UCLouvain

epl

École polytechnique de Louvain

Life cycle assessment of a CO_2 revalorisation process using membrane contactors

Membrane absorption promoted by amino acids followed by membrane distillation-crystallisation

Author: **Béatrice Desclée de Maredsous**
Supervisor: **Patricia Luis Alconero**
Readers: **Yusak Hartanto, Naïma Sallem**
Academic year 2020–2021
Master [120] in Chemical and Materials Engineering

Abstract

Anthropogenic carbon dioxide (CO_2) emissions are largely emitted from fossil fuel combustion. In order to avoid global warming, one potential approach to reduce the carbon footprint of industries could be the capture of CO_2 via membrane technologies. This master thesis aims to study the potential interest of a novel process for carbon capture and utilisation (CCU) using membrane contactors. To do so, the environmental impacts will be evaluated in a life cycle assessment (LCA). The LCA will focus on the CCU process operating in 3 major steps. Firstly, membrane gas absorption uses a novel solvent composed of 0.5M sodium carbonates (Na_2CO_3) and promoted by 0.5M arginine (ARG) or 0.3M sarcosine (SAR). Chemical absorption fixes CO_2 in the form of sodium bircarbonates ($NaHCO_3$) in an aqueous solution. Secondly, the solution is distilled and $NaHCO_3$ crystallised via membrane distillation-crystallisation (MDC). 3 different and potential MDC technologies will be studied: osmotic membrane distillation (OMD), direct contact membrane distillation (DCMD) and vacuum membrane distillation (VMD). Finally, a post-treatment step allows the filtration of $NaHCO_3$ crystals and the recovery of the remaining solution. These crystals could be reused for other commercial purposes. The work of the thesis is 1) to model this CCU process as a continuous process and to scale it up such that material and energy inventories can be collected and 2) to identify key points of the process which are determinant with regards to environmental impacts. For this purpose, the 4-step LCA methodology is followed. The results show that the process, when environmentally optimised, is a possible technology to reduce CO_2 emissions and achieve significant impact reduction in other impact categories. Absorption is also proven to be a key step with regard to emissions, with an emphasis on minimising the use of Na_2CO_3. Indeed, the use of Na_2CO_3 in the solvent is a relatively important factor for environmental concerns. To reduce its use, absorption must be carried out until the solvent is saturated. This minimises the solvent flowrate and thus reduces emissions in the subsequent MDC step. With regard to the preferred MDC, there is no consensus on all impact categories. OMD and VMD have the highest emissions in several categories, whilst DCMD depicts quantitatively intermediate emissions.

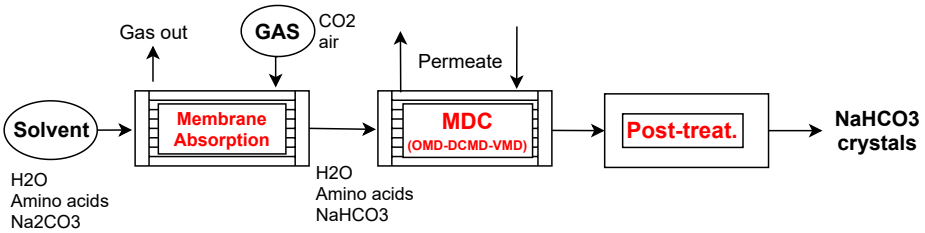

Figure 1 The studied carbon capture and utilisation (CCU) process in 3 steps.

Acknowledgements

First of all, I would like to thank Patricia Luis Alconero for giving me the opportunity to participate in this project and for helping me throughout the work. More generally, I would also like to thank her for the different classes she gave me during my 2 years of master. I particularly liked these subjects, which gave a particular sense to my choice of master and option. Secondly, I would like to thank Marie-Charlotte Sparenberg for her precise comments and her dedicated contribution to my work. I would also like to thank Vida Sang Sefidi for her time and availability to help me or to show me the labs. I would like to express my gratitude to Naïma Sallem and Yusak Hartanto who accepted to be assessors of this master thesis.

I would like to thank in particular my classmates with whom we supported each other during the last semester, despite the distance learning. Finally, a special thanks to my parents and my friends for their daily encouragement during this reflection and, more generally, their support during these five years of academic training.

Contents

Glossary

$A_{m,i}$	Membrane area of process step i $[m^2]$.
a_w	Water activity [-].
C_{fj}	$NaHCO_3$ concentration in the feed at j, i.e inlet or outlet, MDC $[g\,kg^{-1}]$.
c_p	Specific heat capacity of water $[kJ\,kg^{-1}\,K^{-1}]$.
C_{pj}	NaCL concentration in the permeate outlet at j, i.e inlet or outlet, OMD $[g\,kg^{-1}]$.
ΔC	Driving force, absorption $[mol\,m^{-3}]$.
$\Delta\overline{C}$	Mean driving force, absorption $[mol\,m^{-3}]$.
ΔH_{vap}	Enthalpy of vaporisation of water $[kJ\,kg^{-1}]$.
ΔP	Driving force, MDC $[Pa]$.
$\Delta\overline{P}$	Arithmetic mean along the membrane contactor of the driving force, MDC $[Pa]$.
ε	Overall absorption efficiency of CO_2 along the membrane contactor [-].
H^{cp}	Dimensionless Henry solubility, [-].
H^{cp}	Henry solubility defined via concentration, $[mol\,m^{-3}\,Pa^{-1}]$.
J_{abso}	Transmembrane flux, absorption $[mol\,m^{-2}s^{-1}]$.
J_{mdc}	Transmembrane flux, MDC $[m^3\,m^{-2}s^{-1}]$.
κ	CO_2 load in the solvent, absorption $[mol_{CO2}\,kg^{-1}_{solution}]$.
K_{ov}	Overall mass transfer coefficient, absorption $[mol\,m^{-2}s^{-1}]$.
K_{ov}	Overall mass transfer coefficient, MDC $[m^3\,m^{-2}s^{-1}\,Pa^{-1}]$.
M_i	Mass of compound i $[kg]$.
$M_{m,i}$	Molar mass of compound i $[g\,mol^{-1}]$.
m_p	Mass of the polymer of the membrane $[kg]$.

N_{CO2}	Moles of CO_2 absorbed per hour, absorption $[mol\,h^{-1}]$.
N_{H2O}	Mass of H_2O evaporated per hour, MDC $[kg\,h^{-1}]$.
$n_{ij,k}$	Moles of component k in stream i, i.e gaseous or solvent stream, at j, i.e inlet or outlet, absorption $[mol\,h^{-1}]$.
ν	Molar fraction of CO_2 in gaseous stream, absorption [-].
p_{ij}	Pressure in i, i.e feed or permeate side, and at j, i.e the inlet or outlet, MDC $[Pa]$.
p_o	Vacuum pressure, VMD $[Pa]$.
p_{so}	Partial pressure of CO_2 in the gas phase under equilibrium conditions and at the outlet of the membrane, absorption $[Pa]$.
Q_{ij}	Flow rate in i, i.e solvent, feed, gaseous or permeate side, and at j, i.e the inlet or outlet $[kg\,h^{-1}]$.
ρ_{H2O}	Water density $[kg\,m^{-3}]$.
ρ_p	Polymer density of the membrane material $[kg\,m^{-3}]$.
r_j	Radius j, i.e. inner or outer, of the hollow fibers of the membrane $[m]$.
T_{ij}	Temperature in i, i.e feed or permeate side, and at j, i.e the inlet or outlet, MDC $[^\circ C]$.
V_{gj}	Total volume flow rate in gaseous stream and at j, i.e the inlet or outlet, absorption $[m^3\,h^{-1}]$.
V_m	Molar volume $[m^3\,mol^{-1}]$.
χ	Recovery rate from post-treatment to absorption [-].
x_i	Mass fraction of component i [-].

Acronyms

CO_2	carbon dioxide.
K_2CO_3	potassium carbonate.
NH_3	ammonia.
Na_2CO_3	sodium carbonate.
$NaHCO_3$	sodium bicarbonate.
AA	amino acid.
AP	air pollution.
ARG	arginine.
CCS	carbon capture and storage.
CCU	carbon capture and utilisation.
DALY	Disability adjusted life years.
DCMD	direct contact membrane distillation.
DI	deionised water.
DMAC	dimethylacetamide.
EO	ethylene oxide.
FEFANA	EU Association of Specialty Feed Ingredients and their Mixtures.
FU	functional unit.
GHG	greenhouse gas.
GWP	global warming potential.
ILCD	International Reference Life Cycle Data.
IPCC	Intergovernmental Panel on Climate Change.
LCA	life cycle assessment.
LCI	life cycle inventory.
LCIA	life cycle impact assessment.
MC	membrane contactor.
MD	membrane distillation.

MDC	membrane distillation-crystallisation.
MEA	monoethanolamine.
MFC	mass flow controller.
ML	membrane lifetime.
MSG	monosodium glutamate.
OMD	osmotic membrane distillation.
PP	polypropylene.
PTFE	polytetrafluoroethylene.
PVDF	polyvinylidene fluoride.
RO	reverse osmosis.
SAR	sarcosine.
VMD	vacuum membrane distillation.
WWT	wastewater treatment.

List of Figures

List of Tables

Introduction

Mainly responsible for current environmental crises, our society is facing an emergency regarding climate change. We are already aware of the great problem surrounding it, and 195 countries signed the Paris agreement in 2015 to continue their efforts to limit the temperature increase to 1.5°C by 2100.

To keep the temperature below this target, one of the key points is to significantly reduce greenhouse gas (GHG) emissions. Carbon dioxide (CO_2) is one of the most present GHGs in the atmosphere (81% of GHGs) [1]. The presence of CO_2 in the atmosphere is a natural phenomenon partially due to photosynthesis but today, we have reached an extreme level, partially caused by the coal power sector, which, in 2021, accounts for 29% of global CO_2 emissions, while the industry and transport sector each accounts for 23% [2]. In addition, in 2019, fossil fuels were used to produce about 84% of the world's electricity which illustrates their significant contribution to CO_2 emissions into the atmosphere[3]. Global demand for energy services and economic growth suggests that fossil fuels will continue to be widely used in the future. Therefore, in order to reduce emissions whilst meeting the growing demand for energy, technologies must be developed to capture CO_2 released from fuel combustion and industrial activities. [4]

In this thesis, a carbon capture and utilisation (CCU) process is investigated as a potential technology to reduce CO_2 emissions. The specific CCU process analysed in this work is still under research in the laboratories of UCLouvain and is based on membrane technologies. The process flowsheet studied in the present document is outlined in Figure 2. The first step consists of carbon absorption by a membrane contactor, promoted by amino acids and sodium carbonates (Na_2CO_3). In the second step, the captured carbon dioxide is revalorised into sodium bicarbonates ($NaHCO_3$) by membrane distillation-crystallisation (MDC). Different MDC configurations (osmotic membrane distillation (OMD), direct contact membrane distillation (DCMD) and vacuum membrane distillation (VMD)) will be developed and considered in this thesis. Finally, once the $NaHCO_3$ crystals are concentrated and crystallised, a last post-treatment step allows them to grow and to be filtered so that the dried crystals can be revalued for commercial uses.

In order to assess whether the CCU under development could indeed be a potential and interesting technology to reduce CO_2 emissions, the environmental impacts of the whole process are evaluated using the standardised method of life cycle assessment (LCA) in 4 steps. The LCA is carried out taking into account the defined system boundaries of the process and are outlined in Figure 3.

Consequently, the objective of this thesis is to evaluate and highlight potential high environmental impact stages of the process. Several scenarii are studied by varying the operating parameters and changing different baseline assumptions. By doing so, different LCAs can be compared in order to present the best operating conditions and recommendations for the CCU process with regard to environmental concerns.

These recommendations are the result of the following research approach. First, a literature review is carried out with respect to the process studied and the LCA methodology, more specifically on CCU. In order to provide a theoretical background to the process, Chapter I reviews conventional CO_2 absorption by columns and $NaHCO_3$ crystallisation. Additionally, it presents the operating principles of the studied membrane technologies. The choice of solvent in absorption is detailed and the different MDC configurations explained. After the process review, a description of the LCA methodology and the CCU is presented in Chapter II, followed by a state of the art on LCAs of CCU.
Afterwards, the LCA methodology is applied to the current CCU process. The goal and scope (Chapter III) are defined and life cycle inventories required for the process and surrounding aspects are collected (Chapter IV). By this way, experimental data from UCLouvain laboratories is taken into account as well as quantitative data found in the scientific literature. The environmental impacts are then analysed and interpreted in Chapter V. This highlights the system boundaries' stages and the process's operating conditions that have the most damaging environmental effects. Finally, the limitations of the study as well as recommendations for future research are presented and conclusions are drawn (Chapter VI).

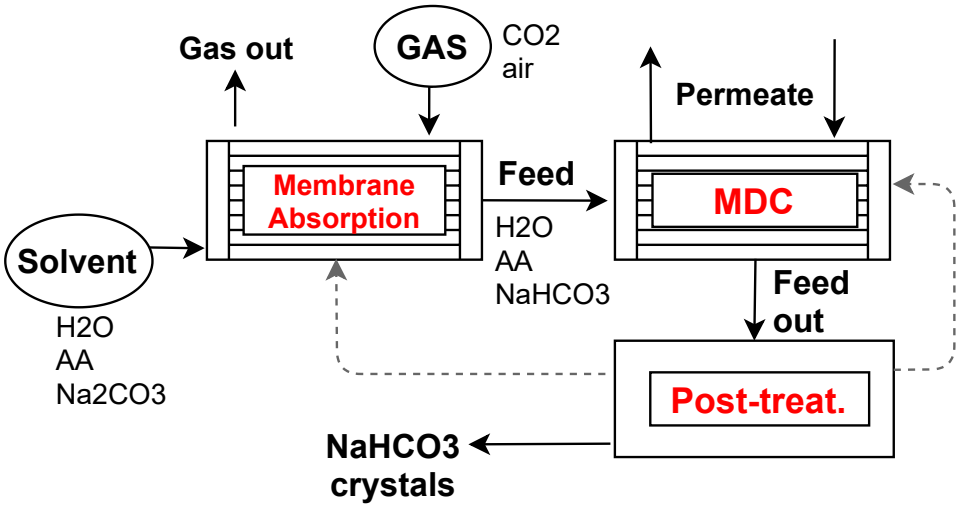

Figure 2 Simplified process flowsheet.

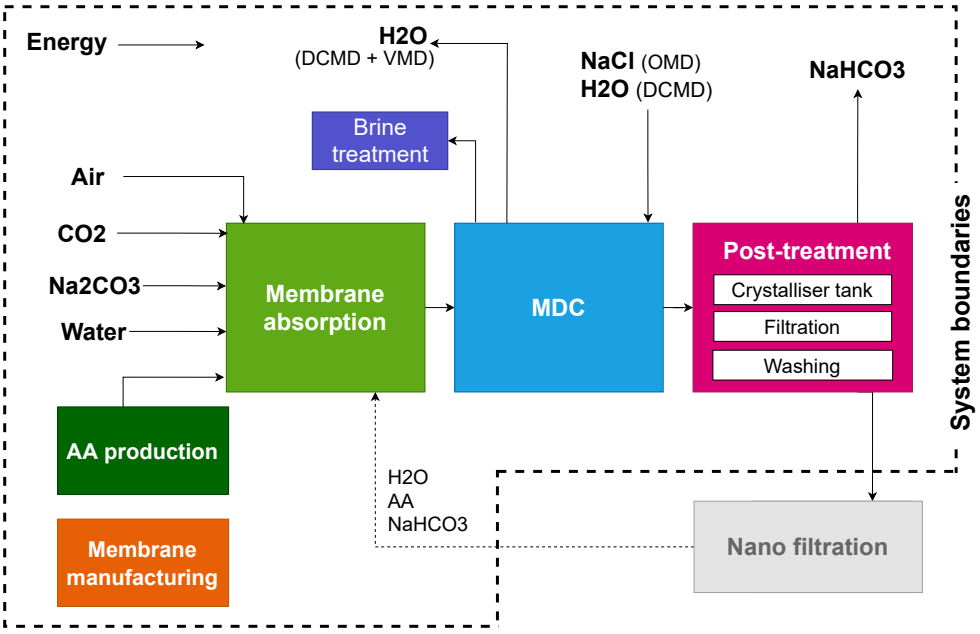

Figure 3 LCA system boundaries.

Chapter I

Literature review of the process

The studied process is on one hand based on the absorption of CO_2 by a chemical solvent, and on the other hand, it lays ground on the crystallisation of the $NaHCO_3$ crystals. Both technologies operate thanks to membrane contactors. A last process's step includes the recovery of $NaHCO_3$ crystals. A simplified flowsheet of the process is shown on Figure 2, and a more detailed one is given at the end of this chapter on Figure 11 and 12 where the composition of the flows and each devices are indicated.

As a matter of fact, the interest of the studied process lies in the use of **post-combustion** flue gases which are captured directly after the combustion stage and produce a flow composed of 10 to 15% CO_2 at atmospheric pressure [5]. This gas mixture is then sent as a gaseous feed to **membrane gas absorption** in order to absorb CO_2 into a liquid mixture. To achieve this, a novel solvent mixture is prepared with sodium carbonates (Na_2CO_3) and amino acids (AAs). Once the solvent has chemically absorbed CO_2, dissolved odium bicarbonates ($NaHCO_3$) are present in the solvent leaving the absorption membrane. However, membrane as an absorption equipment is a novel technology compared to conventional absorption columns. Moreover, the choice of the chemical solvent is crucial. Although a monoethanolamine (MEA) solution is the most widely used solvent, carbonates mixed with AAs appear to be interesting alternatives. Therefore, research in UCLouvain laboratories is performed to characterise absorption performances of CO_2 absorption by membrane and using solvent of Na_2CO_3 promoted by AAs (arginine and sarcosine in the studied case).

After absorption, the aqueous solution is sent as feed to the **membrane distillation-crystallisation (MDC)** to saturate the solution in $NaHCO_3$. Distillation in the membrane evaporates water of the feed to the permeate side, followed by crystallisation of $NaHCO_3$ until saturation is reached. Here again, the studied crystallisation technology is still under development and could be a great alternative to conventional crystalliser and conventional $NaHCO_3$ production by the Solvay process.

This chapter presents a literature review in 2 sections of both the CO_2 absorption step and the crystallisation of $NaHCO_3$. Firstly, the equipment and solvent for CO_2

absorption are studied. Regarding the equipment, the conventional packed column and the main concerns about it are described, whilst the membrane contactor studied for the absorption and its operating principle are explained. Then, conventional MEA as solvent is presented. In addition, advantages of the solvent mixture of carbonates and AAs are listed, and the mass transfer coefficient of the studied absorption process explained. Finally, membrane distillation-crystallisation (MDC) is discussed at length. The conventional crystalliser and the Solvay process are described, while the studied set-up is presented with its advantages, the operating principles and the different membrane configurations studied in more detail in this paper. For both absorption and MDC, mass transfer coefficients and transmembrane fluxes are described.

I.1 CO_2 absorption

CO_2 absorption by a chemical solvent is becoming one of the best available technologies [6]. However, two major bottlenecks must be solved to achieve technico-economical targets: the reduction of the size of the installations and the energy requirements. For this purpose, the choice of the equipment and the solvent are of key importance and are discussed in the following sections. [6]

I.1.1 Equipment

Nowadays, the conventional industrial equipment is a packed column and is considered as the best available technology. However, given the important size of these conventional columns, membrane contactors are seen as a solution to this problem. [6]

This section presents the conventional and the studied membrane equipment, defining their working principles, advantages and application's limitations.

I.1.1.1 Conventional columns

The conventional packed column scheme of a post-combustion process is shown in Figure 4. The data is taken for a coal-fired power plant with a flue gas composition of 15% CO_2 by volume. The absorption unit (A) represents the packed column. On the one hand, the solvent is pumped to the top of the column and sprayed through it so that it also falls by gravity. On the other hand, the gas stream is introduced at the bottom of the column. The **gas-liquid contact** between the CO_2 and the solvent allows the CO_2 to be chemically absorbed by the solvent. [7; 6]

However, the conventional packed column has various **disadvantages** such as the size of its installation. It follows from this that membrane contactors can replace the absorption column, which has many advantages.

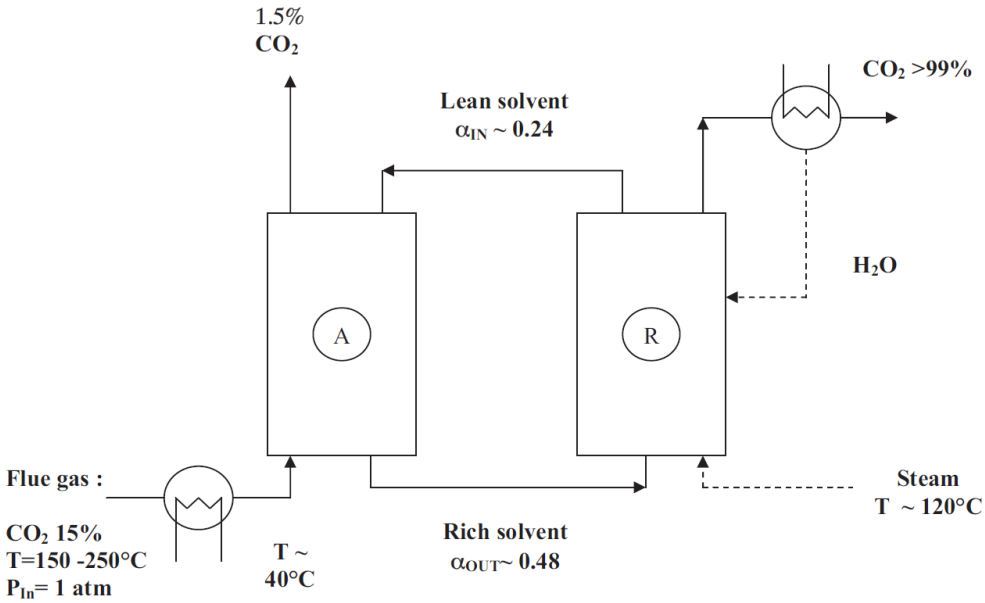

Figure 4 Simple flowsheet with gas absorption in a chemical solvent. The $\alpha_{IN/OUT}$ gives the solvent loading for the inlets and outlets respectively.[6]

I.1.1.2 Studied membrane contactors

The reduction in the size of the conventional installations can be achieved by intensifying the process. To this end, membrane contactor's technology is considered as one of the most promising strategies for intensifying CO_2 capture in gas-liquid absorption.[6]

Regarding the working principle, membrane contractor uses a porous membrane that separates gas from liquid streams and induces gas absorption. The membrane acts as an additional mass transfer resistance that must be taken into account, compared to a conventional gas-liquid absorption column where the contact between the two phases is direct. However, thanks to the membrane, the **interfacial surface area** between the two phases is extremely increased and therefore counteracts the decrease in mass transfer. The total and effective performance of the mass transfer can lead to an interesting intensification of the post-combustion process.[6; 8] A detailed description of the gas-liquid absorption process by membrane is shown in Figure 5, whilst Figure 5A shows the 3 mass transfer resistances due to the gas, the membrane and liquid solvent [6]. The resistance of the gas phase in Figure 5A can be neglected in comparison to the liquid phase boundary. When the membrane is porous, the resistance of the membrane is also relatively very low, as long as the porous membrane is not wetted by the solvent. Nevertheless, the membrane resistance becomes very visible when the pores are wetted, as shown in Figure 5B.

Two types of membranes are available: **hydrophobic** and hydrophilic. In order to avoid the problem of wet pores, the hydrophobic membrane (allowing only the vapour phase to pass through the membrane's pores) must be used with a solvent in aqueous solution. However, the problem of pore's wetting always arises in case

of prolonged use.[8] In the present case of hydrophobic membrane, a "liquid in" configuration is considered, i.e. the solvent flows inside the fibers and the gas stream flows in the membrane shelter. [9].

In addition, the membrane contractor has several other **advantages** over conventional gas absorption in a packed column [10; 6]:

(i) There is no fear of weeping and flooding, as there is no direct contact between the liquid and gaseous phases. Operating conditions also have a larger range, as the choice of gas and liquid flowrates is independent.

(ii) Solvent losses are usually due to aerosol formation and physical training is considerably reduced.

(iii) The use of polymeric membranes can reduce the weight of the installation. This argument could be very decisive for offshore applications.

(iv) The usual corrosion problems of packed columns can be avoided to a large extent through the use of membranes.

For these different reasons, the membrane contactor was chosen as the absorption equipment of the process studied.

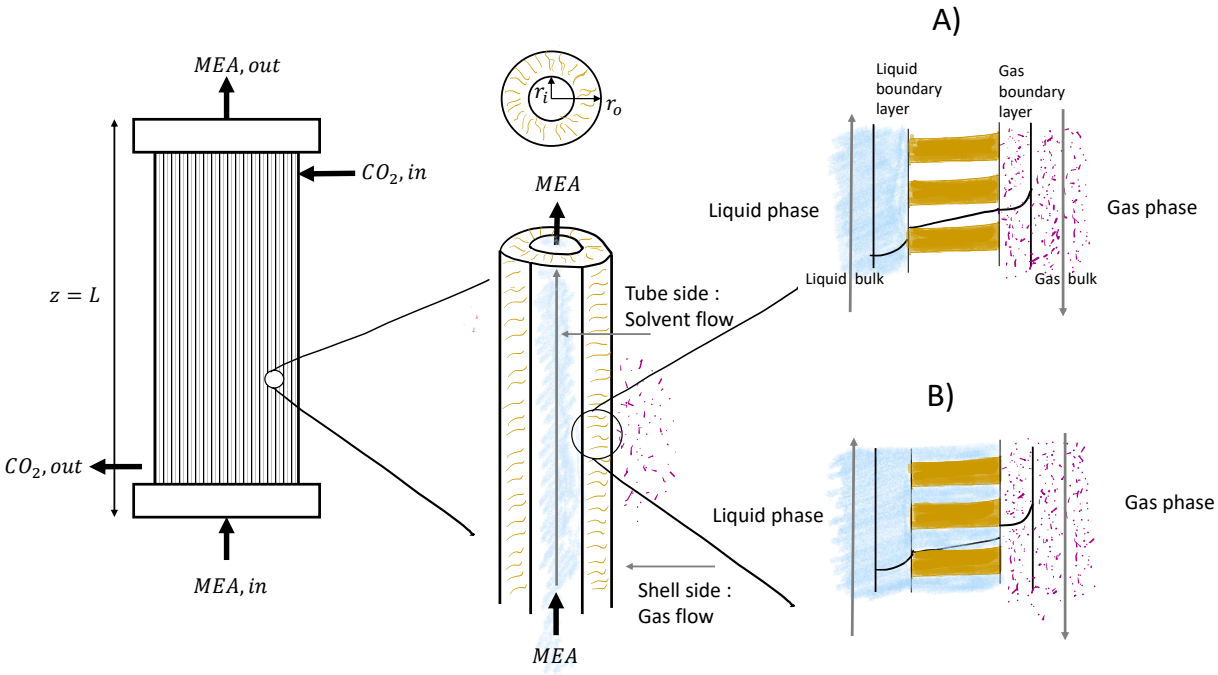

Figure 5 Principle gas–liquid absorption processes for membrane contactor. Array with hollow fibers and made of microporous hydrophobic material. Liquid phase boundary layer resistance with (A) nonwetted mode and (B) wetted mode. Inspired from [6] and [8]

I.1.2 Solvent

CO_2 capture by gas-liquid contact widely uses amines as chemical solvent. As a matter of fact, MEA is the actual benchmark absorbent to absorb CO_2 [11]. However, there are still some gaps in this technology such as the high energy required to regenerate MEA [7; 6]. To address this, a solvent mixture of carbonates promoted by AAs is considered.

This section presents the conventional solvent by MEA and an alternative mixture composed of carbonates and AAs.

I.1.2.1 Conventional MEA

The chemical solvent **MEA** is the actual benchmark absorbent (see structure on Figure 6) and has been widely synthesised in order to absorb CO_2. The cost of production is clearly an **advantage** for the commercial use of MEA, as it can be synthesised from ammonia (NH_3) and ethylene oxide (EO), both chemicals are ranked in the Top 50 of production by mass [12]. MEA has several **advantages** for CO_2 capture: high reactivity and absorption rates, high resistance to thermal degradation, low solubility for hydrocarbons, low cost [8].

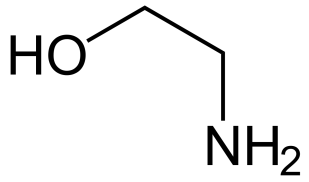

Figure 6 Structure of ethanolamine.[13]

Nevertheless, even if the most extensive capture method is absorption with MEA solvent, this technology still presents some **drawbacks**. The process has a high solvent loss during the process, a high heat demand for regeneration, a low CO_2 loading, a high vapour pressure which leads to vaporisation losses and a high viscosity. For instance, CO_2 packed columns currently requires 3.5 GJ/tonne of CO_2, whereas the EU target is 2 GJ/tonne of CO_2 [5]. MEA also exhibits equipment corrosion, and with regard to the overall process, the production of MEA from NH_3 by the Haber-Bosch process emits a significant amount of CO_2. From a safety point of view, amines are highly toxic compounds. Moreover, the use of the solvent MEA is intended for the sequestration and storage of the captured CO_2, and does not allow for any additional recovery. The presence of impurities in the flue gas, such as SO_x, NO_x, H_2S, fly ash and heavy metals, could also cause the loss of amines and thus reduce the efficiency of CO_2 capture.[8; 12; 7; 14]

I.1.2.2 Studied carbonates promoted by amino acids

To address the drawbacks associated with the use of MEA, alternative technologies using a new solvent must be considered as a key element in the development of a process that allows the capture and reuse of residual CO_2 [7]. A potential alternative solvent is studied in this document, being a mixture of sodium carbonate (Na_2CO_3)

promoted by AAs. Indeed, "*the combination of amine and carbonate solution offers advantages for gas treating in terms of both efficiency (via the amines) and capacity (via the carbonates)* ".[15]

More specifically, the new solvent in question must have characteristics that will allow it to replace the current MEA, such characteristics are [11]:

- **Reactivity**: high reactivity with CO_2 such that the absorption rate and mass flows increase. But a balance must be found between high reactivity and regeneration energy, because high solvent kinetics induce high energy consumption for regeneration as well.
- **Volatility**: not too high, otherwise a high physical loss of the solvent will result in the need for a high compensation.
- **Impurity tolerance**: the post-combustion gas to be treated contains impurities (NO_x, O_2, SO_x and ashes). These can lead to the reaction of impurities such as SO_x with MEA and the formation of corrosive salts. In such a situation of chemical degradation, the active solvent decreases and scrubbers must be placed before the CO_2 is absorbed.
- **Environment friendly**: quality of rejected flows and waste treatment.
- **Production cost**: the solvent must be commercially affordable.
- **Global carbon balance**: the global production of the solvent and more widely the whole capture system should have a positive final carbon balance. These characteristics play key role in the LCA study of this thesis.

Regarding the **carbonate**'s choice, potassium carbonate (K_2CO_3) as a carbonate agent is widespread, but the recycling level of this component is low. However, it is widely accepted that K_2CO_3 has a higher absorption capacity and kinetics than sodium carbonate (Na_2CO_3). Despite these arguments, Na_2CO_3 is more suitable for large-scale industrial applications due to its lower cost. For this reason, this document takes into account the use of Na_2CO_3 as a carbonate agent.[16]

Next, concerning the **AA**, as the high selectivity with respect to CO_2 is the amine group (primary-NH_2, secondary -NH, see structure on Figure 7), the researchers are studying an alternative solvent to MEA with an amine group, non-volatile [8], and which would best meet the above list of required characteristics. It appears that AAs in aqueous solution seem to present **advantages** such as good properties for CO_2 absorption with a high CO_2 solubility [17]. AAs such as glycine, alanine, proline and taurine have a much lower vapour pressure than MEA, which reduces the loss of solvent to the atmosphere. The lower toxicity, greater stability to oxidation and better resistance to degradation make AAs very interesting as alternatives to MEA [18]. However, the use of an AA has the potential **disadvantage** of possible precipitation when absorbing CO_2. For this reason, working conditions play an important role. [19]

In the case studied here, the absorption solvent is composed of Na_2CO_3 mixed separately with 2 types of AAs: arginine (ARG) and sarcosine (SAR). Both cases have been developed and experimented within the laboratories of UCLouvain.

The reaction mechanism of the chemical absorption is also described in Appendix A.1.1.

ARG is composed of an primary amino group as well as a guanidinium group. As with previous MEA, the primary amino group reacts with CO_2. The strong basic chain is always positively charged. The nitrogen double bonds and single nitrogen pairs in the guanidinium group allow the positive charge to be delocalised and participate in many hydrogen bonds. This allows the association with water and promotes the formation of carbamates and the absorption of CO_2. Thanks to these characteristics, arginine should work as well as MEA with comparable reactivity and capacity, but with the advantage of easy regeneration.[20]

SAR is composed of a secondary amino group. In addition, sarcosine is cheaper than arginine. [21] Despite the economical advantage of SAR, it has been experimented in UCLouvain laboratories that SAR shows lower absorption performances as promoter than ARG. First, because a high concentration of SAR in the solution can lead to a reduction of solubility and mass transfer. Secondly, ARG reacts better than SAR thanks to its structure. As a matter of fact, primary amino acid shows better absorption capacity than secondary amines [17]. [21]

To summarise, the studied absorption step is performed using a membrane contactor, where the CO_2 gas is absorbed into a chemical solvent composed of Na_2CO_3 and promoted by AAs (ARG or SAR).

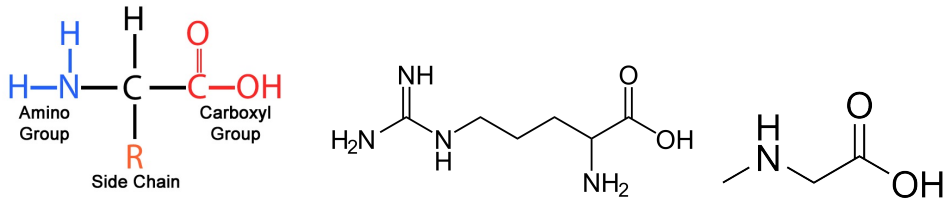

(a) Structure amino acids.[22] **(b)** Structure arginine.[23] **(c)** Structure sarcosine.[24].

Figure 7 Molecular structures

I.1.3 Mass transfer

Mass transfer in membrane-assisted absorption can be expressed in terms of the overall mass transfer coefficient (K_{ov} $[m^3/m^2s]$). The latter is theoretically calculated and allows comparison with other absorption membrane's systems and operating conditions, whereas the transmembrane flux does not. The units of K_{ov} represent the volume of gas stream in m^3 per membrane are in m^2 and per second.

The transmembrane flux J_{abso} $[mol_{CO_2}/m^2s]$ represents the amount of CO_2 moles passing through the membrane per active membrane area per second. The flux J_{abso} is related to the overall mass transfer coefficient and the driving force ΔC (in $[mol/m^3]$) based on the CO_2 concentration gradient:

$$J_{abso} = K_{ov}\ \Delta C \tag{1}$$

Two extreme cases can be distinguished regarding calculations of ΔC: i) when the solvent is fresh and far from saturation and on the other hand, ii) when the solvent reaches saturation. In fact, when the solvent is used until saturation, chemical absorption is almost non-existing and physical absorption takes over.
For a **fresh solvent** running continuously through the membrane contactor, the concentration of CO_2 in the solvent (i.e. C_s in $[mol/m^2]$) is assumed negligible.
But when the **solvent is saturated**, physical absorption should be included in the calculations and C_s becomes non-negligible. The calculation of C_s requires to evaluate the solubility of CO_2 into the liquid solvent. Hence, the Henry constant of CO_2 in aqueous solution is considered (neglecting AA, Na_2CO_3 or $NaHCO_3$ present in the solvent). The latter in found in the literature to be worth $H^{cp} = 3.4 * 10^{-4}\,[mol/m^3 Pa]$ [25]. In addition, the dimensionless Henry solubility H^{cc} is defined as [25]:

$$H^{cc} = \frac{C_s}{C_g}$$

where C_s and C_g are the concentrations of CO_2 $[mol/m^3]$ in the liquid and gaseous phase respectively. Considering ideal gases [25]:

$$H^{cc} = RT \times H^{cp}$$

where R is the gas constant and $T = 298K$. Thus, $H^{cc} = 0.82$ [-].

Subsequently, the driving force varies along the membrane since the concentrations of CO_2 are not the same between the inlet and outlet of the membrane contactor. Therefore an average value of ΔC is calculated (via arithmetic or logarithmic means). Such that:

$$J_{abso} = K_{ov}\ \Delta\overline{C} \tag{2}$$

In addition, on a physical point a view, it is known that a higher $\Delta\overline{C}$ should be observed for a fresh solvent than for a saturated solvent [26; 27]. In order to meet these physical considerations with the mathematical model, arithmetic mean is used for a continuous fresh solvent and logarithmic mean in the saturation case (see Figure A.1 in Appendix) [20; 28; 29; 30]:

$$\Delta\overline{C}_{fresh} = \frac{C_{gi} + C_{go}}{2} \tag{3}$$

$$\begin{aligned}\Delta\overline{C}_{saturation} &= \frac{C_{gi} - (C_{go} - C_{so})}{ln\left(C_{gi}/(C_{go} - C_{so})\right)} \\ &= \frac{C_{gi} - C_{go}(1 - H^{cc})}{ln\left(C_{gi}/(C_{go}(1 - H^{cc}))\right)}\end{aligned} \tag{4}$$

I.2 Crystallisation

The interest of crystallisation for the studied process is the recovery of sodium bicarbonate ($NaHCO_3$) solid crystals. This component is the product of the chemical absorption of CO_2 by the chemical solvent composed of Na_2CO_3 and AAs (see reaction mechanism of absorption in Appendix A.1.1). A detailed scheme of the process' flows and their composition is shown on Figure 11 at the end of the

chapter. As a matter of fact, crystallisation is a solid-liquid separation technique allowing the purification of a chemical species.[31]

In this section, conventional crystallisation is presented with respect to both the conventional columns as equipment and the Solvay process for the production of $NaHCO_3$. Subsequently, the studied case of crystallisation technology by MDC is described in detail.

I.2.1 Conventional columns

Crystallisation and precipitation are often mixed and called by a generic term. Indeed, both refer to a process where a solid is isolated from a supersaturated liquid solution. Nevertheless, a distinction between the two separation techniques must be made according to the speed of the process and the size of the particles formed. Usually, precipitation refers to the rapid formation of small solids, while crystallisation refers to the slow and strictly controlled growth of solid crystals with the desired particle size distribution. Both processes take place in 3 steps: supersaturation, nucleation and solid phase growth.[32]

Crystallisation technology has been widely used since the beginning of the 19th century. Many different industrial sectors (the sugar industry, pharmaceuticals and fine chemicals, microelectronics etc) have started to use this technology. Today, research is being focused on the recovery and removal of crystals present in wastewater, such as phenol, phosphorus or alkali phosphate concentrates. [33; 34]

Conventional crystallisation is traditionally carried out using **crystallisers** or evaporators where precipitation is then generated by cooling or heating devices respectively. However, this technology has the **disadvantage** of high energy consumption, although advances in recent decades have made crystallisation less energy-intensive. To be a sustainable technology, research on crystallisation has increased with the aim of improving design, large-scale operations and increasing efficiency. However, the lack of knowledge on crystallisation kinetics, modeling and prediction of polymorphic crystallisation makes it difficult to improve conventional crystallisation.

Concerning the practical case of $NaHCO_3$ crystallisation, in 1863, **Ernerst Solvay** discovered a new process to produce Na_2CO_3 from sea salt, ammonia and carbonic acid. With this new process, the Solvay group produces $NaHCO_3$ of great purity and is present in more than 55 countries, being the world leader in the production of sodium carbonate and bicarbonate. Also known as BICAR®, $NaHCO_3$ can be used in many application sectors. It can neutralise acids in exhaust gases or even in tomato sauce during cooking, reduce acidity in the stomach by preventing acidosis or prevent corrosion of pipes. The BICAR® also works as a water softener when it dissolves in water and makes it impossible to separate the calcium ion into lime, thus avoiding the lime deposits. But $NaHCO_3$ is also used for daily applications as a cleaning agent, toilet product, odour absorbent, food additive, etc.[35; 36]

Conventional production of refined $NaHCO_3$ is carried out in a large bubble column (20 m high and 2.5 m wide), also known as a **BIR column** (Figure 8), where a

gas mixture of CO_2 and air is dispersed in an aqueous solution of Na_2CO_3 and $NaHCO_3$. The BIR column is nearly isothermal and is divided into two parts: at the top of the column, the cylindrical core is equipped with trays, and at the lower part; with circulation loops. The column works by counter-current injections: at the top, the liquid brine enters the column while the gases are injected at the bottom.[35; 36]

During the reaction, the gaseous CO_2 is transferred into the liquid phases. A supersaturation of $NaHCO_3$ is created by the reactions (5) and (6), leading to the continuous precipitation (fast crystal formation unlike crystallisation) of $NaHCO_3$ at the bottom of the column.[35; 36]

$$CO_{2(g)} \rightleftharpoons CO_{2(l)}$$
$$CO^{+}_{2(l)}OH^{-} \rightleftharpoons HCO_3^{-} \quad (5)$$
$$CO_3^{2-} + H_2O \rightleftharpoons HCO_3^{-} + OH^{-} \quad (6)$$

However, conventional production of $NaHCO_3$ by BIR columns has **drawbacks** such as environmental concerns regarding the disposal of the main by-product $CaCl_2$, extraction of raw materials such as purified brines and $CaCO_3$, ammonia losses, dust, etc.[37; 38]

In this context and taking into account the disadvantages of conventional crystallisers and the conventional $NaHCO_3$ process, a new technology such as membrane crystallisation seems to be an innovative alternative to obtain a better control of the crystallisation and a more environmentally friendly production of $NaHCO_3$.[33; 34]

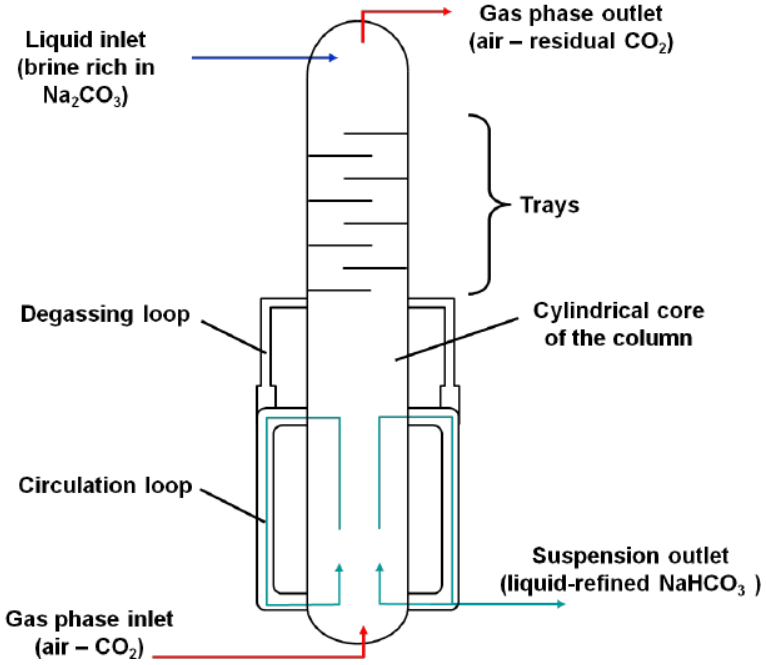

Figure 8 Schematic representation of a BIR column.[35]

I.2.2 Studied membrane distillation-crystallisation

The use of a membrane for crystallisation allows its intrinsic **advantages** to be exploited. Indeed, the porous surface of the membrane favours heterogeneous nucleation mechanisms and the control of the supersaturated solution by regulating the mass transfer through the membrane. Membrane technology also allows well-controlled nucleation and growth kinetics. Moreover, membrane-assisted crystallisation allows nucleation and crystal growth to be induced in two separate compartments, which significantly reduces the risk of membrane clogging. In addition, solid features such as size, shape and purity are easier to adjust than those of conventional devices, and scale-up (or scale-down) the membrane crystallisation process is simpler. Membranes are also very compact (membrane surface area per unit volume) with a specific surface area $> 1000\ m^2/m^3$ for hollow fibre membrane contactors. Finally, compared to conventional methods such as evaporators, membrane-assisted crystallisation reduces energy consumption, as it can be used at room temperature and with the possibility of using waste heat to increase the feed temperature. These latter features play a key role in favour of membrane-assisted crystallisation.[33; 39; 14]

In addition, there are two ways of **classifying** membrane-assisted crystallisation operations. In the studied case, the focus is on the classification where only vapour can pass through the pores. Indeed, the recovery of $NaHCO_3$ crystals is made possible by means of membrane distillation-based processes. In fact, membrane distillation is first carried out and the water is evaporated until the supersaturation level is reached. This is the **membrane distillation (MD)**. Once achieved, it becomes a **MDC** process.[39]

In other words, during the first phase of **MD**, "*the solvent molecules evaporate on the feed side, diffuse through a porous membrane and recondense at the opposite site, under the action of a vapour pressure gradient as driving force*" [39]. In this case, MD is used to concentrate the feed for other applications but not for crystallisation. As with membrane absorption, the membrane acts as a separation barrier between two phases, such that 3 resistances appear: one from the liquid feed side, one from the crystalline phase and the last resistance comes from the membrane itself. In order to concentrate the feed solution, mass transfer occurs as a result of 3 different phenomena: i) diffusion of water from the feed mass into the pores of the membrane, ii) vaporisation and diffusion through the membrane, and iii) condensation and diffusion into the permeate mass.
The permeate side varies according to the **configuration** of membrane. Therefore, it may contain an aqueous solution, air/gas or be connected to a vacuum pump. The type of permeate defines the sources of driving force, which can be caused by temperature, osmosis or vacuum (see later in the Section). From an equipment point of view, a **hydrophobic** membrane must be used to allow only vapour to pass through and to keep the pores theoretically dry. Unfortunately, wetting of the membrane occurs by decreasing the mass transfer and increasing the interfacial area.[33; 34; 39]

Membrane distillation can continue up to very high concentration, "*generating supersaturation in the crystallisation solution*", leading to the second phase of **MDC**

[39]. Heterogeneous nucleation on the feed side is triggered by the **supersaturation** state of the solution, while crystal growth is carried out in a separate crystallisation tank, followed finally by vacuum filtration to recover the solid crystals $NaHCO_3$. In addition to its role as a membrane barrier, the membrane acts as a "*solid support on which the solute molecules can converge forming clusters (nuclei) or growth units, leading to a heterogeneous nucleation, which is desired when crystallising a component since a higher crystal yield can be produced*"[39]. The general process of crystallisation is represented on Figure 9.[33; 34; 39]

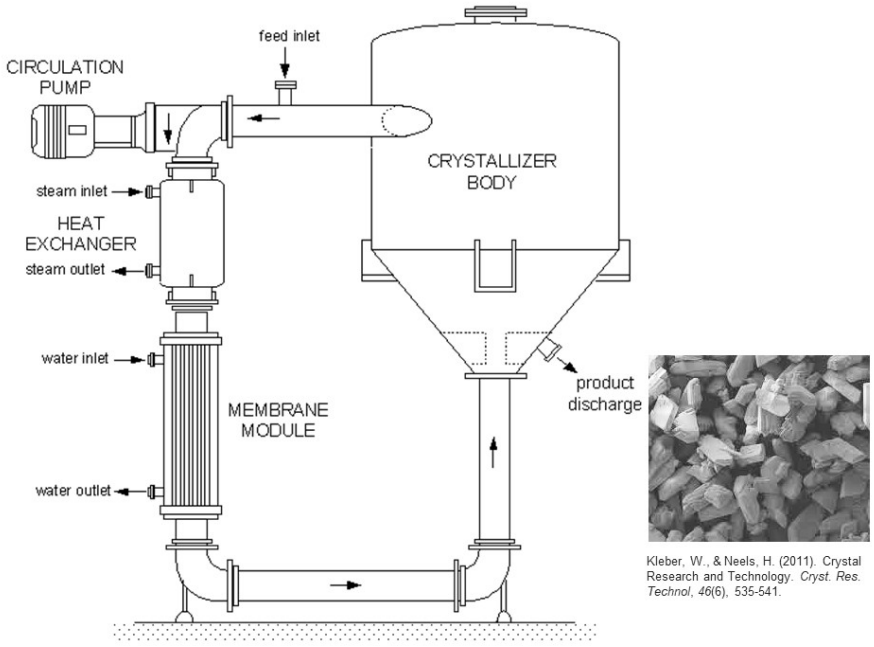

Figure 9 Scheme of membrane distillation and MDC with crystalliser tank (missing here the filtration unit).[39]

The use of the membrane brings an extra resistance which is highly dependent on the **type** of membrane and the kind of configuration.[33] The type membrane, as far as its morphology is concerned presents different characteristics that affect crystallisation. For example, it depends on the thickness of the membrane, its porosity, the inlet pressure of the liquid, the size of the pores and the thermal conductivity.[33; 40]

In addition to the type of membrane, several **configurations** have been developed for membrane-assisted crystallisation. The removal of water from the liquid feed is highly dependent on this, which determines the sources of the driving force. In the case studied in this document, the crystallisation of $NaHCO_3$ is achieved via 3 different configurations represented on Figure 10:

(i) **Direct Contact Membrane Distillation** (DCMD - Figure 10a): the permeate side is composed of a cooler aqueous solution kept in contact with the hotter feed by a hydrophobic membrane that prevents liquid water from entering the pores. The temperature difference between the two sides of the

membrane induces evaporation of the feed. Volatile molecules pass through the pores of the membrane on the permeate side, where they condense.[41]

The driving force ΔP_{dcmd} in $[Pa]$ enables the evaporation of water and is due to a of vapor pressure gradient between the 2 two sides.

$$\Delta P_{dcmd} = a_{wf} p_f - a_{wp} p_p \tag{7}$$

Where a_{wi} represents the water activities. The vapor pressure p depends on the water temperature which can be calculated via the empirical Antoine's equation [42; 41]:

$$p(T) = exp\left(23,1964 - \frac{3816,44}{46,13 + T}\right) \tag{8}$$

The vapor pressure in Antoine's equation is given in $[Pa]$ and the temperature T in $[K]$.

The water activity in the permeate side a_{wp} is worth 1, since it is pure water. However, the water activity of the feed a_{wf} which is an aqueous solution containing 2 solutes is estimated by the following equation [43]:

$$a_w = a_i \times a_j \tag{9}$$

where a_i and a_j are the water activity of each component in the solution respectively. Therefore, the water activity of the feed (a_{wf}) entering MDC and being composed of AAs and $NaHCO_3$ can be estimated by substituting water activity of the pure aqueous solution with ARG (or SAR) (a_i) and with $NaHCO_3$ (a_j). These are found in the literature and are attached in Appendix B.5.2.

(ii) **Osmosis Membrane Distillation** (OMD - Figure 10a): the process works in a similar way to DCMD, but in this case an osmotic agent is used instead of a cold permeate solution. In the present study, NaCl (non-volatile) is used as an osmotic agent. OMD is an athermal process, which has the advantage of operating under mild conditions. The driving force for the mass transfer of water is induced by the difference in vapour pressure across the membrane. The latter is made possible by the concentration gradient between the feed and permeate sides. The latter enhanced by the lower water activity in the permeate [44]. The water evaporates from the feed solution with a higher vapour pressure, diffuses through the pores and condenses in the demineralised solution at the permeate side.[45] The driving force ΔP_{omd} is expressed:

$$\Delta P_{omd} = p\ (a_{wf} - a_{wp}) \tag{10}$$

where the vapour pressure at the feed and permeate sides are equal since the temperature is the same in both sides, such that $p_f = p_p = p$, and p is obtained via Antoine's equation (8). The water activities a_{wp} of the osmotic permeate is given in Figure B.14 and a_{wf} is calculated like in DCMD.

(iii) **Vacuum Membrane Distillation** (VMD - Figure 10b): The driving force is induced by a vacuum pump system connected to the permeate side. In order to create a driving force, the vacuum must be lower than the saturation pressure of the volatile molecules on the feed side. Once the vapour passed through the pores, it is sucked out of the permeate side and a condenser must be added to further condense it.[33] Here again, the driving force ΔP_{vmd} is expressed [41]:

$$\Delta P_{vmd} = (a_{wf} p_f - p_o) \tag{11}$$

p_o is the vacuum pressure $[Pa]$, constant in the permeate side, p_f obtained via Antoine's equation and a_{wf} like explained in DCMD.

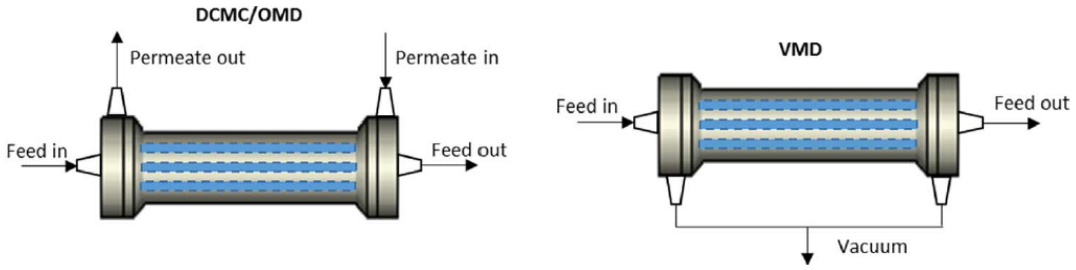

(a) direct contact membrane distillation (DCMD), osmotic membrane distillation (OMD). **(b)** vacuum membrane distillation (VMD).

Figure 10 Membrane distillation configurations.[33]

I.2.3 Mass transfer

Like for absorption, the overall mass transfer coefficient K_{ov} is a good indication of the mass transfer of water between the feed and the permeate. It allows a fair comparison of the 3 different MDC configurations operating at different conditions while excluding the effect of the driving force. K_{ov} in expressed in $[m^3/m^2 s]$ and represents the amount of water going through the pores per second and per membrane active area. It can be obtained from the experimentally calculated transmembrane flux. [28]

The overall mass transfer coefficient linked with the driving force ΔP in $[Pa]$ (see above section for its full mathematical expression) varies for each MDC configuration and gives the transmembrane flux J_{mdc} in $[m^3/m^2 sPa]$. However, since the temperature of both sides and the concentrations of the feed change along the membrane, an arithmetic mean of driving force is introduced, subsequently noted $\Delta\overline{P}$ $[Pa]$. The flux is therefore expressed as follows:

$$J_{mdc} = K_{ov}\ \Delta\overline{P} = K_{ov}\ \frac{\Delta P_{in} + \Delta P_{out}}{2} \tag{12}$$

Note that the choice for an arithmetic mean of $\Delta\overline{P}$ is explained in Appendix B.5.1.

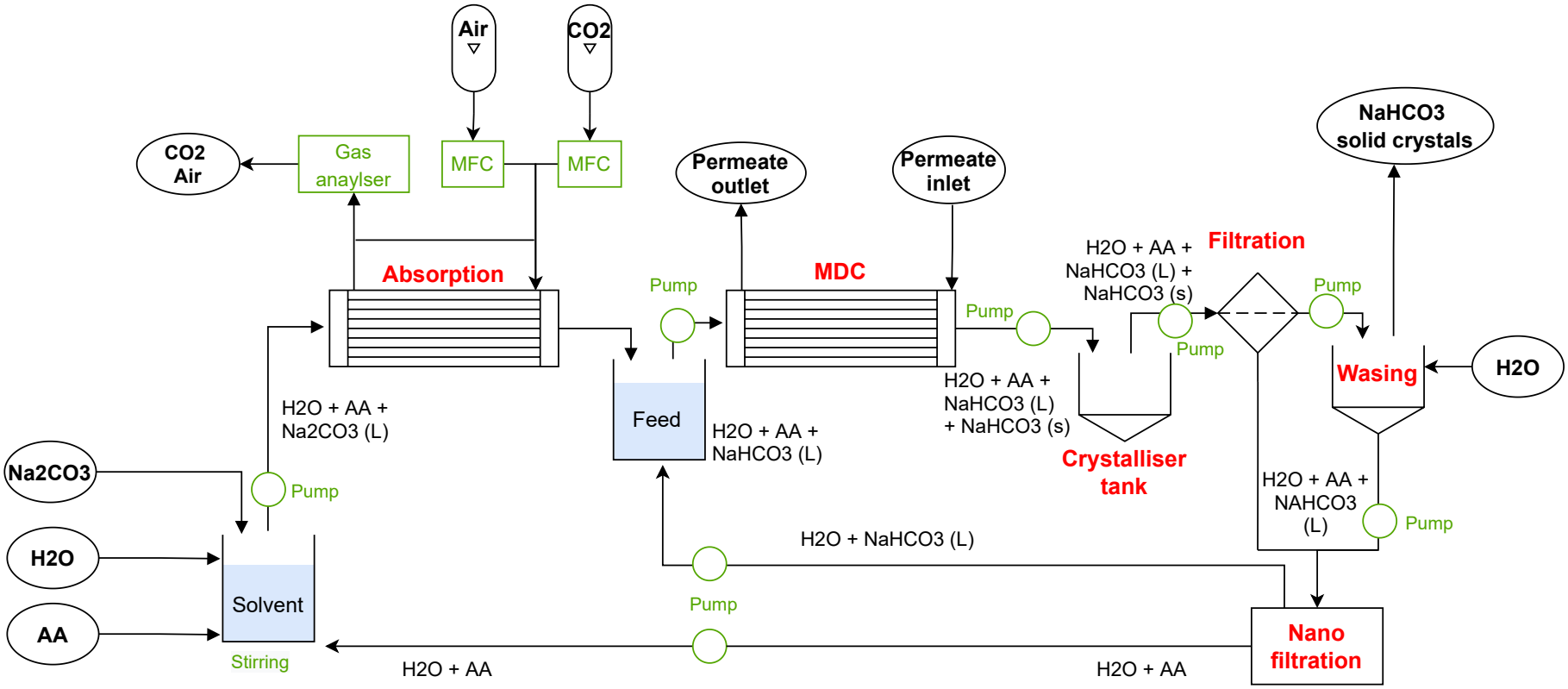

Figure 11 Complete flowsheet of the process. The composition of the streams is described, as well as the main electronic devices.

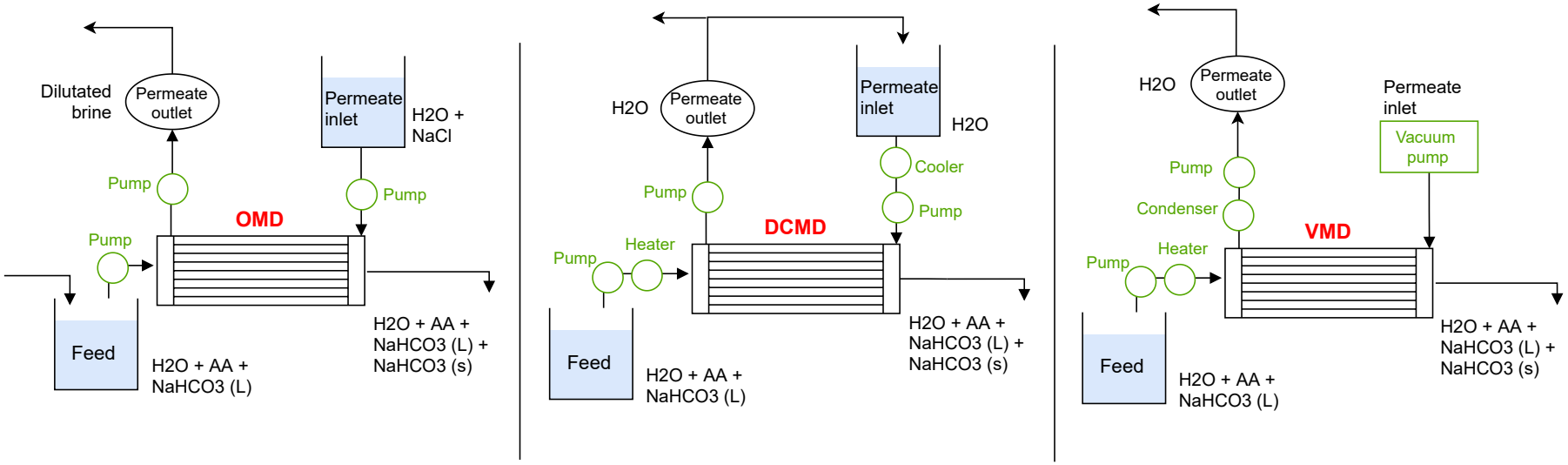

Figure 12 Detailed zoom on MDC configurations and their flowsheets. The solution at the permeate outlet either undergoes further post-treatment (for OMD, see Appendix B.6 for explanation on the brine post-treatment) or is recycled inside the process (for DCMD and VMD).

Chapter II

Literature review of LCA on CCU processes

In order to quantify the environmental impacts of the process described in the previous chapter, it is possible to carry out an life cycle assessment (LCA) within a structured methodology. As LCA is a standardised method. The ISO standards provide a guiding framework and divide an LCA method into different well-defined steps. In addition, several LCAs of carbon capture and utilisation (CCU) have already been carried out and are available in the scientific literature. It is then interesting to look at LCAs on CCU as a basis and potential key references for the case studied here.

This chapter first presents the general LCA methodology that will be followed to carry out the LCA on the CCU of interest. Then, the CCU concept is presented and a state of the art on previous LCAs of CCU is provided.

II.1 LCA methodology

In order to confirm the environmental benefit of recycling captured CO_2 into solid sodium bicarbonates ($NaHCO_3$), an environmental impact assessment must be developed by means of a LCA. LCA is a structured, comprehensive and standardised method for quantifying emissions and resource use taking into account the entire life cycle (cradle-to-gate/cradle) of the studied product and focusing on the relevant environmental impacts. [46]

As LCA is a standardised method, ISO standards 14040 and 14044 provide a framework for guidance, but leave some flexibility to respond to the wide variety of questions addressed in the LCA [46]. To be systematic, the ISO standards divide LCA into 4 steps which are defined iteratively in time and effort [47; 48] :

(1) **Goal and scope definition**: the first step aims at describing the purpose of the study and the conditions, assumptions and limitations of the system. The functional unit (FU) and system boundaries are also defined during this phase (Chapter III).

(2) **Life Cycle Inventory Analysis (LCI)**: it quantifies the mass and energy inputs and outputs of each process's stage within the system boundaries (Chapter IV).

(3) **Life Cycle Impact Assessment (LCIA)**: the elementary flows of inputs and outputs collected in the previous inventory stage are translated into environmental impacts related to human health, the natural environment and the depletion of resources [46]. Within the framework of this phase, LCA requires mandatory steps: selection of impact categories, indicators and methods, classification (into impact categories) and characterisation (use of characterisation factors to express different pollutants of the same impact categories as equivalent or the same pollutant) (Chapter V).

    Additional and optional steps can be allowed (in function of the LCA context): normalisation (to express the results in relation to a reference), grouping and weighting of impact categories (weighting factors, based on choices of values, but involving a certain subjectivity).

(4) **Interpretation**: in the last phase, significant results are identified. Uncertainties are studied, sensitivity studies can be examined. In addition, the limits of the LCA are highlighted, and recommendations are drawn (Chapter V).

II.2 Carbon capture and utilisation

Carbon capture utilisation (CCU) differs from carbon capture and storage (CCS) in the way that it aims to recycle the captured CO_2 as a raw material to produce valuable chemicals or by-products, instead of permanent geothermal sequestration. In other words, "*CCU retains the benefits of CCS but additionally yields value-added products*" [47].

CCS is composed of different processes separated in three main stages: the capture and compression of CO_2 through a separation process, followed by the transport of the captured CO_2 (most often in a pipe) and geological storage [6]. A very large number of studies are dedicated to address the unsolved challenges of storage, such as "*CO_2 leaks, destruction of the saline solution, ground disturbance and the triggering of an earthquake*" [49]. In addition to the storage' risk faced by CCS, this CCS process presents a high and costly energy expenditure where the capture stage represents 60 to 80% of the cost of the overall CCS chain [50]. Therefore, it is also of major importance for engineers to design the most efficient process. For instance, and in comparison with CCS, it is estimated that CCU reduces CO_2 emissions by consuming less energy and being more financially attractive. [49]

II.3 State of the art about LCA of CCU technologies

Several life cycle analyses have already been carried out on different carbon capture and storage/utilisation techniques (CCS/CCU) by studying and comparing LCAs in the case of different sources of CO_2 and different uses of the captured CO_2.

A report published in 2018 by the enterprise CE Delft [51] has studied 9 different routes of CCU and compared their environmental impacts based on "1 tonne of CO_2 captured in 2030 and subsequent utilisation" (FU). The 9 pathways combine LCA with three sources of CO_2 emissions (municipal waste incineration, blast furnaces, fossil oil refining from a hydrogen plant (including a membrane separation unit in the process)) with the use of CO_2 revalorisation in three different application sectors (horticulture, mineralisation, methanol production). The study showed that the use of CO_2 for methanol production avoids net CO_2 emissions when renewable energies are used for methanol and hydrogen production. On the contrary, if fossil-based electricity is used in the process, more CO_2 is emitted than captured (in total, more than 1500 [kg CO_2-eq/tonne captured] emitted). It should be noted, however, that the use of CO_2 in methanol production is not the only possible chemical industry (e.g. ethylene, dimethyl carbonate [52], polyols for the production of polyurethanes). Afterwards, the use of CO_2 for mineralisation gives the best emission reductions (about 1000 [kg CO_2-eq/tonne of CO_2 captured]), which lead to a balanced CO_2 emission-reduction. However, the 9 pathways have been compared to conventional CCS from the different 3 CO_2 sources. Their LCAs showed that CCS avoided more CO_2 emissions than CCU for horticulture and methanol production. [51]

Next, other studies have compared several LCAs. This is the case of an article by Cuéllar-France & Azapagic [53], published in 2015, that compares 11 studies on CCSs and 16 on CCUs. On one hand, CCS studies suggest that the global warming potential (GWP) of power plants could be reduced by 63-82%. Among the others, the lowest reductions are achieved by post-combustion capture in combined cycle gas turbine power plants, whilst the highest reductions are achieved by oxy-fuel combustion in pulverised coal and integrated gasification combined cycle. In the other hand, for CCU, CO_2 savings largely depends on utilisation option and emission reductions on the impact category studied. For CCU in the production of chemicals, in particular dimethylcarbonate, the use of CO_2 reduces GWP by 4.3 times and ozone depletion by 13 times compared to conventional dimethylcarbonate production.[53] Finally, comparing CCS and CCU, the study pointed out that, on average, the GWP of CCS is significantly lower than for CCU applications. But other environmental impacts of CCS are higher than those of the CCU. Exception should be noted for the production of dimethylcarbonate, with acidification being 320 times higher, ozone layer depletion and photochemical oxidants around 2.8 times higher and eutrophication 20% higher than average emissions of all CCS options.[53]

For the 6th European Conference on Renewable Energy Systems (2018), results of a LCA on CO_2 capture and revalorisation into sodium carbonates (Na_2CO_3) was presented. The LCA compares 2 absorption technologies using the same solvent

(NaOH): 1) packed columns and 2) membrane contactor. For both technologies, the environmental impacts increase with increasing solvent concentration. In addition, the study shows that the membrane contactor has higher environmental impacts due to its lower CO_2 absorption efficiency compared to conventional packed columns. Finally, the climate change gives the highest impact due to the need to produce NaOH.[54]

Least recently, in 2006, Khoo & Tan compared membrane separations with cyrogenic absorption, pressure swing absorption and monoethanolamine (MEA) for CCS. Two impacts were taken into account: GWP and air pollution (AP). The study suggested that absorption with MEA has the lowest GWP but the second highest AP (after cryogenic separation).[55]

A recent article of this year 2021 [56] showed through an in-depth review of the literature on CCU a growing in publications since 2012 on the subject. It demonstrated the increase in research and interest in this sector. Nonetheless, it identified different methodological choices in LCA on CCU, making the results non-comparable. The study highlighted the need to harmonise the LCA methodology on CCU studies since different LCAs on the same CCU technology often give divergent results. [56] Finally, even if researches on CCU increased the last decade, it should be noticed that it is difficult to compare LCAs because of different assumptions, system boundaries and life cycle stages (see Chapter III).[47]

Chapter III

Goal and scope

As the LCA process and methodology have been described in the previous chapters, the LCA can now be carried out on the process of interest.

In this chapter, following the first step of the LCA methodology, the goal and scope of the process are defined. Indeed, the first phase of a life cycle assessment (LCA) aims to describe the purpose for the study and the conditions, assumptions and limitations of the system. Therefore, the functional unit (FU) and the impact categories must be defined in accordance with the goal of the study, while the system boundaries are closely related to the definition of the scope. [47; 48; 57]

III.1 Functional unit and reference flow

The FU is essential because it serves as a basis for the uniform comparison of the different carbon capture and utilisation (CCU) pathways, for different amino acids (AAs) and different configurations of membrane distillation-crystallisation (MDC). Several FUs can be chosen, but the final choice depends on the objective of the LCA.

For example, if the purpose is to produce $NaHCO_3$ by an alternative process, it is more common to use the mass of $NaHCO_3$ produced in a given time periode as FU (e.g. 1 kg of $NaHCO_3$ produced), since the structure and chemical composition is identical to that of conventional $NaHCO_3$. However, this FU focusing on the product does not allow direct comparison of several LCAs on CCUs that would produce different products. [47]

Moreover, another possible function of the CCU is to capture CO_2. It is therefore logical to consider the absorbed CO_2 as a FU and hence, makes it possible to compare the CCS and the CCU. This has the advantage of being independent of the final product and the source of the CO_2. Therefore, the main function of the LCA turns out to be a technology for capturing CO_2 and not $NaHCO_3$ itself.

The CCU being a multifunctional system, it provides 1) the service of capturing CO_2, and 2) the use by-products. Therefore, the FU will define how to demonstrate the benefits of the technology [51]. In the present case, one of the objectives of the

LCA is to allow the future comparison of LCA results with other CCU (or CCS) technologies, such as the study of LCA on a CCU by mineralisation of CO_2 [47]. In the latter, 1 tonne of stored CO_2 was taken for the FU. For this reason, the FU in the present study is: 1 kg CO_2 absorbed per hour. Nevertheless, it should be reminded that the comparison is a delicate task because the assumptions and limitations of the system can differ according to the studies. Comparison of the present CCU with other CCUs could be the focus of further research.

Next, the reference flows quantify needs and key parameters to fulfil the function of defined FU [48]. They are given in Table 3.

Table 3 Functional unit and reference flows.

Function	CO_2 capture
Functional unit	1 $kg\,CO_2$ absorbed per hour
Reference flows	Absorption by membrane contactor into a solution solvent of 0.5M Na2CO3and 0.5M ARG or 0.3M SAR, further revalorised into NaHCO3 crystals. The solvent flowrate varies in function of the operating conditions. It ranges from 40 to 82 kg/h with ARG. And the membrane lifetime is fixed at 5 years. In the generic scenario, the flowrate are 82 kg/h with arginine and 689 kg/h with sarcosine.

III.2 System boundaries

The system boundaries in Figure 13 define the stages of the CCU's life cycle that are considered in the LCA to fill the previously defined FU. In general, the system boundaries should cover the entire life cycle (from cradle-to-grave): from raw material manufacture to the recycling stage. However, a cradle-to-gate approach is considered sufficient. On the one hand, given the LCA goal defined in the above section, $NaHCO_3$ is not the focus of CCU and can therefore be considered as a by-product or a waste with commercial added value. And on the other hand, when the use phase, technical performance and end-of-life treatment of the by-product are similar to the conventional counterparts as well as the associated environmental impacts, a cradle-to-gate approach is considered sufficient. This is the case of $NaHCO_3$ produced. This by-product obtained is assumed to be similar to conventional $NaHCO_3$, so that the two products cannot be differentiated. [57] Therefore, the use phase or end of life of $NaHCO_3$ crystals is not relevant for the defined objectives such that they are not included in the system boundaries.

Several raw materials are used as part of CCU process. Air and CO_2 represent together the **gaseous mixture** to be absorbed wherea the aqueous solution with Na_2CO_3 and AAs defines the **solvent mixture** supply. The latter is prepared in the right quantities and concentrations. Upstream, the production step of AAs is part of the LCA scope.

In addition, the **membrane manufacturing** is included inside the system boundaries. These polymeric hollow fibers constitute the membrane. They are prepared

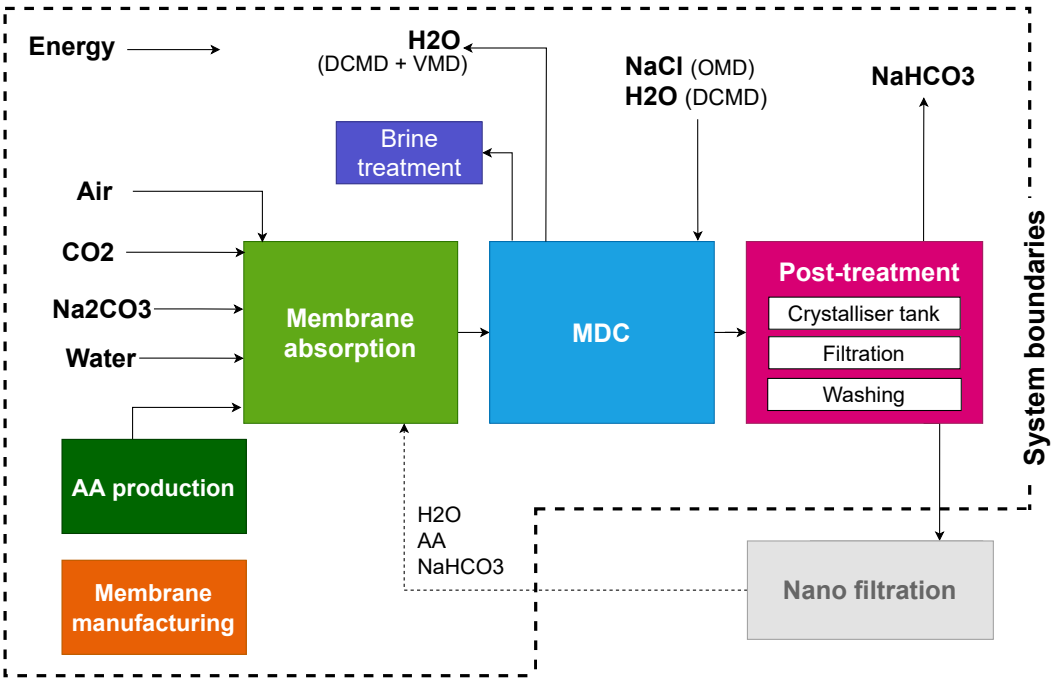

Figure 13 System boundaries of the generic process.

by means of a spinning process [58] and a solvent is also required. Indeed this stage's consideration is important since CCU is based on membrane technologies. This potential crucial differentiation from other CCUs should be environmentally quantified. In addition, the hollow fibers membrane manufacturing is *"far from sustainable and environmentally friendly"* [58]. For this other reason, the membrane manufacturing is modelled in SimaPro in the foreground database.
It should be noted that other equipment is needed to operate the process (pumps, stirring tank, heater, cooler, etc.) However, for these devices, only the energy consumption is taken into account and their manufacture is left out.

In the **membrane absorption's** stage, the energy consumption of stirring tank, pumps, mass flow controller (MFC) and a CO_2 gas analyser is taken into account. In addition, the capture stage includes materials of the membrane manufacturing for a specific membrane's size as well as its own lifetime.

In the next stage, **MDC** depends on membrane configurations types and the use of an additional solvent at the inlet of the permeate side, the temperature gradient or vacuum pump. Again, the membrane manufacturing and lifetime is taken into account. Different types of permeate are also required for each MDC configurations as well as energy inputs. To recall, there are 3 MDC processes studied in the present document: osmotic membrane distillation (OMD), direct contact membrane distillation (DCMD), vacuum membrane distillation (VMD).

As last stage, **post-treatment** of $NaHCO_3$ summarises the steps required to prepare the product for market. The crystallisation tank, filtration, and washing are taken into account and enable $NaHCO_3$ crystals recovery. [47; 57]

A **brine treatment** stage is also included within the system boundaries for saline water leaving OMD (more information about the type of brine treatment selected in Section IV.2.1).

Note that, as shown in the process flowsheet (Figure 11) and in the above Figure, the whole process includes a **nano-filtration** step. But, as defined by the system boundaries, this step is not considered in the LCA because it is not yet studied and optimised. However, the recycling of materials has significant environmental impacts. This is why **recycling of AAs**, from nano-filtration to absorption, is included in the scope of the study and reduces the real material need in AAs. Note that water and residual $NaHCO_3$ particles are also recycled within the process in order to minimise losses.

III.3 Impact categories selection

The environmental impacts of each LCA step can be quantified and presented in different forms or may be linked to different areas of emissions. Consequently, the sorting of environmental impacts into *impact categories* is necessary and even mandatory for the 3rd step of a LCA: the life cycle impact assessment (LCIA).

The main objective of CCU is to absorb 1 kg CO_2 while avoiding that the CCU technology emits more than it absorbs. Therefore, the selection of the climate change impact category (in kg CO_2-eq to air) is essential.

However, in order to have the most complete LCA analyse, other impact categories must be studied. For instance, water consumption (m^3 water-eq consumed) or materials or fossil resources (in kg CU-eq and kg-oil eq) are important aspects that should be mentioned. The full list of impact categories oriented problem is given in Appendix (Figure B.2).

Note that impact categories also depend on the magnitude of the impact. Therefore, at a worldwide scale, impact categories like climate change, ozone layer depletion or resources consumption (energy and materials) are considered. At continental scale, acidification or eutrophication are more relevant. Finally, regarding the regional scale (<100km), human toxicity, ecotoxicity are taken into account. [48]

Chapter IV

Life cycle inventory

The life cycle inventory (LCI) quantifies the mass and energy inputs of each stage within the system boundaries. Part of the data for LCIs is taken from the **Ecoinvent v.3** [59] database available in **SimaPro**. This database is considered as background data. In this database, the natural gas consumption, the production of the plant infrastructures, the consumption of substances for sub-operations are included. In other words, background data are more generic data for materials, transport, energy or waste treatment. In addition, different libraries are available in Ecoinvent. The choice is made to use the APOS library, which is further described in Appendix B.2.
Other required data for the LCA is found in the **scientific literature** or during **experiments** carried out in the laboratories of UCLouvain. This is more specific data needed to model the system and is called the foreground database. [47; 48; 59]

It is also important to note that the laboratory experiments were carried out at the laboratory scale and in batch mode. Therefore, in order to use the laboratory data in the LCA study, a transition to continuous mode and a scaling up to LCA-scale must be carried out during the LCI.

In order to clearly define the LCIs, this chapter presents each step of effective process inside the system boundaries (absorption, OMD, DCMD, VMD and post-treatment). They are analysed in detail to collect all necessary data. Data are collected with the consideration of a baseline case with specific assumptions. Each section (absorption, MDC configurations and post-processing) details the calculation steps, the assumptions made and presents the inventories in tables. In addition, a final table (Table 19) at the end of the chapter summarises all LCI inputs entered into SimaPro. Tables 20-23 outline technical data for calculations of the LCIs.

IV.1 Absorption

The overall mass transfer coefficient and therefore the corresponding CO_2 load in the solvent are 2 parameters fixed and known by experiments performed in

UCLouvain laboratories. These parameters and the functional unit (FU) (i.e. 1 kg of CO_2 absorbed per hour) lead to the determination of the amount of solvent mixture and the membrane surface area.

The generic and reference cases take the assumption of the **highest** K_{ov}, such that a fresh solvent is continuously running through the membrane. Two absorption scenarii are derived for the two amino acids (AAs) (arginine (ARG) and sarcosine (SAR)), and are labelled **absoA.s0** and **absoS.s0** respectively.

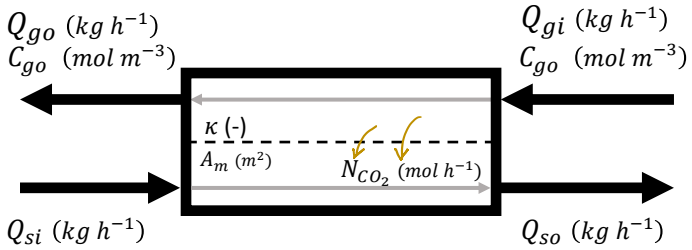

Figure 14 Absorption schema, symbols are summarised in the Glossary list and defined in the following sections.

IV.1.1 Solvent mixture

In this section, solvent composition is defined as well as the inventories of AAs production. Moreover the amount of solvent flowrate Q_s is calculated based on the CO_2 load in the solvent.

The solvent supply for absorption is an aqueous mixture of water (H_2O) with anhydrous sodium carbonate (0.5 mol/kg_{H2O} Na_2CO_3) and AAs. Two cases of absorption are studied with different AAs: 0.5 mol/kg_{H2O} of ARG and 0.3 mol/kg_{H2O} of SAR. The mass composition of the solvent required by the FU is shown in Table 4.

Regarding the **AA production**, since they are not provided by Ecoinvent, their production as part of the system boundaries was modelled in SimaPro as foreground database. The choice of the production model is explained in detail in Appendix B.4. Finally, the inputs required to produce 1 kg of ARG and SAR are indicated in Tables 5 and 6 respectively.

Moreover, the solvent is recycled thanks to a post-treatment followed by a nanofiltration step. However, a small fraction of AAs is lost during these steps such that AA losses in the generic case is about 1 %/h [60]. Indeed, the recovery χ from post-treatment and nanofiltration is worth 99%.

In addition, note that Na_2CO_3 in the background database of Ecoinvent exists as $Na_2CO_3 \cdot 7\,H_2O$, such that it is composed by 46%wt of Na_2CO_3. The amount of $Na_2CO_3 \cdot 7\,H_2O$ entered in SimaPro is therefore higher, but at the same time less pure water is also needed.

Finally, the solvent flowrate is calculated. During laboratories experiments, the

solvent was running under batch mode in a loop through the membrane. To transit to a continuous mode, the CO_2 load of the solvent (κ) is used as well as the natural logarithmic mean (ln) of K_{ov}. Indeed, the absorption performance varies along the membrane so that overall mass transfer coefficient K_{ov} is not constant. For this reason, the logarithmic mean of K_{ov} is considered. Furthermore, the associated CO_2 load in the solvent κ in [mol/kg] represents the cumulative amount of CO_2 that the solvent can absorb. These 2 experimental parameters are presented in Figure 15.

For the reference case, the **maximum** K_{ov} and its corresponding κ are considered. The values are presented in Table 20. With this reference scenario, one tries to operate absorption with the maximum absorption performance. Finally, the total inlet solvent flowrate Q_{si} (in [kg/h]) required to absorb 1 kg CO_2 per hour is obtained by:

$$Q_{si} = \frac{N_{CO2}}{\kappa} \tag{13}$$

where N_{CO2} refers to the amount of moles CO_2 absorbed per hour $[mol/h]$. It can be computed by the following equation and by remembering the FU:

$$N_{CO2} = \frac{1000}{44} = 22.73 \quad [mol/h]$$

As a result, the total composition and amount of the solvent mixture required by the FU are shown in Table 4 for absoA.s0 and absoS.s0 respectively. It should be noted that a difference must be made between the actual composition of the solvent mixture required by the process and the hypothetical inputs into the LCA model. Indeed, due to the recycling of AAs and different types of carbonates, the LCI in SimaPro does not represent the actual mass balance that takes place during gas absorption in the membrane. Therefore, Q_{si} does not represent the sum of all LCI entries in SimaPro but represents the total flowrate of the real and effective absorption process.

Table 4 LCI inputs for the production of solvent mixture. The generic scenario considers the maximum value for K_{ov}. The AA loss is 1 %/h. One column represents the composition of the solvent in the real effective absorption process. The second column is the case is dedicated to the LCA case.

Component	**Amount process**	**Amount LCA**	**Unit**
H_2O	71.44	66.8	kg/h
Na_2CO_3	3.78	-	kg/h
$Na_2CO_3 \cdot 7\,H_2O$	-	8.3	kg/h
ARG	6.22	0.062	kg/h
Q_{si} **absoA.s0**	81.5	81.5	kg/h
H_2O	638	596	kg/h
Na_2CO_3	33.75	-	kg/h
$Na_2CO_3 \cdot 7\,H_2O$	-	73.9	kg/h
SAR	17.22	0.172	kg/h
Q_{si} **absoS.s0**	689	689	kg/h

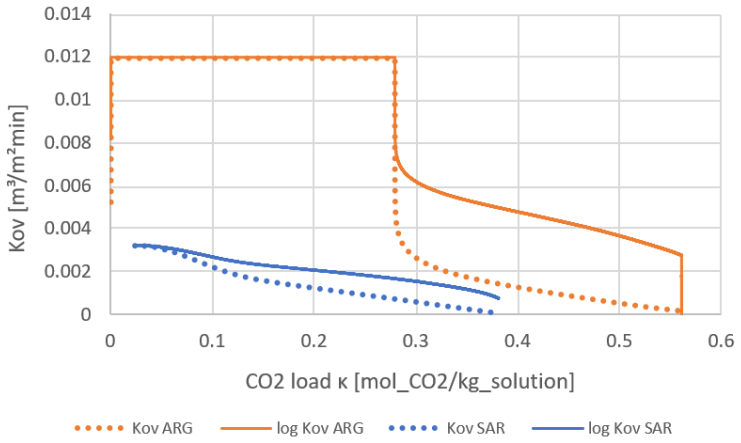

Figure 15 Experimental data of absorption, K_{ov} vs CO_2 load κ, obtained from UCLouvain experiments. The solid lines stand for the natural logarithmic mean of K_{ov} along the membrane contactor. The dotted lines are the values of K_{ov} at a given CO_2 load in the solvent and along the membrane.

Table 5 LCI inputs for the production of 1kg ARG by lysine.[61]

Component	Amount	Unit
Sugar	1	kg
Maize starch	0.5	kg
Wheat starch	0.5	kg
Liquid ammonia	0.3	kg
Energy		
Electricity mix	18	MJ
Natural gas	18	MJ

Table 6 LCI inputs for the production of 1kg SAR by methionine.[61]

Component	Amount	Unit
Propylene	0.43	kg
Hydrogene sulfide	0.27	kg
Methanol	0.39	kg
Hydrogen cyanide	0.21	kg
Energy		
Electricity mix	3.7	MJ
Natural gas	3.7	MJ

IV.1.2 Gaseous mixture

The objective here is to evaluate the LCI of the gaseous stream. Therefore, the composition of the gaseous mixture at the inlet in terms of CO_2 and air with respect to K_{ov} and the FU is computed. Furthermore, the concentrations of CO_2 at the inlet and outlet of the membrane are respectively noted C_{gi} and C_{go} are computed for further use (see later in the next Section IV.1.3).

For each given logarithmic mean K_{ov}, an overall CO_2 absorption efficiency ε along the membrane is given and presented in Figure 16. ε represents the percentage of CO_2 in the gas stream absorbed by the liquid solution and averaged along the membrane length. Moreover the molar composition ν of CO_2 in the gaseous inlet stream is fixed at 15%. With these operating conditions, the gaseous composition can be determined.

The generic case takes the maximum K_{ov} where the corresponding ε is close to 100% for ARG and SAR. Then the amount of moles of CO_2 and air entering the membrane is expressed as (in $[mol/h]$):

$$\begin{aligned} n_{gi,CO2} &= \frac{N_{CO2}}{\varepsilon} \\ n_{gi,air} &= \frac{n_{gi,CO2}}{\nu}(1-\nu) \\ n_{go,CO2} &= n_{gi,CO2}\,(1-\varepsilon) \end{aligned}$$

With this, the LCI of the total gaseous mixture required to absorb 1 kg of CO_2 per hour is given in Table 7, using the molar mass of CO_2 and air.

Then, the total gaseous volume at the inlet and outlet respectively noted V_{gi} and V_{go} ($[m^3/h]$) is computed :

$$\begin{aligned} V_{gi} &= (n_{gi,air} + n_{gi,CO2})\; V_m \\ V_{go} &= (n_{gi,air} + n_{gi,CO2}\,(1-\varepsilon))\; V_m \end{aligned}$$

where taking the V_m as the molar volume for the temperature $25°C$ and the pressure 1 atm:

$$V_m = \frac{V}{n} = \frac{R\,T}{P} = 0.0248 \quad [m^3/mol]$$

CO_2 concentrations are hence obtained (in $[mol/m^3]$):

$$\begin{aligned} C_{gi} &= \frac{n_{gi,CO2}}{V_{gi}} \\ C_{go} &= \frac{n_{go,CO2}}{V_{go}} \end{aligned}$$

The calculated data of the volumes and concentrations of the reference case is resumed in Table 20.

Table 7 LCI inputs in production of the gaseous feed for the reference case absoA.s0 (with ARG) and absoS.s0 (with SAR). The CO_2 molar composition is $\nu = 15\%$.

Component	**absoA.s0 Amount**	**absoS.s0 Amount**	**Unit**
CO_2	1000	1010	g
Air	3728	3766	g
Total	4728	4776	g

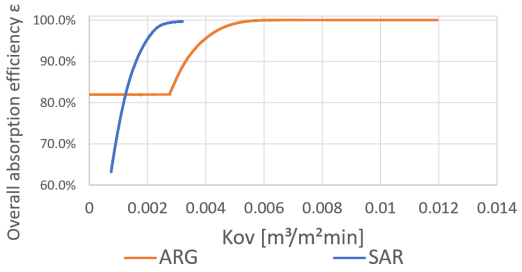

Figure 16 Absorption experimental data, K_{ov} vs the overall absorption efficiency ε.

IV.1.3 Membrane gas absorption

In this section, the rest of inventories for the absorption step are computed. Indeed, the membrane area is calculated and the materials and energy inputs required by the PP membrane manufacturing is derived. In addition, the energy consumption of secondary devices is considered.

The solvent and gaseous streams enter the membrane contactor in a counter-current mode (see Figure 14). But, to absorb the amount of CO_2 defined by FU, the membrane area $A_{m,a}$ in $[m^2]$ must be adjusted. To do so, the relation between $A_{m,a}$ and the transmembrane flux J_{abso} is expressed as follows:

$$A_{m,a} = \frac{N_{CO2}}{J_{abso} * 3600} \tag{14}$$

The flux J_{abso} is obtained as described in Section I.1.3 by the equation (2) via the driving force $\Delta\overline{C}_{fresh}$ and K_{ov}. As a reminder, $\Delta\overline{C}_{fresh}$ is obtained considering a fresh solvent. Indeed, the reference scenario of absorption considers the maximum value of K_{ov}. The latter is ensured at the beginning of the experiments when the solvent is still fresh. $\Delta\overline{C}_{fresh}$ is defined by the equation below. CO_2 concentrations C_{gi} and C_{go} in $[mol/m^3]$ respectively at the inlet and outlet of the membrane, are considered using the data defined in the above Section IV.1.2. Data is summarised in Table 20.

$$\Delta\overline{C}_{fresh} = \frac{C_{gi} + C_{go}}{2}$$

In addition, the membrane lifetime is considered to be worth 5 years [62]. Therefore, the actual surface area of the membrane as LCI is less than the calculated area $A_{m,a}$ which is divided by the total number of working hours of the membrane over its lifetime (5 years × 365 days × 24 hours). This final area input in the LCI is presented in Table 10.

Afterwards, the hollow fibers **membrane manufacturing** is modelled in SimaPro in the foreground data base. The production of polymeric membrane involves energy and solvents with important environmental impacts. In the present case of polypropylene (PP) membranes, a possible solvent for the spinning of the fibers is dimethylacetamide (DMAC) [63; 58]. The total inputs required for the production

of a polymeric membrane with a membrane area of 1000 m^2 are available in Table 8. The mass of polymer is adjusted to the studied case taking the PP density and with the membrane characteristics given in Table B.1 of Appendix B.3.

$$m_p = \rho_p \; A_{m,a}(r_o - r_i) = 900 * 1000 * (150 - 120) * 10^{-6} = 27 \quad [kg]$$

Table 8 LCI inputs of membrane manufacturing. Production of 1000 m^2 hollow fibers membrane [58].

Component	Amount	Unit
Tap water	3000	L
Polymer	27	kg
Solvent (DMAC)	320	kg
Nitrogen	0.561	L
Electricity	2832	kWh

In the absorption step, $CaCl_2$ granulars are also used on the equipment as water trapping. During the running of the process, water evaporates from the solvent and can affect the performance of the process. To avoid this, the membrane contactor is connected to a water trap filled with $CaCl_2$ granulars to absorb the excess vapour. After 4 to 5 experiments each of 8 hours and conducted in UCLouvain laboratories, for a membrane having an active surface area of 0.18 m^2, an average mass of 5.5 g $CaCl_2$ must be replaced in the water trap. Therefore, it is considered that 0.85 $g/m^2\,h$ of fresh $CaCl_2$ are necessary.

Finally, energy is required to move and to control the membrane gas absorption step. Two mass flow controllers (MFCs) are placed to control the gas flows and a gas analyser measures the CO_2 concentration. A stirring system also mixes the solvent solution which is moved with a pump. The total energy inputs are given in Table 9.

Note that concerning pumps, moving in and out the the solvent could concerns bigger amounts closer to industrial pumps. Consequently, pumping power E^p can be estimated based on a heuristic expression as follows [64]:

$$E^p = \frac{P\;Q}{\eta} \quad [W]$$

where P in [Pa] is the pressure (1 atm), Q is the flowrate in $[m^3/s]$ to be displaced and η is the pump efficiency (about 0.5-0.85) [64]. However, this expression gives a lower energy consumption for absoA.s0 and absoS.s0 than the pump's data sheet (80 W). The latter is considered as the wort case and taken into account for the following. As a result, it should be noted that this pump can move from 0.3 to 360 L/h, so that the application range is considered suitable for the studied cases [65].

At the end, material and energy inputs required for the membrane gas absorption step are summarised in Table 10. Note that Q_{so} represents the output solvent of membrane gas absorption step that absorbed 1 kg of CO_2.

Table 9 Devices and power required for absorption step.

Device	Amount	Unit
MFC [66]	16	W
Gas analyser [67; 68]	60	W
Pump [65]	80	W
Stirring [69; 70]	370	W

Table 10 LCI inputs and outputs of membrane absorption process for ARG and SAR (absoA.s0 and absoS.s0), during 1 hour and for the generic case with maximum K_{ov}. The membrane lifetime is 5 years [62].

Component	absoA.s0 Amount	absoS.s0 Amount	Unit
Inputs			
Solvent mixture Q_{si}	81.5	689	kg
Gas mixture	4728	4776	g
Membrane area $A_{m,a}$	2.4	8.8	cm^2
$CaCl_2$	8.86	33	g
Electricity	1896	1896	kJ
Output			
Solvent Q_{so}	82.5	690	kg

IV.2 Distillation-crystallisation

In this section, inventories of membrane distillation-crystallisation (MDC) are provided for each configuration (OMD, DCMD, VMD). The objective is to determine solution flowrates at the permeate inlet/outlet, energy inputs and the membrane area. These are obtained by determining the desired final $NaHCO_3$ crystals and using experimental data.

After absorption step, a liquid stream composed of water, sodium bicarbonate ($NaHCO_3$) and deactivated AAs leaves the membrane and is directly sent to the MDC step as feed. Therefore, the leaving solvent flowrate from absorption is the entering feed flowrate of MDC. It can be written as:

$$Q_{fi} = Q_{so}$$

The objective of MDC is to concentrate the feed solution into $NaHCO_3$ up to the desired level (C_{fo}). Indeed, during the running of MDC, water evaporated from feed solution such that the solution becomes more concentrated with $NaHCO_3$. For this purpose, the initial concentration of $NaHCO_3$ in the feed inlet C_{fi} $[mol/kg_{H2O}]$ needs to be determined. The latter depends on the CO_2 load κ and the solvent flowrate Q_{so} in the absorption stage. To facilitate calculations, the following reaction is considered as source of $NaHCO_3$ production in the solvent (see Appendix A.1.1 for the full reaction mechanism):

$$CO_2 + H_2O + Na_2CO_3 \rightleftharpoons 2\,NaHCO_3$$

Given that $N_{CO2} = 22.73$ mol/h of CO_2, the final concentration of solvent leaving the membrane and entering MDC is then expressed as follows:

$$C_{fi} = \frac{2 * N_{CO2}}{x_{H2O}\, Q_{so}} \tag{15}$$

where x_{H2O} is the mass fraction of water in the solvent stream, and is worth 88% and 93% for the ARG and SAR case respectively. For the reference scenario, only the MDC with former absoA.s0 as feed stream is considered, i.e. with ARG instead of SAR, since the SAR case follows the same logic. Hence, the concentration is worth $C_{fi} = 0.64\ mol/kg_{H2O}$. Further, the generic cases are noted as **omd.s0**, **dcmd.s0** and **vmd.s0** for OMD, DCMD and VMD respectively.

Note that in function of the CO_2 load κ in the solvent in the gas absorption, the solvent mixture may contain residual Na_2CO_3 components. However, these are not considered in MDC (e.g for the water activities calculations).

Regarding the final desired concentration of $NaHCO_3$ in the feed leaving the membrane (C_{fo}), the latter is determined thanks to the relation between the outlet temperature of the feed T_{fo} and $NaHCO_3$ saturation concentration on Figure 17.

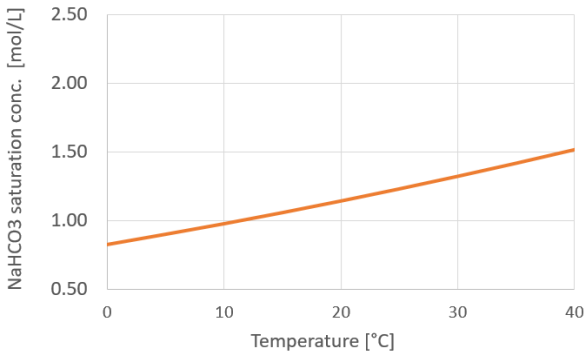

Figure 17 Saturation $NaHCO_3$ concentration as a function of temperature [71].

Then, knowing the feed flowrate Q_{fi} entering MDC, its initial concentration of $NaHCO_3$ (C_{fi}) and the final desired saturation concentration at the outlet feed (C_{fo}), the required amount of water to be evaporated to the permeate side can be calculated. The latter is noted N_{H2O} in $[kg_{H2O}/h]$:

$$N_{H2O} = x_{H2O}\, Q_{fi}\ (1 - \frac{C_{fi}}{C_{fo}}) \tag{16}$$

To evaporate N_{H2O}, the membrane area $A_{m,mdc}$ in $[m^2]$ must be adjusted. The relation between N_{H2O}, $A_{m,mdc}$ and the transmembrane flux J_{mdc} is expressed as:

$$A_{m,mdc} = \frac{N_{H2O}}{J_{mdc}\ \rho_{H2O} * 3600} \tag{17}$$

The transmembrane flux J_{mdc} is described in the Section I.2.3 and depends on the overall mass transfer coefficient K_{ov} and the driving force $\Delta\overline{P}$, whose expression

differs for each MDC configuration. Each $\Delta\overline{P}$ are given in Section I.2.2. In the following sections, a LCI is derived for each MDC configuration.

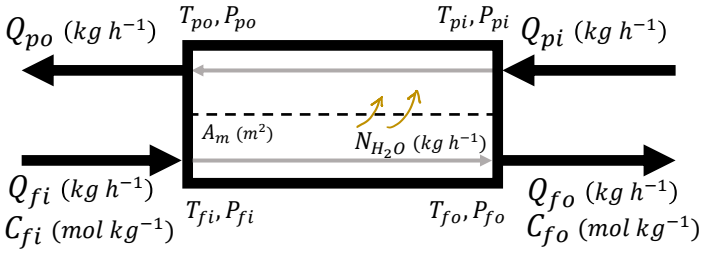

Figure 18 MDC schema, symbols are summarised in the Glossary list and defined in the following sections.

IV.2.1 Osmotic membrane distillation

Feed side

The feed Q_{fi} comes directly from the previous step, the membrane gas absorption absoA.s0 and is at room temperature (25 °C). As mentioned above, the stream is composed of $NaHCO_3$ and AAs (here ARG). For the generic case, the $NaHCO_3$ concentration at the feed inlet is $C_{fi} = 0.64\ mol/kg_{H2O}$, whilst the outlet concentration at room temperature (Figure 17) is fixed at 1.23 mol/kg_{H2O}. Given these concentrations, the amount of water evaporated from the feed side to the permeate side, N_{H2O}, is computed by the equation (16) and presented in Table 21.

Permeate side

The osmotic solution entering the permeate side is composed of a 300 g/kg_{H2O} NaCl solution and its material inputs for the LCA are presented in Table 11.

Table 11 LCI inputs in production of 1.3 kg of osmotic permeate OMD.

Component	Amount	Unit
H_2O	1	kg
NaCl	0.3	kg

The flowrate at the permeate inlet must also be scaled-up. In experiments, inlet flowrates of the feed and permeate are similar. Therefore:

$$Q_{pi} = Q_{fi}$$

which is worth 83 kg/h for omd.s0.

Membrane distillation-crystallisation

To reach the level of saturation, the transmembrane flux J_{omd} is expressed as given by the equation (12), depending on both the overall mass transfer coefficient K_{ov}

and the driving force $\Delta\overline{P}_{omd}$ and permits calculations of $A_{m,o}$ by the equation (17).

Concerning the overall mass transfer coefficient K_{ov}, this is obtained through laboratory experiments. Indeed, the K_{ov} with the presence of AAs and for the given C_{fi} are not yet experienced. However, it is known that in the case of OMD, the K_{ov} with 1 mol/kg_{H2O} $NaHCO_3$ and 0.5 mol/kg_{H2O} ARG is 86% about the one with only 1 mol/kg_{H2O} $NaHCO_3$. This ratio is used to obtain K_{ov} with other operating conditions. Hence, in the case of $C_{fi} = 0.64$ $mol/kgH2O$ and with 0.5 mol/kg_{H2O} ARG, the associated K_{ov} is worth:

$$K_{ov} = 0.86 * 6.06\,10^{-11} = 5.18\,10^{-11} \quad [m^3/m^2\,s\,Pa]$$

Regarding calculations of $\Delta\overline{P}_{omd}$ as expressed in equation (10), it is assumed that the temperature:

$$T = T_{pi} = T_{po} = T_{fi} = T_{fo} = 25 \quad [^\circ C]$$

such that from Antoine's equation (8):

$$p = p_{pi} = p_{po} = p_{fi} = p_{fo} = 3155 \quad [Pa]$$

Further, with both feed and permeate concentrations at the inlet and outlet known, the water activities of each components can be found in Appendix B.5.2. The water activities of each mixture is computed and presented in Table 21. Finally, by equations (10) and (12), the mean driving force $\Delta\overline{P}_{omd}$ and J_{omd} are obtained, and by equation (17) the total membrane area $A_{m,o}$ is computed. The values are presented in Table 21. In addition, the membrane lifetime must be taken into account (5 years [62]).

Subsequently, the manufacturing of the membrane is similar to that of the absorption, such that inputs for the production of an hollow fibers membrane in Table 8 are considered valid for membranes used in MDC.

Lastly, to complete the inputs required in OMD, the energy inputs are collected. 3 pumps are used to move the feed and permeate solution in and out the membrane, each having a power about 80 W [65].

At the end, total material and energy inputs required for OMD are summarised in Table 12.

Table 12 LCI inputs and outputs of OMD for ARG (omd.s0), during 1 hour. absoA.s0 is taken as the previous absorption step and $C_{fi} = 0.64$ mol/kg_{H2O}. The membrane lifetime is 5 years [62].

Component	**Amount**	**Unit**
Inputs		
Feed side Q_{fi}	83	kg
Permeate side Q_{pi}	83	kg
Membrane area	79	cm^2
Electricity	864	kJ
Output		
Feed side Q_{fo}	48	kg
Permeate side Q_{po}	116	kg

Brine treatment

A post-treatment is considered regarding the permeate leaving the membrane. The latter forms a diluted brine that should be treated before its discharge since it is a very saline solution. The amount of osmotic solution leaving OMD is given by $Q_{po} = (Q_{pi} + N_{H2O})$ in [kg/h] and is entered in SimaPro datasheet as *outputs to technosphere: discharge of water from oil extraction*. The choice of this treatment is extensively explained in Appendix B.6.

IV.2.2 Direct contact membrane distillation

Feed side

Like for osmotic membrane distillation (OMD), the feed Q_{fi} in a direct contact membrane distillation (DCMD) configuration comes directly from the membrane gas absorption (83 kg/h with absoA.s0). The feed is heated up to 40°C. However, the outlet temperature is lower and worth 19°C. The generic case also takes $C_{fi} = 0.64\ mol/kg_{H2O}$, and the final saturation concentration here is about C_{fo}=1.12 mol/kg_{H2O} (from Figure 17, taken for the outlet feed temperature at 19°C). N_{H2O} is also computed and given in Table 22.

Permeate side

The solution at the inlet permeate side of DCMD is composed of pure water entering the membrane in a counter current mode and at $T_{pi} = 5$°C. Its leaving temperature is fixed by experiments in laboratories and is worth $T_{po} = 27$°C.

The required amount of flowrate Q_{pi} in $[kg/h]$ is estimated thanks to an energy balance : the permeate side is heated up by the energy released by the feed side. Indeed, the feed has a temperature gradient known from experiments, such that:

$$Q_{fi}\ c_p\ (T_{fi} - T_{fo}) = Q_{pi}\ c_p\ (T_{pi} - T_{po})$$

with c_p being the heat specific capacity of water about 4.18 $kJ/kg\,K$. The inlet flowrate at the permeate side is expressed as:

$$Q_{pi} = Q_{fi}\,\frac{(T_{fi} - T_{fo})}{(T_{pi} - T_{po})} \tag{18}$$

Finally, note that the outgoing permeate is pure water, so it can partially be recycled directly to the inlet of permeate side (see Figure 12 of the process flowsheet).

Membrane distillation-crystallisation

Again, like in OMD, the objective is to compute the required membrane area $A_{m,d}$ to reach the evaporation performance and thus, the desired saturation concentration. $A_{m,d}$ is expressed in function of N_{H2O} and J_{dcmd} by the equation (17). The transmembrane flux J_{dcmd} is given by the equation (7) depending on K_{ov} and the driving force $\Delta\overline{P}_{dcmd}$.

Concerning K_{ov}, this is obtained through laboratories experiments. Indeed, for DCMD and VMD, the K_{ov} with the presence of AAs are not yet experienced.

However, it is known that in the case of OMD, the K_{ov} with 1 $mol/kgH2O$ $NaHCO_3$ and 0.5 $mol/kgH2O$ ARG is 86% about the one with 1 $mol/kgH2O$ $NaHCO_3$. This ratio is used to obtain K_{ov} of the other MDC configurations. As a result and when C_{fi} is about 0.64 mol/kg_{H2O}:

$$K_{ov} = 0.86 * 2.3\,10^{-11} = 1.97\,10^{-11} \qquad [m^3/m^2\,s\,Pa]$$

Regarding calculations of $\Delta\overline{P}_{dcmd}$ by the equation (7), different temperatures are summarised in Table 22 as well as their corresponding vapour pressures obtained via Antoine's equation (8). Further, with feed concentrations given in Table 22, water activities of each components are found in Appendix B.5.2 and the water activities of the mixtures is obtained. Finally, by equations (7) and (12), the driving force $\Delta\overline{P}_{dcmd}$ and J_{dcmd} are obtained as well as the total membrane area $A_{m,d}$ by the equation (17). The values are presented in Table 22. Note that the membrane lifetime is considered about 5 years.

Lastly, to complete the LCI of DCMD, the energy inputs are collected. 3 pumps are used to move the feed and permeate in and out the membrane contactor, as well as heating and cooling systems of the feed and permeate inlet streams. Regarding the pumps, they have a power of about 80W, which is found in the pump data sheet [65]. Moreover, the streams must be heated (E^h_{fi}) or cooled (E^{cooler}_{pi}). Concerning the permeate, the outlet permeate can be partially recycled and sent to the inlet permeate side. Therefore the cooling of solution at the inlet of permeate side depends on its outlet temperature. The required energies are expressed as follows:

$$E^h_{fi} = Q_{fi}\,c_p\,(T_{fi} - 25) \qquad [kJ]$$
$$E^{cooler}_{pi} = Q_{pi}\,c_p\,(T_{po} - T_{pi}) \qquad [kJ]$$

The total energy inputs for each equipment are available in Table 13.

Table 13 Devices and energy required for DCMD.

Components	**Amount**	**Unit**
Pump (3×)	864	kJ
E^h_{fi}	4473	kJ
E^{cooler}_{pi}	7299	kJ

At the end, the total material and energy inputs required for the DCMD step are summarised in Table 14.

Table 14 LCI inputs and outputs of DCMD for ARG (dcmd.s0.1), during 1 hour. absoA.s0 is taken as the previous absorption step and $C_{fi} = 0.64\ mol/kg_{H2O}$. The membrane lifetime is 5 years [62].

Component	Amount	Unit
Inputs		
Feed side Q_{fi}	83	kg
Permeate side Q_{pi}	78	kg
Membrane area	37	cm^2
Electricity	12	MJ
Output		
Feed side Q_{fo}	51	kg
Permeate side Q_{po}	109	kg

IV.2.3 Vacuum membrane distillation

Feed side

The feed coming from absorption, as for DCMD is heated up to 40°C. Contrary to DCMD, the outlet temperature of the feed is worth 37.5°C and the corresponding saturated concentration is $C_{fo} = 1.47\,mol/kg_{H2O}$ (see Figure 17) where $C_{fi} = 0.64\ mol/kg_{H2O}$. Hence, N_{H2O} can be calculated and is given in Table 23.

Permeate side

The permeate side of the membrane is connected to a vacuum pump, so that the vacuum pressure p_o on the permeate side is set to 30 mbar as established in laboratory experiments, and $Q_{pi} = 0$. At the outlet of the permeate side, the flowrate Q_{po} in $[kg/h]$ represents the total evaporated water though the pores:

$$Q_{po} = N_{H2O}$$

Membrane distillation-crystallisation

Here again, the approach is to compute $A_{m,v}$ required to evaporate the amount N_{H2O} of water. $A_{m,v}$ is expressed in function of N_{H2O} and the transmembrane flux J_{vmd} by the equation (17) which itself depends on K_{ov} and the driving force $\Delta\overline{P}_{vmd}$.

On the one hand, the K_{ov} is given by experiments and via the ratio obtained in OMD:

$$K_{ov} = 0.86 * 4.8\,10^{-11} = 4.10\,10^{-11} \quad [m^3/m^2\,s\,Pa]$$

On the other hand, $\Delta\overline{P}_{vmd}$ is calculated by the equation (11) and based on the vapour pressures p and water activities presented in Table 23. Indeed, in the same way as DCMD, water activities of the feed can be found in Appendix B.5.2, based on feed concentrations presented in Table 23. By equations (11) and (12) the $\Delta\overline{P}_{vmd}$ and J_{vmd} are obtained as well as the total membrane area by the equation (17). These values are shown in Table 23.

Then, the energy inventories are evaluated. Two pumps, each having a power about 80W [65], are used to move the feed inlet stream and evacuate the condensed permeate stream. Regarding the energy used to operate the vacuum pump, a heuristic expression could be used to express its energy consumption as a function of N_{H2O}. However, this method is more suitable for commercial scales. For this reason, the data sheet from the scaled up vacuum pump is used which consumes 40W [72]. A heater also raises the temperature of the feed inlet, while a condensing device condenses the evaporated water into the permeate:

$$\begin{aligned} E_{fi}^{h} &= Q_{fi}\, c_p (T_{pi} - 25) \quad [kJ] \\ E_{po}^{cond} &= \Delta H_{vap}\, Q_{po} \qquad\quad [kJ] \end{aligned} \tag{19}$$

where ΔH_{vap} is the heat of vaporisation about 2257 kJ/kg [73]. The details of each energy input per device are shown in Table 15.

Table 15 Devices and energy required for vacuum membrane distillation (VMD).

Components	**Amount**	**Unit**
Pump (2×)	576	kJ
E^{vacuum}	144	kJ
E_{fi}^{h}	4473	kJ
E_{pi}^{cond}	92 550	kJ

Finally, the total material and energy inputs required for VMD are summarised below in Table 16.

Table 16 LCI inputs and outputs of VMD (Vmd.s0), during 1 hour. AbsoA.s0 is taken as previous absorption step operating with ARG and at maximum K_{ov}. Initial $NaHCO_3$ concentration is $C_{fi} = 0.64\ mol/kg_{H2O}$. The membrane lifetime is 5 years [62].

Component	**Amount**	**Unit**
Inputs		
Feed side Q_{fi}	83	kg
Membrane area	18	cm^2
Electricity	98	MJ
Output		
Feed side Q_{fo}	42	kg
Permeate side Q_{po}	41	kg

IV.3 Post-treatment

The post-treatment inventories mainly include energy inputs and the production of marketable $NaHCO_3$ crystals. It is assumed that crystals recovery is about 99%. This generic situation is noted **post.s0**. However, it should be noted that post-processing experiences at UCLouvain laboratories have not yet been thoroughly investigated and optimised to maximise the recovery of crystals of $NaHCO_3$.

Regarding energy, the post-treatment involves a crystallisation tank, followed by a scroll decanter [74; 75] for the filtration and washing stages [76] (see Figure 11

of the process flowsheet). Pumps, each with a power of about 80 W [65], are also required to move the streams. The energy of the crystalliser tank is taken into account by its agitation system [77]. Note that in industrial applications, filtration and washing are usually carried out in one step by one piece of equipment [76]. The total energy inputs are described in Table 17 and their energy consumption is found as an indication of the total energy supply.

Afterwards, the washing step includes water as a washing agent which is decided to be worth 10 kg of H_2O.

Finally, the percentage of crystals recovery even if not yet optimised, is assumed to be $\chi = 99\%$. Where $NaHCO_3$ crystals not yet recovered in the first process cycle are recycled and returned to the absorption's or MDC's stage. This product is assessed in the inventories (as *avoided products*). Also, the mass of $NaHCO_3$ produced (M_{NaHCO3} in [kg/h]) depends on the solvent flowrate in the absorption step Q_s, the initial concentration C_{fi} considered in the MDC and the percentage of recovery χ of the post-treatment step:

$$M_{post,NaHCO3} = \chi \, C_{fi} \, x_{H2O} \, Q_{so} \, M_{m,NaHCO3} \tag{20}$$

where $M_{m,NaHCO3}$ is the molar mass of $NaHCO_3$ and is 0.084 kg/mol. Moreover, a recycled stream mainly composed of residual H_2O, AAs and some $NaHCO_3$ particles is recovered at the end of the post-treatment. This could be reused for the absorption step. The AAs recycling has already been considered in the membrane absorption stage, whilst the amount of water recovery M_{H2O} in [kg/h] is taken into account as an *avoided product* in the post-treatment stage for more clarity of the results (i.e. the amount of recycled H_2O depends on the MDC configurations).

$$M_{post,H2O} = (x_{H2O} \, Q_{so} - N_{H2O,mdc} + Q_{washing}) * \chi$$

The total inputs to the post-treatment step are shown in Table 18.

Table 17 Devices and energy required for post-treatment.

Components	**Amount**	**Unit**
Pump (4 ×) [65]	1152	kJ
Crystalliser tank [69; 70]	432	kJ
Scroll decanter [75]	8640	kJ
Washing [76]	8640	kJ

Table 18 LCI inputs and outputs of post-treatment post.s0, during 1 hour. The recovery is $\chi = 99\%$, and the amount of water recovered $M_{post,H2O}$ is based on DCMD data (dcmd.s0).

Component	**Amount**	**Unit**
Inputs		
Water $Q_{washing}$	10	kg
Electricity	18.86	MJ
Output		
$NaHCO_3$, $M_{post,NaHCO3}$	3.82	kg
Recycled water, $M_{post,H2O}$	50	kg

Table 19 LCI total inputs of all processes. The membrane lifetime is 5 years, and the recovery rate $\chi = 99\%$.

Process stage		Name	Amount	Unit
Gaseous mixture absoA.s0	Material inputs	CO2	1000	g
		Air	3728	g
	Outputs	Gaseous mixture	4728	g
Gaseous mixture absoS.s0	Material inputs	CO2	1010	g
		Air	3766	g
	Outputs	Gaseous mixture	4776	g
ARG production	Materials inputs	Sugar	1	kg
		Maize starch	1	kg
		Liquid ammonia	0.3	kg
	Energy inputs	Electricity high voltage, production mix	18	MJ
		Electricity high voltage, natural gas	18	MJ
	Outputs	Arginine	1	kg
SAR production	Materials inputs	Propylene	0.43	kg
		Hydrogen sulfide	0.27	kg
		Hydrogen cyanide	0.21	kg
		Methanol	0.39	kg
	Energy inputs	Electricity high voltage, production mix	3.7	MJ
		Electricity high voltage, natural gas	3.7	MJ
	Outputs	Sarcosine	1	kg
Solvent mixture with ARG	Materials inputs	Deionised water	66.8	kg
		Na_2CO_3, soda ash light heptahydrate	8.3	kg
		Arginine	0.062	kg
	Outputs	Solvent mixture	81.5	kg
Solvent mixture with SAR	Materials inputs	Deionised water	638	kg
		Na_2CO_3, soda ash light heptahydrate	73.6	kg
		Sarcosine	0.172	kg
	Outputs	Solvent mixture	689	kg
Membrane manufacturing	Materials inputs	Tap water, conventional	3000	kg
		Polypropylene, granulate	27	kg
		Dimethylacetamide (DMAC)	320	kg
		Nitrogen liquid	0.451	kg
	Energy inputs	Electricity medium voltage	2832	kWh
	Outputs	Membrane area	1000	m2
Membrane absorption (**absoA.s0** for 1 hr)	Materials inputs	Solvent mixture with ARG	82	kg
		Gaseous mixture	4728	kg
		Membrane area $A_{m,a}$	2.4	cm^2
		CaCl2	8.86	g
	Energy inputs	Electricity medium voltage, production mix	1896	kJ
	Outputs	absoA.s0	83	kg
Membrane absorption (**absoS.s0** for 1 hr)	Materials inputs	Solvent mixture with SAR	689	kg
		Gaseous mixture	4776	kg
		Membrane area $A_{m,a}$	8.8	cm^2
		CaCl2	33	g
	Energy inputs	Electricity medium voltage, production mix	1896	kJ
	Outputs	absoS.s0	690	kg
Osmotic permeate	Materials inputs	Deionised water	1	kg
		Sodium chloride powder	300	g
	Outputs	Osmotic permeate	1.3	kg
OMD (**omd.s0** for 1 hr from absoA.s0)	Materials inputs	absoA.s0	83	kg
		Osmotic permeate	83	kg
		Membrane area $A_{m,o}$	79	cm^2
	Energy inputs	Electricity medium voltage, production mix	864	kJ
	Outputs	Feed out OMD	48	kg
		Brine waste, Water discharge from petroleum extraction	116	kg
DCMD (**dcmd.s0** for 1 hr from absoA.s0)	Materials inputs	absoA.s0	83	kg
		Deionised water, permeate	78	kg
		Membrane area $A_{m,d}$	37	cm^2
	Energy inputs	Electricity medium voltage, production mix	12	MJ
	Outputs	Feed out DCMD	51	kg
		Deionised water, *avoided product*	109	kg
VMD (**vmd.s0** for 1 hr from absoA.s0)	Materials inputs	absoA.s0	83	kg
		Membrane area $A_{m,v}$	18	cm^2
	Energy inputs	Electricity medium voltage, production mix	98	MJ
	Outputs	Feed out VMD	42	L
		Deionised water, *avoided product*	41	kg
Post-treatment post.s0	Materials inputs	Deionised water	10	kg
	Energy inputs	Electricity medium voltage, production mix	18.86	MJ
	Outputs	NaHCO3 crystals	3.82	kg
		Deionised water, *avoided product*	50	kg

Table 20 Data for the calculation of the LCI of membrane gas absorption. The reference and generic case is considered, taking the maximum K_{ov} and is noted absoA.s0 (with ARG) and absoS.s0 (with SAR). The molar CO_2 composition in the gaseous stream at the inlet is $\nu = 15\%$. The solvent is composed with 0.5 mol/kg_{H2O} Na_2CO_3 and 0.5 mol/kg_{H2O} ARG or 0.3 mol/kg_{H2O} SAR.

Component		**absoA.s0 Amount**	**absoS.s0 Amount**	**Unit**
Overall mass transfer coef.	K_{ov}	$1.2\,10^{-2}$	$3.2\ 10^{-3}$	$m^3/m^2 min$
Solvent CO_2 load	κ	0.280	0.033	mol/kg
Solvent flowrate	Q_s	81	689	kg/h
Overall abso. efficiency	ε	~ 100	99	%
CO_2 absorption	N_{CO2}	22.73	22.73	mol/h
Moles gas mixture	$n_{gi,CO2}$	22.73	22.96	mol/h
	$n_{go,CO2}$	~ 0	0.23	mol/h
	$n_{gi,air}$	128.79	130.09	mol/h
Volume gas mixture	V_{gi}	3.76	3.80	m^3/h
	V_{go}	3.19	3.23	m^3/h
Conc. CO_2 gas mixture	C_{gi}	6.05	6.05	mol/m^3
	C_{gi}	~ 0	0.071	mol/m^3
Driving force	ΔC_{fresh}	3.02	3.06	mol/m^3
Transmembrane flux	J_{abso}	$6.05\,10^{-4}$	$1.63\,10^{-4}$	$mol/m^2\,s$
Membrane area	$A_{m,a}$	10.44	39	m^2

Table 21 Data for the calculation of the LCI of OMD noted omd.s0. The feed comes from the previous reference absorption case, absoA.s0, taking the maximum K_{ov}. The final feed concentration C_{fo} corresponds to the saturation concentration.

Component		**omd.s0 Amount**	**Unit**
Inlet flowrate feed side	Q_{fi}	82	kg/h
Inlet flowrate permeate side	Q_{pi}	82	kg/h
$NaHCO_3$ feed side concentration	C_{fi}	0.64	mol/kg_{H2O}
	C_{fo}	1.23	mol/kg_{H2O}
ARG feed side concentration	$C_{arg,i}$	0.5	mol/kg_{H2O}
	$C_{arg,o}$	0.96	mol/kg_{H2O}
NaCl permeate side concentration	C_{pi}	5.17	mol/kg_{H2O}
	C_{po}	3.45	mol/kg_{H2O}
Water activities feed side	$a_{w,fi}$	0.973	-
	$a_{w,fo}$	0.953	-
Water activities permeate side	$a_{w,pi}$	0.742	-
	$a_{w,po}$	0.848	-
Temperature	T	25	$°C$
Vapour pressure	p	3155	Pa
H_2O evaporation	N_{H2O}	34	kg_{H2O}/h
Overall mass transfer coef	K_{ov}	$5.18\,10^{-11}$	$m^3/m^2\,s\,Pa$
Driving force	ΔP_{omd}	524	Pa
Transmembrane flux	J_{omd}	$2.72\,10^{-8}$	$m^3/m^2\,s$
Membrane area	$A_{m,o}$	352	m^2

Table 22 Data for the calculation of the LCI of DCMD noted dcmd.s0. The feed comes from the previous reference absorption case, absoA.s0, taking the maximum K_{ov}. The final concentration C_{fo} corresponds to the saturation concentration.

Component		**dcmd.s0 Amount**	**Unit**
Inlet flowrate feed side	Q_{fi}	83	kg/h
Inlet flowrate permeate side	Q_{pi}	71	kg/h
$NaHCO_3$ feed side concentration	C_{fi}	0.64	mol/kg_{H2O}
	C_{fo}	1.12	mol/kg_{H2O}
ARG feed side concentration	$C_{arg,i}$	0.5	mol/kg_{H2O}
	$C_{arg,o}$	0.88	mol/kg_{H2O}
Water activities feed side	$a_{w,fi}$	0.973	-
	$a_{w,fo}$	0.940	-
Temperature feed side	T_{fi}	40	$°C$
	T_{fo}	19	$°C$
Temperature permeate side	T_{pi}	5	$°C$
	T_{po}	27	$°C$
Vapour pressure feed side	p_{fi}	7300	Pa
	p_{fo}	2152	Pa
Vapour pressure permeate side	p_{pi}	843	Pa
	p_{po}	3510	Pa
H_2O evaporation	N_{H2O}	31	kg_{H2O}/h
Overall mass transfer coef	K_{ov}	$2.22\,10^{-11}$	$m^3/m^2\,s\,Pa$
Driving force	$\Delta\overline{P}_{dcmd}$	2400	Pa
Transmembrane flux	J_{omd}	$5.31\,10^{-8}$	$m^3/m^2\,s$
Membrane area	$A_{m,d}$	162	m^2

Table 23 Data for the calculation of the LCI of VMD noted vmd.s0. The feed comes from the previous reference absorption case, absoA.s0, taking the maximum K_{ov}. The final concentration C_{fo} corresponds to the saturation concentration.

Component		**vmd.s0 Amount**	**Unit**
Inlet flowrate feed side	Q_{fi}	83	kg/h
$NaHCO_3$ feed side concentration	C_{fi}	0.64	mol/kg_{H2O}
	C_{fo}	1.47	mol/kg_{H2O}
ARG feed side concentration	$C_{arg,i}$	0.5	mol/kg_{H2O}
	$C_{arg,o}$	1.18	mol/kg_{H2O}
Water activities feed side	$a_{w,fi}$	0.973	-
	$a_{w,fo}$	0.951	-
Temperature feed side	T_{fi}	40	$°C$
	T_{fo}	37.5	$°C$
Temperature permeate side	T_{po}	37.5	$°C$
Vapour pressure feed side	p_{fi}	7300	Pa
	p_{fo}	6377	Pa
Permeate side vacuum pressure	p_p	30	mbar
H_2O evaporation	N_{H2O}	41	kg_{H2O}/h
Overall mass transfer coef	K_{ov}	$4.10\,10^{-11}$	$m^3/m^2\,s\,Pa$
Driving force	$\Delta\overline{P}_{dcmd}$	3586	Pa
Transmembrane flux	J_{omd}	$1.47\,10^{-7}$	$m^3/m^2\,s$
Membrane area	$A_{m,v}$	77	m^2

Chapter V

Impact assessment and interpretation

In this chapter, the 3rd and 4th steps of the LCA methodology are applied to the process studied: i) the life cycle impact assessments (LCIAs) are provided and ii) interpretations of these results are made. This is made possible using the **SimpaPro** software. This chapter presents the LCIA results and discussions where assumptions are varied to optimise the whole carbon capture and utilisation (CCU) process from an environmental point of view.

The 3rd phase of an LCA is the **LCIA**. It translates the elementary flows of inputs and outputs collected in the previous inventory stage into environmental impacts related to human health, the natural environment and the depletion of resources [46].

Within the framework of the LCIA, mandatory steps are required: **classification** and **characterisation**, where a method is selected which is designed to carry out LCAs. The one used for the present LCA is **Recipe 2016 (H) at midpoint** [78; 48], so that the impact categories and environmental impacts are examined in accordance with the previously defined goal and scope described in Section III of Chapter III. More information on the method selection is described in Appendix C.1.1.

Classification consists in the selection of a method consistent with the goal and scope of the LCA. Characterisation uses characterisation factors to express different pollutants of the same impact categories as equivalent or the same pollutant. These characterisation factors can be derived in 2 mainstreams : at midpoint or endpoint. [78; 48]

Additional and optional steps are allowed in the LCIA: normalisation (to express the results in relation to a reference), grouping and weighting of impact categories (weighting factors, based on choices of values, but involving a certain subjectivity). These 2 last steps are not included in the Recipe midpoint method and are not shown in this document. [47; 48]

The last phase of the LCA methodology is **interpretation**, comparable to a discus-

sion of the previous life cycle results. Here, significant results and key parameters are identified. A sensitivity analysis based on the choice of the LCA method can be performed. This analysis is outlined in Appendix C.2.1. Interpretation is also used to check whether the conclusions are well drawn. To do this, uncertainty analyses are carried out concerning either uncertainties in the data (i.e. the maximum or minimum initial concentration of $NaHCO_3$) or variations in the models (such as energy source or desalination plants for OMD). [59]
As recommended by Pré Sustainability [59], an additional sensitivity analysis on assumptions can be performed. Assumptions on the operating conditions are changed and the LCA is recalculated. For this purpose, the use of parameters in SimaPro throughout the LCA is of great help. [59]

In this chapter, global LCIAs of the generic LCIs is firstly presented in order to have an overview on the trend of the whole LCA. Next, the 2nd Section provides a focus on each step of the process where LCIAs and interpretation are carried out. At the same time, the main influencing factors are highlighted and several potential optimisation routes specific to each process' step are proposed in order to reduce environmental impacts. Afterwards, all steps are resumed with their specific optimisation routes. Subsequently in the 3rd Section, some general assumptions are changed on the whole process to further reduce environmental emissions. Once, the LCA (with specific and general optimisations) is finally optimised, each step is summarised.

In addition and based in the references cases, a sensitivity analysis of the choice of the LCA method is also provided in Appendix C.2.1 with, among others, a focus on the global warming indicator.
Note that for better readability on the LCIA graphs, the names of the impact categories are displayed with abbreviations defined in Table 24.
Finally, note that, taking into account the defined FU, the whole process would be interesting regarding carbon footprint, if the total emissions in [$kgCO_2$-eq] of the full LCA (absorption + MDC + post-processing) are lower than 1 $kgCO_2$-eq. However, other environmental concerns are highlighted in conjunction with global warming.

Table 24 Impact categories abbreviations

Abbreviation	**Impact category**	**Abbreviation**	**Impact category**
GW	Global warming	TEco	Terrestrial ecotoxicity
O3Depl	Stratospheric ozone depletion	FEco	Freshwater ecotoxicity
IR	Ionizing radiation	MEco	Marine ecotoxicity
O3F-HH	Ozone formation, Human health	HTCarc	Human carcinogenic toxicity
finePM	Fine particulate matter formation	HTnCarc	Human non-carcinogenic toxicity
O3F-TE	Ozone formation, Terrestrial ecosystems	Land use	Land use
TAcid	Terrestrial acidification	MRS	Mineral resource scarcity
FEutro	Freshwater eutrophication	FRS	Fossil resource scarcity
MEutro	Marine eutrophication	H2OCons	Water consumption

V.1 Overview of the generic LCI

In this section, the environmental impacts of the generic life cycle inventories studied in Chapter IV are assessed using Recipe 2016 from a hierarchical (H) and midpoint perspective. Figures 19 to 21 present a breakdown of the results in all impact categories considering generic absorption, the 3 different configurations of membrane distillation-crystallisation (MDC) and the post-treatment. The characterisation and normalisation steps are indicated. LCIA results by Recipe (H) endpoint are shown in Appendix C.2.2. Note that each step of the generic scenarii is redefined in Table 25.

Table 25 Abbreviations of generic LCIs with the operating conditions considered.

absoA.s0	Absorption considering ARG and the maximum K_{ov}.
absoS.s0	Absorption considering SAR and the maximum K_{ov}.
omd.s0	OMD treating the previous absoA.s0.
dcmd.s0	DCMD treating the previous absoA.s0.
vmd.s0	VMD treating the previous absoA.s0.
Post.s0	Post-treatment considering a recovery $\chi = 99\%$.

Particular attention is paid to the global warming of each step in Figure 19. It can be seen that the recovery of $NaHCO_3$ crystals has a truly reducing effect on carbon footprint (with *avoided product* approach). However, the full process from absorption to post-treatment would emit more CO_2 than it absorbs it. Indeed, starting with absorption, for 1 $kgCO_2$ absorbed, 3.39 $kgCO_2$-eq are emitted. The latter accumulated with MDC, makes the net carbon balance positive. For example, the absorption followed by DCMD emits in total 3.39 + 3.36 $kgCO_2$-eq. However, note that the whole process by DCMD (i.e. absoA.s0 followed by dcmd.s0 and post.s0) has a net carbon balance about 1.81 $kgCO_2$-eq. This represents until now, the best scenario, even if it does not yet lead the CCU to a net negative carbon balance (i.e <1 $kgCO_2$-eq).

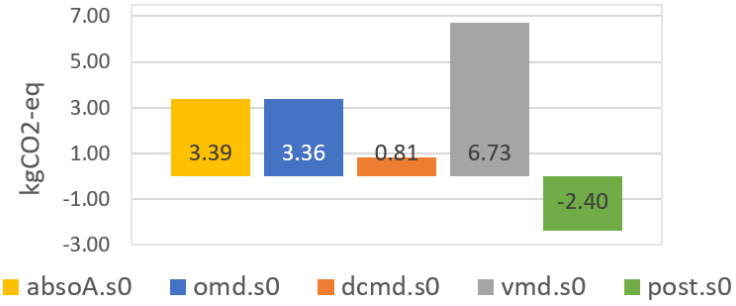

Figure 19 LCIA of the generic steps, global warming - characterisation. The 5 steps refer to reference cases. AbsoA.s0 is absorption considering ARG and the maximum K_{ov}. Omd.s0, dcmd.s0 and vmd.s0 are for OMD, DCMD and VMD treating the former absoA.s0. Post.s0 is post-treatment with a recovery $\chi = 99\%$.

As mentioned earlier, a combination of several emissions categories provides a more complete life cycle analysis. This is why the other impact categories of the Recipe method are presented in Figures 20 and 21.

In Figure 20 and with regard to the characterisation results, it can be seen that in general, omd.s0 is the worst process step in many impact categories (8). Nevertheless, vmd.s0 also scores in some categories (6) whilst post.s0 has the best positive impact in other categories (3). This confirms the importance of selecting several impact categories in a LCA study. Indeed, on the one hand, if only global warming is considered, it could be concluded that the selection of VMD as a step in the MDC should be excluded. On the other hand, if several impact categories are considered, the choice of OMD would be excluded. Note that Figure C.23 in Appendix compares LCIAs of OMD, DCMD and VMD processes together.

Afterwards, impact categories are normalised in Figure 21. Although this step is not mandatory in the LCA methodology. Normalisation of results can be used to simplify the interpretation of results. It extends an impact category to show its relative high or low value in relation to a baseline. This additional step in the LCA methodology also solves the problem of incompatible units [59]. LCA normalisation translates scores for every impact categories to a reference situation. Recipe 2016 considers the year 2000 as reference year and 2 geographic level: European and global level. [79]
The Recipe 2016 normalisation factors were used for Figure 21 and reveal that marine ecotoxicity (MEco) has the highest impact, followed by freshwater ecotoxicity (FEco), mainly for the OMD. Indeed, MEco with regard to OMD is impacted by the discharge of saline water in the seawater (by 41%) and by the use of NaCl (by 59%). For FEco, NaCl in the osmotic solution is responsible for almost 100% in this category. Therefore, the use of NaCl and discharge to the seawater generate this difference between OMD and other MDC configurations.
In addition, the presence of Na_2CO_3 particles in the absorption solvent has a global high impact on MEco and FEco too.
Note that NaCl in OMD and Na_2CO_3 in absoA.s0 also causes the high impact in human toxicity carcinogenity (HTCarc) accounted by the chemical factory construction in Ecoinvent database.

A first conclusion would therefore suggest that in the generic case, absoA.s0 as a common step with respect to any MDC configurations, should be strongly optimised. DCMD has the best environmental results in the most impact categories compared to OMD and VMD. However, to conclude that DCMD is environmentally better than other MDC, DCMD should have the lowest emissions in *every* impact categories. Lastly, even if a focus is given on carbon footprint, when normalised, LCIA results show that ecotoxicity (marine and fresh) and carcinogenicity have relatively way higher environmental impacts compared to global warming and other categories.

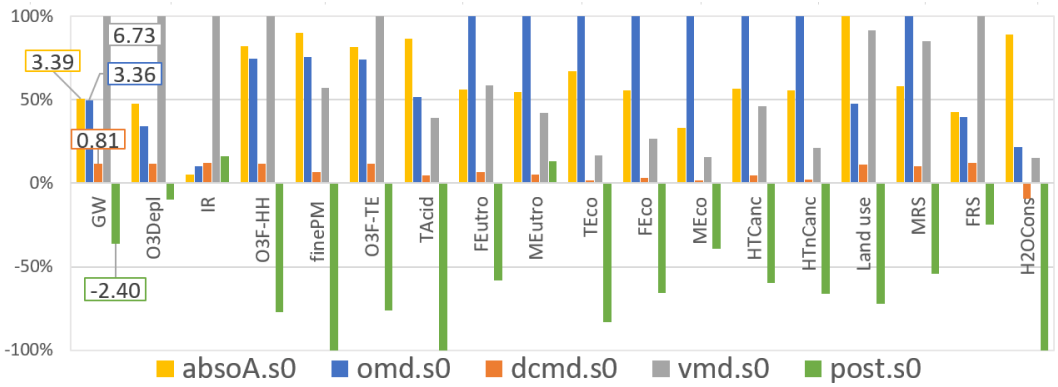

Figure 20 LCIA of the generic LCA for each step - characterisation. The 5 steps refer to reference cases. AbsoA.s0 is absorption considering ARG and the maximum K_{ov}. Omd.s0, dcmd.s0 and vmd.s0 are for OMD, DCMD and VMD treating the former absoA.s0. Post.s0 is post-treatment with a recovery $\chi = 99\%$. Abbreviations on the x-axis refer to Table 24.

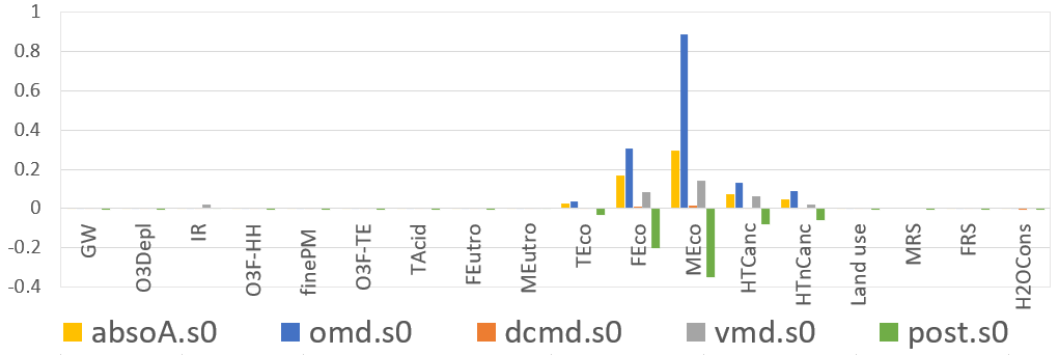

Figure 21 LCIA of generic LCA per steps - normalisation. The 5 steps refer to reference cases. AbsoA.s0 is absorption considering ARG and the maximum K_{ov}. Omd.s0, dcmd.s0 and vmd.s0 are for OMD, DCMD and VMD treating the former absoA.s0. Post.s0 is post-treatment with a recovery $\chi = 99\%$. Abbreviations on the x-axis refer to Table 24.

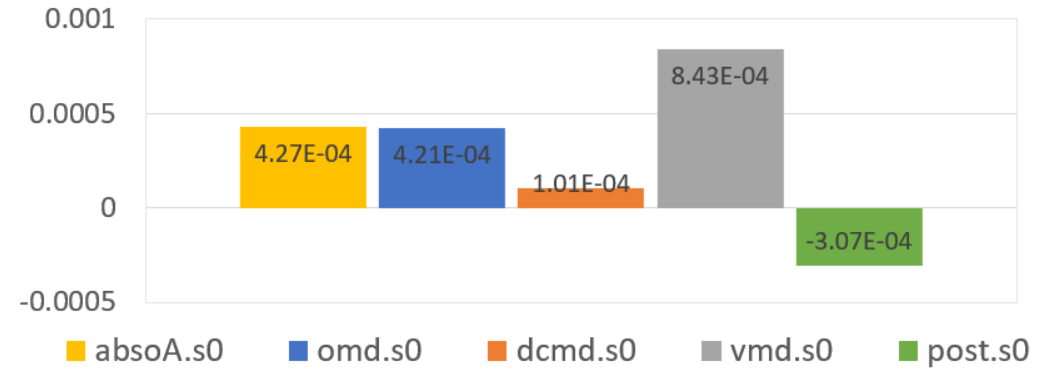

Figure 22 LCIA of generic LCA per steps - zoom on normalisation of global warming. The 5 steps refer to reference cases. AbsoA.s0 is absorption considering ARG and the maximum K_{ov}. Omd.s0, dcmd.s0 and vmd.s0 are for OMD, DCMD and VMD treating the former absoA.s0. Post.s0 is post-treatment with a recovery $\chi = 99\%$.

V.2 Analysis of each LCA step

Starting from the baseline scenarios, environmental impacts of each step are studied. At the same time, different optimisation paths specific to each process's step are proposed. This allows later for a comparison of the optimised OMD, DCMD and VMD in order to determine the technology with the least environmental impacts. In addition, this section is concluded with a summary of the LCA on CCU including all possible optimisation pathways per step. As such, an overall comparison highlights the main environmental issues of the CCU.

V.2.1 Membrane gas absorption

The first step of the process being CO_2 absorption, it is one of the key points for the whole LCA on a CCU technology. It this therefore of key importance to obtain the most environmentally friendly membrane absorption process regarding simultaneously global warming and other emissions categories.

Firstly, the generic LCI on absoA.s0 (i.e. with ARG and maximum K_{ov}) is analysed. The environmental impacts are presented based on characterisation factors and showing the most important input factors. Points of attention are highlighted in order to optimise the process step, with particular attention to solvent mixture. Optimisation of absorption is then provided based on the solvent load. Finally, absorption with ARG and SAR is compared with respect to the generic and most optimised cases.

V.2.1.1 Reference case absoA.s0 analysis

Here, absoA.s0 is analysed in order to highlight important spots in membrane gas absorption. This is intended to establish potential further optimisations of the process's stage.

First of all and with regard to the reference case of absoA.s0 with ARG and the maximum K_{ov}, Figure 23 shows that in terms of global warming, gas absorption by membrane is mainly impacted by the solvent mixture inputs (Q_{si}=81 kg). It represents 96% of the total emissions (or 3.25 kgCO_2-eq). The impacts due to the production of the membrane are almost negligible, as it was assumed in the LCI chapter that membranes have a lifetime of 5 years. In other impact categories, the solvent also seems to be the determining factor. An exception is ionising radiation (IR). As will be explained later, these emissions are mainly due to nuclear power generation.

Afterwards, the environmental impacts of the solvent mixture are studied in Figure 24. The use of Na_2CO_3 as a promoter is found to be the main contributor in almost all impact categories. For the LCI, Na_2CO_3 is taken in SimaPro from the Ecoinvent background database as soda ash produced by the Solvay process. The Ecoinvent *Unit* database allows to analyse the network and the different actors behind the production of Na_2CO_3. For example, in the global warming category, the components of Na_2CO_3 have a significant participation due by 61% to the production of energy and heat by the coal-fired furnaces, 21% to the use of NaCl

and to 18% to the construction of the chemical plant (Figure C.32).
Nevertheless, it appears from Figure 24 that, with respect to marine eutrophication (MEutro), the most contributing factor is ARG and not Na_2CO_3. From the network produced by SimaPro in this impact category (Figure C.34), the use of maize starch for the production of ARG is responsible for 50% of these emissions in [kg N-eq]. Indeed, the production of maize starch requires maize grains and green manure. The latter contains nitrogen-fixing agent. The excess of nitrogen can be washed from farm field during rain days or snow melts and ends up in oceans causing marine eutrophication [80].
Ionising radiation (IR) is nonetheless proportionally more impacted by electricity than in other categories. Electricity represents a Belgian electricity mix partially composed of nuclear generation. In the mix, this nuclear power is greatly responsible for IR emission (see SimaPro network in Figure C.43).
Stratospheric ozone depletion (O3Depl) is relatively more influenced by ARG than in other categories like IR and MEutro. This is due to the use of sugar beet starch and maize requiring green manure. The latter participates in the increase of N_2O contributes to the destruction of the stratospheric ozone [81].

With these LCIA results, it can be estimated that a significant way to decrease the impacts generated by absorption would be to reduce the amount of Na_2CO_3 in the solvent mixture. However, the concentration being fixed (0.5M), the solvent flowrate Q_{si} should thus be the parameter to decrease. This optimisation is presented in the following sections.

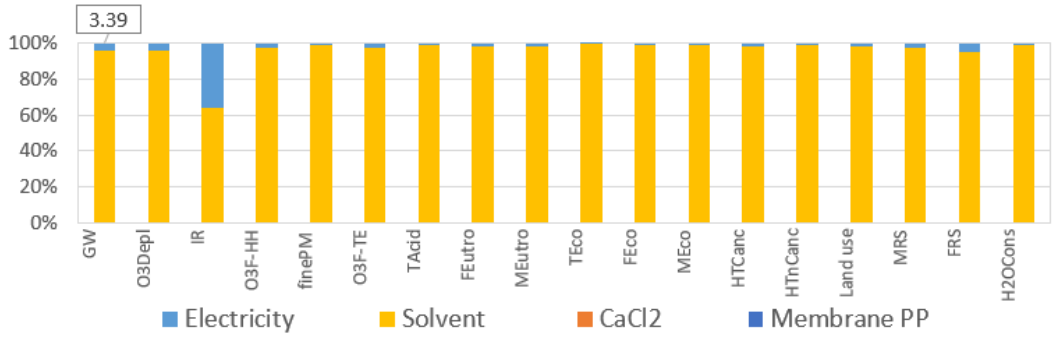

Figure 23 LCIA of absoA.s0, standing for absorption with ARG and maximum K_{ov}. The data label on the bar chart represents the total global warming emissions in [$kgCO_2$-eq]. Abbreviations on the x-axis refer to Table 24.

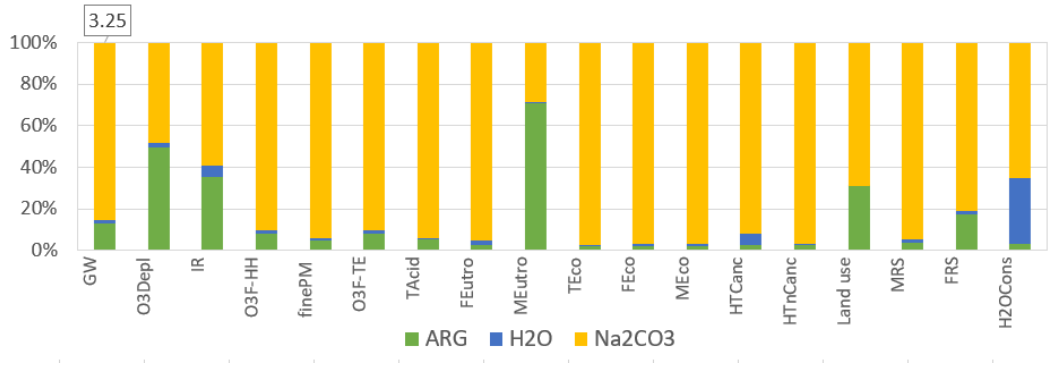

Figure 24 LCIA of solvent mixture for absoA.s0, standing for absorption with ARG and maximum K_{ov}. The amount of solvent mixture is worth 81 kg (see LCI Table 4). The data label on the bar chart represents the total global warming emissions in [kgCO_2-eq]. Abbreviations on the x-axis refer to Table 24.

V.2.1.2 Saturation of the solvent

In order to reduce the amount of solvent mixture entering the membrane gas absorption step, and given equation (13), CO_2 load κ in [mol/kg] should be maximised. This would also lead to an absorption saturation of the solvent. This section presents the LCI followed by the LCIA of an absorption scenario promoted by ARG with the maximum κ. This scenario is noted **absoA.kMax**. In addition, absorption with fresh solvent (i.e. the generic case with a maximum K_{ov}) is compared to absorption with saturated solvent.

As a reminder, κ (in $[mol_{CO2}/kg_{solution}]$) represents the cumulative amount of CO_2 absorbed and loaded into the solvent solution. In other words, κ indicates the saturation level of the solvent to absorb CO_2.
The generic cases initially considered maximising the absorption performance by taking operating conditions with the highest K_{ov} (in $[m^3/m^2min]$). A fresh solvent was therefore always running through the membrane contactor keeping the absorption performance at the most. Being always fresh, the solvent could not reach saturation before leaving the contactor. However, it emerged in the previous section that the solvent flowrate is a key parameter for environmental concerns. In order to reduce the flowrate, this section suggests running the absorption at high κ (i.e until saturation). In fact, to technically reach a high κ (i.e saturation), the residence time of the solvent inside the membrane must be as high as possible. This simultaneously results in a decrease of absorption performance due to a lower K_{ov}. The relationship between κ and K_{ov} is illustrated in Figure 15.
From a physical point of view, when κ increases, more AAs are deactivated in the solvent. In addition, sodium salts of AAs are formed in the solution. These salts increase the viscosity of the solvent, which in turn increases the resistance to mass transfer. Therefore, as a solvent becomes more saturated and κ increases, the K_{ov} decreases. [21]

Nevertheless, when the solvent is used until saturation, chemical absorption becomes almost non-existing and physical absorption takes over. In the generic case with maximum K_{ov}, it has been considered that the solvent is far from saturation since it

is continuously fresh. Hence, in calculation of $\Delta\overline{C}_{fresh}$ by the equation (3), the CO_2 concentration in the solvent (C_s) was assumed negligible. But when the solvent is saturated, physical absorption should be included in the calculations. And C_{so} becomes non-negligible. Therefore the driving force $\Delta\overline{C}_{saturation}$ is calculated via equation (4). For more information, the driving force calculation was more fully described in Section I.1.3. Note than only 2 extreme scenarii are considered (fresh and saturated solvent), since the in-between solution is not known with competition between chemical and physical absorption. For this reason, no in-between value of κ are taken into account.

Consequently, absorption with ARG is first optimised by performing the LCI for maximum κ (see Table 26). Then, the LCAs is run on SimaPro and the LCIA is presented in Figure 25.

In Table 26, one observed that for a high κ, the amount of required solvent mixture decreases whilst the incoming gaseous mixture increases. Indeed, for the maximum κ, the overall absorption efficiency ε decreases. Hence, to keep the FU's goal (absorb 1 kg of CO_2 per hour), more CO_2 must be introduced at the inlet of the membrane contactor. Moreover, as the molar concentration of CO_2 in the fresh gas mixture is kept constant (ν=15%), the inputs of CO_2 and air are adapted to ε.
According to Figures 15 and 16, when maximising the load of CO_2, K_{ov} decreases as well as the overall absorption efficiency ε. Indeed, if the solvent is used up to its maximum cumulative CO_2 load, absorption will start in the membrane with abundant fresh solvent and with an initial high K_{ov} and ε. However, the more the solvent absorbs CO_2, the more saturated the solvent and therefore the less efficient the overall gas absorption along the membrane. Note that, as shown in Figure 15, an average K_{ov} is calculated along the membrane. Since K_{ov} varies along the contactor, so that is it high at the beginning and lower at the end, an average value is calculated between these 2 extremes. These averaged values were taken into account in Table 26.

Additionally, based on Table 26, membrane area $A_{m,a}$ shows a increasing trend with high κ. As a matter of fact, $A_{m,a}$ is calculated via equation (14) which depends on the transmembrane flux J_{abso}. The latter is computed via K_{ov} and the driving force $\Delta C_{saturation}$ (equation (4)). And both decrease with a higher κ, leading to an increase of A_m.

Afterwards, Figure 25 shows the LCIA for these 2 different κ. The general trend in all categories is the same: all environmental impacts are positively impacted by the augmentation of κ and the reduction of solvent mixture, and thus by the use of Na_2CO_3. Note that the IR category (ionising radiation) decreases less than the others. IR is mainly influenced by the production of electricity. For absoA.s0, 67% of the IR impacts are due to the production of the solvent mixture, and the remaining 33% due to the electricity needed to operate the membrane gas absorption. Then, for the absoA.kMax, IR is caused by 51% from the solvent and 49% from the electricity of the absorption LCI. As the electricity input to the LCI is considered constant (1896 kJ, see Table 26), the reduction of IR emissions is slightly different than of other categories.
As a matter of fact, the electricity source selected in Ecoinvent is an Belgian

electricity mixed composed of different generation technologies: hard coal, nuclear energy, natural gas, heat and power co-generation, importation and treatment of the wasted gas from blast furnace (see Figure C.43 and C.42). And IR is causes by electricity generation from nuclear power (see Figure C.43) where uranium milling and mining, electricity generation from power reactor and fuel reprocessing contributes to radiation exposures [82].

In summary, the primary interest in absorption was the maximisation of absorption performance by a high K_{ov}. However, from an environmental point of view, the CO_2 load in the solvent turns out to be the key point. Indeed, to reduce emissions, the solvent must be used up to saturation. This leads to a high CO_2 load κ associated to a lower K_{ov}.
A link can be established with the results of the LCA study of CCU based on membrane absorption promoted by NaOH for CO_2 revalorisation. [54]. The study concluded that minimising the amount of NaOH in the solvent was the key point for reducing environmental impacts. To do this, the concentration could be reduced in the case of the article. But in our case studied, the concentration of Na_2CO_3 in the solvent is fixed at 0.5M. Therefore, in the same logic of minimising the amount of solvent, the flow rate of the solvent must be reduced here.

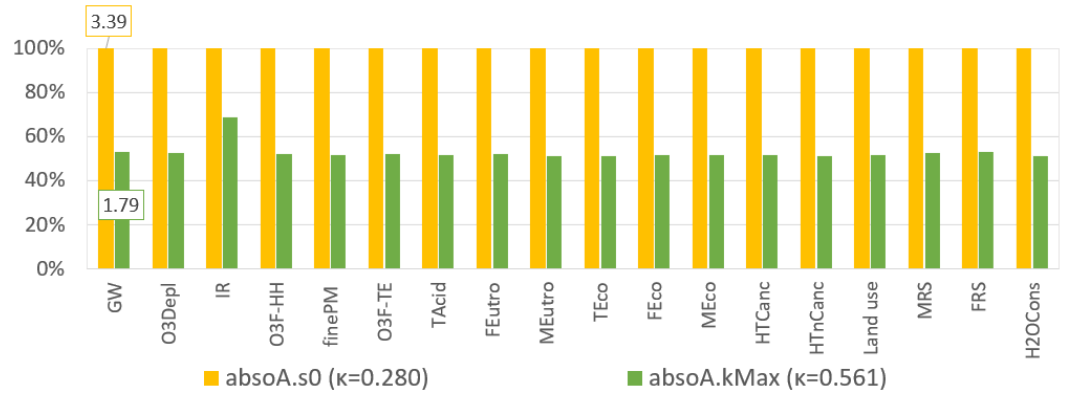

Figure 25 LCIA of absorption with ARG and fresh solvent or saturation. AbsoA.s0 stands for absorption with ARG and maximum K_{ov} where $\kappa = 0.280$ [mol/kg] (fresh solvent). AbsoA.kMax stands for optimised absorption with ARG and maximum CO_2 load $\kappa = 0.561$ [mol/kg] (saturation). Abbreviations on the x-axis refer to Table 24.

Table 26 Characterisation data for calculation of the LCIA and LCI inputs for absorption with ARG or SAR and with solvent saturation. Membrane lifetime is 5 years.

Characterisation data for calculation					
Component	**absoA.s0 fresh**	**absoA.kMax saturation**	**absoS.s0 fresh**	**absoS.kMax saturation**	**Unit**
CO_2 load κ	0.280	0.561	0.033	0.412	mol/kg
Overall mass transf. coef. K_{ov}	1.20E-02	2.75E-03	3.20E-03	7.53E-04	$m^3/m^2\,s$
Driving force $\Delta\overline{P}$	3.02	2.87	3.06	2.87	$m^3/m^2\,s$
Overall abso. efficiency ε	∼100	81.8	99	63	%
LCI					
Inputs					
Solvent mixture Q_{si}	82	41	689	55	kg
Gas mixture	4728	5780	4776	7505	g
Membrane area $A_{m,a}$	2.4	11	8.8	40	cm^2
$CaCl_2$	8.9	41	33	149	g
Electricity	1896	1896	1896	1896	kJ
Output					
Solvent Q_{so}	83	42	690	56	kg

V.2.1.3 Comparison of absorption with ARG and SAR

Since it has been proven in the previous sections that the amount of Na_2CO_3 is the main problem of absorption, it can easily be deducted that for the generic case absoS.s0, where the maximum value of K_{ov} is considered to lead to a solvent flow of 699 kg (and 74 kg of Na_2CO_3), absoS.s0 will definitely not be a feasible and applicable case from an environmental and operational point of view. Indeed, by using nearly 700 kg of solvent for the absorption of 1 kg of CO_2, the environmental effects are devastating compared to absoA.s0 (Figure 26). However, this section presents a comparison between ARG and SAR regarding the generic cases and the most optimised scenarii regarding κ.

Figure 26 presents among other things, a comparison of the generic LCIs for absorption with ARG (absoA.s0) and SAR (SAR.max), and optimised cases where κ was maximised for both AA scenarii (absoA.kMax and absoS.kMax). As a result, the preferred situation in almost all environmental categories was observed for absoA.kMax where the minimum solvent flowrate Q_{si} is obtained (Table 26). Nevertheless, absoS.kMax shows lower emissions in marine eutrophication (MEutro). In addition, the gap between optimised absoA.kMax and absoS.kMax is less significant than between absoA.s0 and absoS.s0, such that absoS.kMax could eventually be intended.

Regarding global warming of the best scenario absoA.kMax, for 1 kg CO_2 absorbed, the net emissions balance would be worth 0.79 kgCO_2-eq. Therefore, the isolated absorption step as a CCU technology still would need improvements to reach a negative net carbon balance.

Finally, marine eutrophication (MEutro) is substantially less impacted by a decrease of solvent flowrate. Indeed, optimised absorption with ARG (absoA.kMax) becomes worse than optimised SAR (absoS.kMax) in this category. Indeed, ARG is produced by fermentation using maize starch requiring green manure and nitrogen-fixing bacteria whilst SAR is chemically synthesised generating lower MEutro (more

explanation on AA production in Appendix B.4). This is shown by SimaPro networks on Figures C.34 and C.35. As general remark, it should be noticed that in ARG production, the chemical organic factory construction contributes to emissions, whereas the latter is not considered in SAR production (i.e. the chemical compounds inputs for SAR production from Ecoinvent database does not include infrastructure). Consequently, it could be suggest that if infrastructure uses were included in the background database [83], SAR production would emit slightly more than in presents results.

A physical explanation can also highlight the reasons for a lower maximum κ for SAR compared to ARG. As a reminder, κ represents the cumulative load of chCO2 in the solvent, where CO_2 is absorbed in the solution by chemical and/or physical absorption [19]. Therefore, for a higher κ, the solvent is more saturated. And ARG has a higher maximum κ, showing a higher absorption capacity compared to the SAR. This phenomenon can have different explanations.
First of all, less active SAR is initially present in the solution (0.3M SAR versus 0.5M ARG). It should be noted that these AA concentrations were fixed in the laboratory in order to maximise the K_{ov}. For example, it was observed that a high concentration of SAR (0.5M) decreased the mass transfer due to a reduction of solubility in the aqueous solution. Therefore, the optimal concentration of SAR was set at 0.3M (against to 0.5M for ARG).
Secondly, ARG has a better absorption capacity due to its chemical structure. Indeed, ARG has a primary amine group which has a better absorption performance compared to secondary amines as for SAR. [21]
A solvent with 0.5M ARG is thereby able to absorb more CO_2 leading to a higher κ. Hence, less solvent is required for absorption by ARG, leading to lower environmental impacts.

In conclusion, the best membrane gas absorption scenario regarding environmental concerns should work with the lowest solvent flowrate. Therefore, solvent with ARG should be preferred to SAR. Indeed, its loading of CO_2 can reach a higher value such that less solvent is needed to absorb the same amount of kgCO_2. To conclude that optimised ARG is better than SAR scenario in every categories, it should be assumed that infrastructure contribution in the latter scenarii would exceed absoA.kMax emissions.

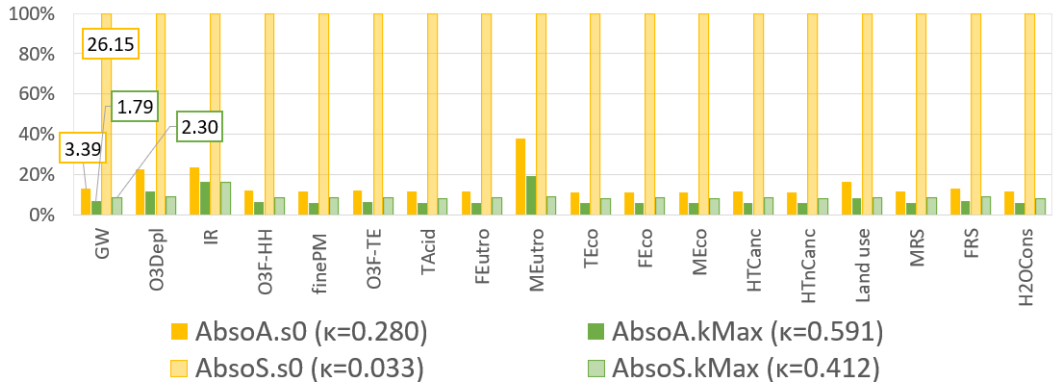

Figure 26 LCIA comparison of absorption with ARG and SAR and solvent saturation. AbsoA.s0 and absoS.s0 stand for reference absorption with ARG and SAR respectively and maximum K_{ov} where $\kappa = 0.280$ and $\kappa = 0.033$ [mol/kg] respectively (fresh solvent). AbsoA.kMax and absoS.kMax denominate absorption with ARG and SAR respectively and maximum CO_2 load $\kappa = 0.561$ and $\kappa = 0.412$ [mol/kg] respectively (saturation). The data labels on the bar chart represent the CO_2 emissions in [kgCO_2-eq]. Abbreviations on the x-axis refer to Table 24.

V.2.2 Osmotic membrane distillation

This section presents the results of the LCIA and the potential optimisation pathways specific to OMD. The generic case of the OMD (noted omd.s0) treating the previous absoA.s0 is analysed in order to determine the main key points of the environmental emissions. Results also compare the distillation by OMD of different absorption up-streams like the generic case (absoA.s0) and the optimised one (absoS.kMax). Only optimised absorption promoted by SAR can be described given the saturation concentration decided in the first assumptions. Indeed, absoA.kMax generates an already highly concentrated solution in $NaHCO_3$ so that OMD noed not need to distil it more. Subsequently, an optimisation scenario is proposed by coupling OMD with desalination plants.

V.2.2.1 Reference case omd.s0 analysis

Here, omd.s0 is analysed to highlight the important points of OMD, which appears to be mainly the osmotic solution. This section also aims to establish potential further optimisations of the process step. As a reminder, the generic omd.s0 deals with a Q_{fi} feed flowrate coming from the generic absorption's stage, absoA.s0.

To begin with, the global warming category is given in Figure 27. The different contributions to the CO_2-eq are illustrated such that the osmotic solution is the main component of the carbon footprint. It accounts for 98% of carbon emissions.

Hence, a focus on the LCIA of the osmotic solution at the permeate inlet is provided in Figure 28. The use of NaCl is the main reason for environmental impacts generated by the use of osmotic permeate in OMD. NaCl powder was taken from the Ecoinvent database available in SimaPro. Further analysis with the Ecoinvent *Unit* database shows that heat (10%, energy (51%) and the chemical factory construction (34%) are the main reasons for the CO_2 emissions caused by

the use of NaCl compounds. The network of NaCl emissions on global warming is represented in Figure C.36. In view of these results, the use of OMD would make sense if a mixture of pure NaCl and pure water were not used, but if it were coupled to a recycled brine. This scenario is studied in Section V.2.2.2.

In addition, the LCIA of the omd.s0 can be studied in depth with regard to other impact categories. In Figure 27, the influence of the saline solution leaving the membrane is shown (more information on the selection of the brine post-treatment in Appendix B.6). As a result, marine ecotoxicity (MEco) is strongly impacted by the discharge of brine into seawater and the production NaCl for the osmotic solution. Moreover, normalised LCIA of OMD shows that MEutro is the most important category. Normalisation on LCIA results of omd.s0 are shown in Appendix (Figure C.26). In fact, and as mentioned before, absorption also has a high normalised impact on MEco (Figure 21) due to the use of Na_2CO_3 in the solvent. This can be explained by the fact that Na_2CO_3 also requires the production of NaCl (Figure C.33).

Afterwards, it is interesting to display the LCIA results of OMD treating solutions from an optimised absorption (i.e. absoA.kMax and absoS.kMax). However, absoA.kMax produces a solution already highly concentrated in $NaHCO_3$ with $C_{fi} = 1.26\, mol/kg_{H2O}$. The calculations of C_{fi} were extensively explained in Section IV.2. Hence it reaches before passing through the MDC, the final saturation concentration set at $C_{fo} = 1.23\, mol/kg_{H2O}$ for a room temperature. For absoS.kMax, this does not represent a problem since $C_{fi} = 0.89\, mol/kg_{H2O}$. The LCIA of the OMD with previous absoS.kMax is given in Figure 29. The final concentration C_{fo} is nevertheless a parameter of interest that can be modified to provide a sensitivity analysis and where an LCIA of the OMD coupled to the absoA.kMax can be performed (see later in Section V.2.6).

In the end, it was found that since the osmotic solution is the key point of environmental impacts, a potential optimisation would be to apply OMD to a previous absorption stage producing a relatively small amount of feed solution Q_{si}. By doing so, thanks to the osmotic flowrate Q_{pi} correlated to Q_{si}, the osmotic flowrate Q_{pi} would also reduce. In addition, it could be suggested to use recycled brine made of high saline solution to minimise the effects of permeate (see next Section).

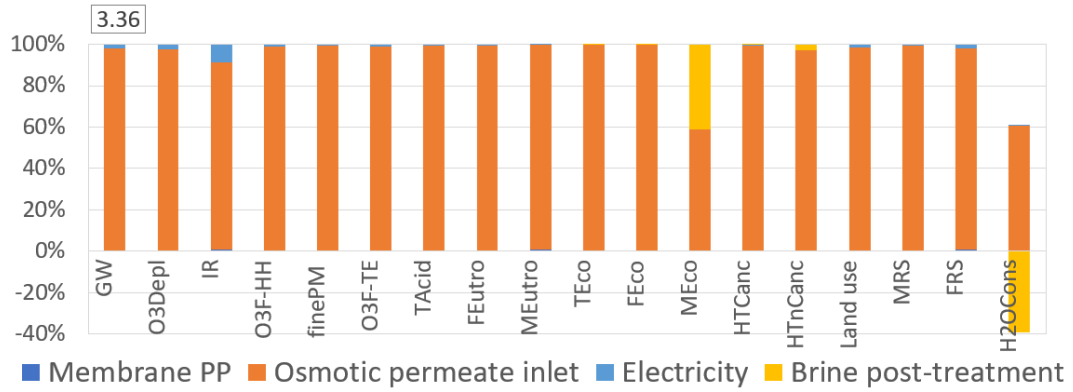

Figure 27 LCIA of generic OMD (i.e omd.s0) treating previous absoA.s0 that represents absorption with ARG and maximum K_{ov} - characterisation. The data label on the bar chart represents the overall CO_2 emissions in [kgCO_2-eq]. Abbreviations on the x-axis refer to Table 24.

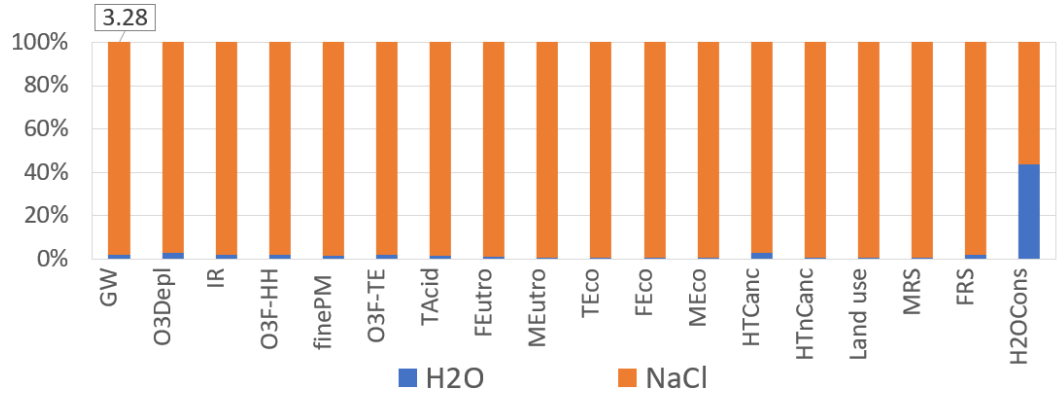

Figure 28 LCIA of the osmotic solution at inlet of the permeate side. The solution is used for generic OMD (i.e. omd.s0) treating previous absoA.s0 that represents absorption with ARG and maximum K_{ov} (see LCI Table 12) - characterisation. The data label on the bar chart represents the CO_2 emissions in [kgCO_2-eq] Abbreviations on the x-axis refer to Table 24.

V.2.2.2 Coupling OMD with desalination plant

The production of the osmotic solution from NaCl powder is not relevant from an environmental point of view when we know that in other industrial fields, after reverse osmosis (RO) in a desalination plant, very salty brines are obtained. Indeed, during desalination, a seawater supply is separated into two streams: fresh water (the marketable product) and brine (by-product). Generally, these very high salinity brines are released into the environment. [84] In the context of desalination, brine as a by-product or waste could be revalorised and used as osmotic permeate for OMD. Consequently, this section assessed the environmental impacts of OMD when coupled to a desalination plant.

For sake of consistency with the selected library model (APOS, see Appendix B.2 for more information on the library selection), the recycling of brine from desalination plant must be credited by allocation factors. Brine being a secondary

product of desalination plants, upstream activities should be allocated to the brine with a certain factor. Economic allocation is the most common in Ecoinvent [83]. Therefore brine and produced drinking water from desalination plants have an allocation factor about 90% and 10% respectively [85; 86]. Regarding mass balance, it is known that drinking water is produced with 40% recovery from seawater. The remaining 60% is considered as a brine.[83] Given this, it is possible to calculated allocated emissions of brine from an equivalent amount of tap water produced by RO. The material "*tap water produced by RO*" is already available in Ecoinvent database.

From the amount of brine required for OMD (Q_{pi}), the amount of produced tap water ($Q_{tapwater}$) can be computed as:

$$Q_{tapwater} = Q_{pi} * \frac{60}{40}$$

Next, it is assumed that the Ecoinvent database allocates 100% of the emissions to tap water by RO since no information on the allocation factor is detailed [83]. Therefore, the equivalent emissions allocated to brine recovery are about $Q_{tapwater} * 0.90$ of the emissions from tap water production.

Finally, brine post-treatment can be removed from the LCI when considering OMD coupled with desalination plants. Indeed, the production of tap water by RO already takes into account brine removal. The same is true for the credits allocated to brine recovery in tap water production.

The LCIA results are presented in Figure 29, so that OMD combined with desalination plants is an environmentally and globally attractive MDC option. Nevertheless, stratospheric ozone depletion (O3Depl) emits more when considering recycled brine from desalination than with freshly prepared osmotic solution. Indeed, the production of tap water by RO requires polyvinylidene chloride (Figure C.38) for all the water pre-treatment stages (chlorination, coagulation, flocculation, clarification, sludge sedimentation, etc.) [83]. Thus, polyvinylidene chloride introduces CFC particles increasing O3Depl emissions. Finally, note that in these LCIA results, no transport emissions have been taken into account, since it is assumed that the CCU process would take place on the desalination site, and in the vicinity of the sea coast (for access to seawater for the desalination plant and for the discharge of the permeate).

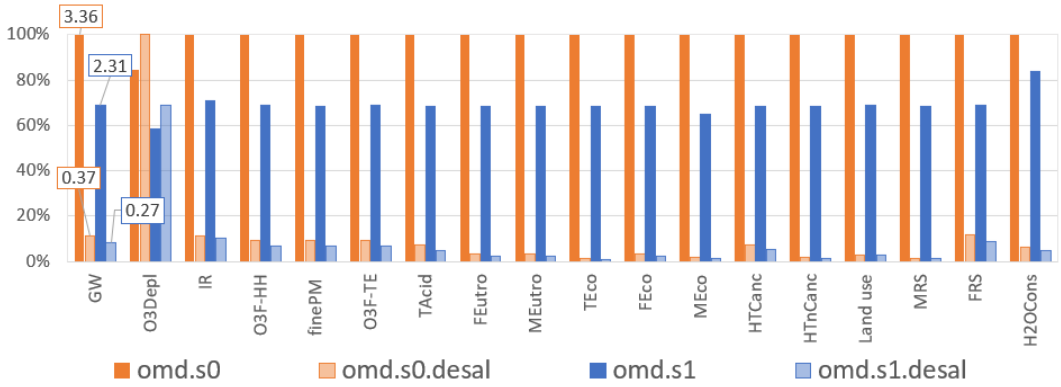

Figure 29 LCIA of different OMD cases (with a fresh osmotic solution and with recycled brine from desalination plants) with different previous absorption cases (s0 or s1). Omd.s0 is OMD treating generic absorption absoA.s0 with ARG and maximum K_{ov}. Omd.s0.desal is omd.s0 with same previous absorption step and coupled with a desalination plant. Omd.s1 represents OMD treating previous absorption absoS.kMax, with SAR and maximum $\kappa = 0.412$ [mol/kg]. omd.s1.desal is omd.s1 coupled with a desalination plant. Abbreviations on the x-axis refer to Table 24.

V.2.3 Direct contact membrane distillation

Different distillation and crystallisation processes to concentrate Na_2CO_3 are considered in this document. After OMD, direct contact membrane distillation (DCMD) is assessed based on the generic dcmd.s0 case derived in the previous chapter. In addition, environmental impacts are compared when the temperatures of the feed and permeate inlet sides are varied.

V.2.3.1 Reference case dcmd.s0 analysis

The LCIA results of the generic LCI on DCMD, noted dcmd.s0, with the previous absoA.s0 in absorption, are presented in this section. The key points on environmental emissions are highlighted.

First, Figure 30 outlines the global warming due to dcmd.s0. In fact, water recovery and the recirculation of the permeate inside DCMD appears to have a real positive impact on the carbon footprint. Moreover, the energy demand provided as electricity shows to be the most consequent part (by 83%) of the CO_2-eq emissions. This electricity is required to heat (to T_{fi}) and cool (to T_{fo}) the feed and permeate streams respectively and entering the membrane.

In addition, other impact categories resulting from the dcmd.s0 are presented in Figure 30. Electricity inputs score as expected in almost all impact categories, whilst permeate and H_2O recovery are the main factors in the category concerning water consumption (H2OCons). Water recovery is one of the main difference between DCMD and OMD. In DCMD pure water is collected from the permeate, whilst brine solution in OMD must undergo a waste-treatment.

A first conclusion on the environmental results suggests that, in order to further reduce emissions, electricity demands should be minimised. To achieve this, a

sensitivity analysis can be carried out by varying the temperature of the feed and permeate inputs, denoted T_{fi} and T_{fo} respectively (see the following 2 Sections V.2.3.2 and V.2.3.3) as well as the source of electricity (see Section V.3.3).

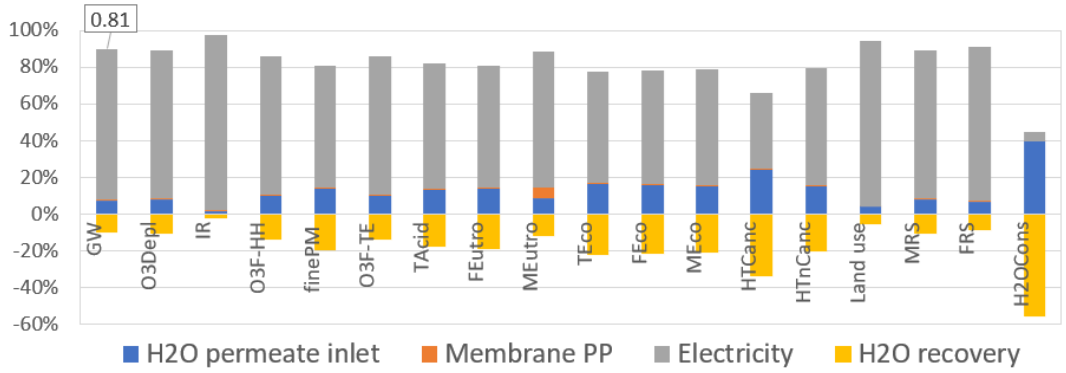

Figure 30 LCIA of reference DCMD (i.e dcmd.s0) with previous absoA.s0 that represents absorption with ARG and maximum K_{ov} (see LCI Table 14) - characterisation. The data label on the bar chart represents the overall CO_2 emissions in [$kgCO_2$-eq]. Abbreviations on the x-axis refer to Table 24.

V.2.3.2 Temperature at feed inlet T_{fi}

In the laboratory, the set ups of DCMD operating with different feed inlet temperatures T_{fi} have been experimented, whilst the associated K_{ov} has been recorded. Therefore, T_{fi} can be considered as a parameter to vary in order to reduce environmental emissions. A sensitivity analysis on T_{fi} is performed considering different values of T_{fi}: 40 (reference case noted dcmd.s0 or dcmd.s0.tfi40), 35, 30 and room temperature 25 °C.

When T_{fi} is reduced, different operating conditions are accordingly changed. New feed and permeate outlet temperatures (T_{fo} and T_{po}) are measured during the laboratory experiments, so that the final $NaHCO_3$ concentration C_{fo} (Figure 17) and thus the amount of water to be evaporated N_{H2O} (equation (16)) changes. Moreover, the different vapour pressures p (equation (8)) lead to a new driving force. With the adapted driving force ΔP and K_{ov}, the flux J_{abso} is also impacted as well as the membrane area (equation (17)). Then, the amount of permeate flow Q_{pi} entering the membrane at T_{pi}=5°C is also influenced by the modification of T_{fi} since it is calculated via equation (18).
From experimental data, one observes that for different T_{fi}, K_{ov} shows a relatively constant profile, suggesting that temperature polarisation can be neglected in this range of temperatures [28]. However, it could be expected that with a lower T_{fi}, the driving force decreases because of equation (7).

The different scenarii with T_{fi} are calculated taking the previous absoA.s0 case as absorption. The different data such as temperatures and C_{fo} needed to determine the LCI is all presented in Table 27. The resulting LCIAs from this table are presented in Figure 31. It appears that reducing T_{fi} significantly reduces the electrical inputs, resulting in a reduction in environmental impacts. However, the lower T_{fi} is, the lower K_{ov} (and the driving force) becomes. Leading to an

expansion of the membrane area (equation (17)). Even if this last factor is less important than electricity, attention should be paid to it if the membrane lifetime is assumed to be shorter (5 years in the present calculations [62]). This membrane lifetime is subject to a sensitivity analysis later in Section V.3.2.

In Figure 31, it is observed that for a decreasing T_{fi}, the emissions reduction from water consumption (H2O) varies relatively less than other impacts. A detailed graph on water consumption is shown in Figure C.27. In fact, compared to the other categories, electricity has less influence on the overall H2OCons. Therefore, since water recovery decreases only slightly with lower T_{fi} and the contribution of electricity is relatively smaller, the overall decreases in H2OCons show a flatter profile.

In fact, the lower T_{fi}, the lower T_{fo} and C_{fo} and thus the lower Q_{pi} and N_{H2O}. Consequently, the recovery of water leaving the permeate $Q_{po} = Q_{pi} + N_{H2O}$ decreases H2OCons with a decreasing T_{fi}. However, H2OCons is also sensible to water demand from electricity production. Indeed, the contribution of a high electricity consumption causes by a high T_{fi} increases the water consumption. Therefore, the overall H2OCons decreases slower when electricity consumption is slightly changed.

Finally, we note that marine eutrophication (MEutro) decreases relatively less for $T_{fi} = 25°C$ than for other temperatures. In this case, MEutro emissions due to membrane production become significant, whereas for other higher T_{fi}, MEUtro is mainly impacted by electricity (see Figure C.28).

Table 27 Data and LCI for sensitivity analysis of DCMD when changing T_{fi}. The LCIs are calculated with absoA.s0 as previous absorption step and considering 1 hour of running. Membrane lifetime is 5 years [62]. The different temperatures were experimentally measured.

Components	**dcmd.s0**	**dcmd.s0.tfi35**	**dcmd.s0.tfi30**	**dcmd.s0.tfi25**	**Unit**
T_{fi}	40.00	35.00	30.00	25.00	°C
T_{fo}	19.00	16.63	14.39	12.24	°C
T_{pi}	5.00	5.00	5.00	5.00	°C
T_{po}	27.00	24.28	21.46	18.47	°C
K_{ov}	2.22E-11	1.88E-11	2.14E-11	1.71E-11	$m^3/m^2\,Pa\,s$
C_{fo}	1.12	1.08	1.04	1.01	mol/kg_{H2O}
LCI					
Inputs					
Feed Q_{fi}	83	83	83	83	kg
Permeate Q_{pi}	78	78	78	78	kg
Membrane area	37	59	74	137	cm^2
Electricity	12	9.6	7.2	4.7	MJ
Outputs					
Feed Q_{fo}	51	53	54	56	kg
Permeate Q_{po}	109	108	106	104	kg

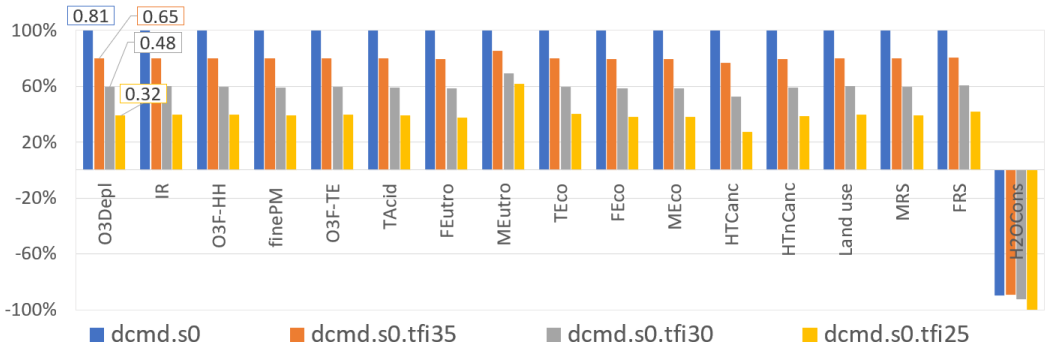

Figure 31 LCIA of DCMD with different feed inlet temperature T_{fi} - characterisation. The previous absorption step of all DCMD cases is absoA.s0 with ARG and maximum K_{ov}. dcmd.s0 represents the reference case of DCMD working at 40°C. The data labels on the bar charts represent CO_2 emissions in [kgCO_2-eq]. Abbreviations on the x-axis refer to Table 24.

V.2.3.3 Temperature at permeate inlet T_{pi}

Further experiments were carried out in the laboratory to characterise DCMD. The inlet temperature of the aqueous permeate T_{pi} was modified and the associated K_{ov} was recorded. T_{pi} can be considered, like T_{fi}, as a parameter to be varied in order to reduce emissions. A sensitivity analysis is carried out by taking different T_{pi}: 5 (reference case noted dcmd.s0 or dcmd.s0.tpi5), 10, 15 and 20°C.

The impact of a changing T_{pi} on the other operating parameters is similar to that of T_{fi} in the previous Section. Different inlet and outlet temperatures are measured during the laboratory experiments. The saturation concentration changes. The amount of water to be evaporated as well as the surface area of the membrane. In addition, the permeate flowrate Q_{pi} (equation (18)) and the electricity to cool it must be adjusted. It also follows from laboratory experiments that K_{ov} remains constant with a variation of T_{pi}.

The results are calculated by taking the previous generic absorption case absoA.s0 with ARG and its maximum K_{ov}. The different data allowing to calculate the LCI are presented in Table 28. Figure 32 presents the resulting LCIs. It appears that the reduction of T_{pi} has a positive impact on the environment. This is mainly due to the reduction in electricity needed to cool the permeate. Therefore, the preferred T_{pi} is the highest at 20°C. However, this case is still less cost effective than a lower inlet temperature $T_{fi} = 25°$. Therefore, the DCMD should be optimised by decreasing T_{fi} rather than increasing T_{pi}.

Table 28 Data and LCI for sensitivity analysis of DCMD when changing T_{pi}. The LCIs are calculated with absoA.s0 as previous absorption step and considering 1 hour of running. Membrane lifetime is 5 years [62]. The different temperatures were experimentally measured.

Components	dcmd.s0	dcmd.s0.tpi10	dcmd.s0.tpi15	dcmd.s0.tpi20	Unit
T_{pi}	5.00	10.00	15.00	20.00	°C
T_{po}	27.00	28.81	30.37	31.54	°C
T_{fi}	40.00	40.00	40.00	40.00	°C
T_{fo}	19.00	21.08	22.39	25.79	°C
K_{ov}	2.22E-11	1.97-11	1.97E-11	1.97E-11	$m^3/m^2\ Pa\ s$
C_{fo}	1.12	1.16	1.18	1.24	mol/kg_{H2O}
LCI					
Inputs					
Feed side Q_{fi}	83	83	83	83	kg
Permeate side Q_{pi}	78	82	94	101	kg
Membrane area	37	48	57	67	cm^2
Electricity	12	11.3	10.9	9.7	MJ
Outputs					
Feed side Q_{fo}	51	50	49	47	kg
Permeate side Q_{po}	109	115	127	136	kg

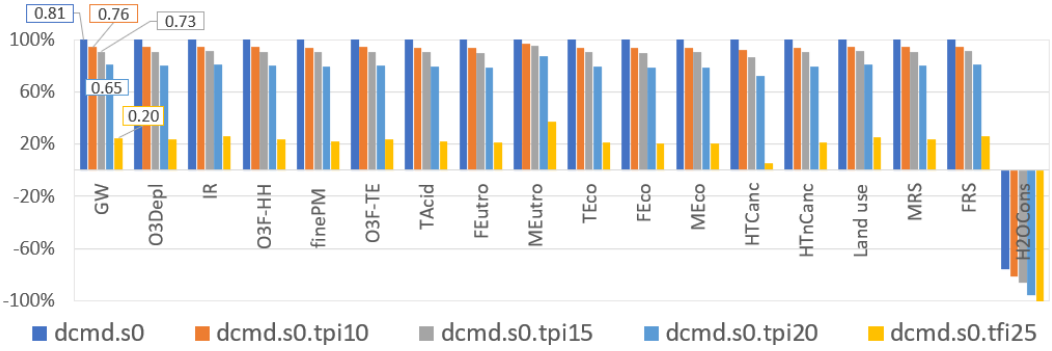

Figure 32 LCIA of DCMD with different feed inlet temperature T_{pi} - characterisation. The previous absorption step of all DCMD cases is absoA.s0 with ARG and maximum K_{ov}. dcmd.s0 represents the reference case of DCMD working at $T_{fi} = 40°C$ and $T_{pi} = 5°C$. dcmd.s0.tfi25 represents DCMD working at $T_{fi} = 25°C$ and $T_{pi} = 5°C$. The data labels on the bar charts represent CO_2 emissions in [$kgCO_2$-eq]. Abbreviations on the x-axis refer to Table 24.

V.2.4 Vacuum membrane distillation

As the last MDC configuration studied, vacuum membrane distillation (VMD) is here evaluated. First, the generic case of VMD, vmd.s0, is analysed and compared with different upstream absorption cases: absoA.s0 and the optimised case absoS.kMax. Afterwards, a first optimisation of VMD consisting in decreasing the inlet temperature T_{fi} is presented.

V.2.4.1 Reference case vmd.s0 analysis

Here, environmental impacts of vmd.s0 are studied in order to understand key points on this process stage. Vmd.s0 is the reference case of VMD where the LCI is given in Table 16, and where it is assumed that the upstream feed solution from absorption is the generic case absoA.s0.

To begin with, global warming impacts are available in Figure 33 where it clearly

appears that electricity has a major responsibility in carbon emissions. This electricity demand is required to heat the feed stream but mostly to condense the vapour permeate leaving the membrane (equation (19)) which represents near 94% of energy inputs.

Further, a larger view on all impact categories is outlined is Figure 33 where the effect of electricity consumption is widely confirmed. However, it should be noted that the overall water consumption (H2OCons) is positive. In this way, the recovery of water from the permeate does not compensate for the upstream water consumption required for electricity generation. This makes a difference between DCMD and VMD, where DCMD showed in figure 30 a negative overall water consumption.

A potential way to reduce emissions generated by energy, would be to reduce T_{fi} and the amount $Q_{po} = N_{H2O}$ of water to be condensed, or to change the energy source to renewable energies (see Section V.3.3). Note that in order to decrease N_{H2O}, the initial and final $NaHCO_3$ concentrations (C_{fi} and C_{fo} respectively) play an important role by the equation (16).
For instance, VMD with upstream absoA.s0 (generic absorption with ARG) and absoS.kMax (optimised absorption with SAR) are compared in Figure 34. In this figure, vmd.s0 refers to the upstream absoA.s0. Vmd.s1.tfi40 refers to the upstream absoS.kMax. The main point here is that each scenario produces a feed solution with a different flowrate Q_{fi} (82 vs 55 kg/h for absoA.s0 and absoS.kMax respectively) and different C_{fi} (0.64 and 0.89 mol/kg_{H2O} for absoA.s0 and absoS.kMax respectively). As a result, absoS.kMax represents only 50% of absoA.s0 emissions since N_{H2O} is lower with absoS.kMax (41 vs 20 kg_{H2O}/h). Optimisation of absorption is thus a win-win situation in order to reduce emissions of VMD and absorption at the same time.

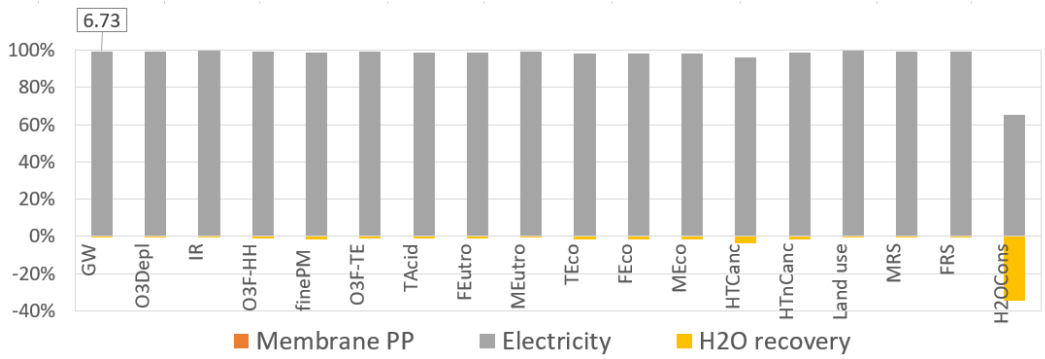

Figure 33 LCIA of reference VMD (i.e vmd.s0) treating previous absoA.s0 that denominate absorption with ARG and maximum K_{ov} (see LCI Table 16) - characterisation. Abbreviations on the x-axis refer to Table 24.

V.2.4.2 Temperature at feed inlet

As for DCMD, a first optimisation pathway for VMD consists of decreasing T_{fi}, which has an impact on the inputs of LCI with regard to electricity, membrane area and flowrates Q_{fo} and Q_{po} at the outlet. A sensitivity analysis on T_{fi} is performed

in this section, taking different values of T_{fi}: 40 (generic case noted vmd.s0 or vmd.s0.tfi40), 35 and 30 °C. Note that in the laboratory, VMD was also performed for T_{fi} = 25°C. However, the experimental feed solution was composed only of water and $NaHCO_3$ such that no AA were present. Nevertheless, when considering AAs in the feed stream, the overall driving force in the membrane becomes negative due to the consideration of AA water activities in the driving force calculations (see equations (9) and (11)).

As explained in Section V.2.3.2, when T_{fi} is changed, many operating parameters are also changed. The different T_{fi} are calculated taking into account the absoA.s0 reference case as previous absorption scenario. The different temperatures and C_{fo} needed to calculate the LCIs are presented in Table 29. It can be observed that the reduction of T_{fi} decreases the final desired concentration C_{fo} (Figure 17). Therefore, less water N_{H2O} must be evaporated, less membrane area is required and less water must be condensed. Indeed, in Table 29, LCI inputs of electricity are constantly decreasing. However, membrane area increases with the reduction of T_{fi}. In fact, although N_{H2O} decreases, the transmembrane flux J_{vmd} decreases due to a lower driving force $\Delta\overline{P}_{vmd}$ (equation (11)) and requires a higher membrane area. Note that K_{ov} keeps a constant profile.

Figure 34 quantifies the LCI entries of Table 27 in terms of environmental impacts. It shows a reduction in emissions when VMD is operated at a lower T_{fi}. In addition, as with DCMD, it should be noted that as the membrane area increases, the process could emit more when the membrane lifetime is assumed to be shorter. This is discussed further in the following section V.3.2. Furthermore, Figure 34 compares a reduction of T_{fi} with VMD in the case of an optimised upstream absorption, noted vmd.s1 . Consequently, it can be concluded that it would be interesting to integrate the two optimisations: an optimised absorption producing less feed solution Q_{fi} and VMD operating at a lower T_{fi}. This is shown on Figure 34 with vmd.s1.tfi30 showing the lowest emissions (39% of vmd.s0).

Table 29 Data and LCI for sensitivity analysis of VMD when changing T_{fi}. The LCIs of vmd.s0 are calculated with absoA.s0 as previous absorption step and considering 1 hour running. For vmd.s1, LCI are based on optimised absorption absoS.kMax. Membrane lifetime is 5 years [62].

Component	**vmd.s0.tfi40**	**vmd.s0.tfi35**	**vmd.s0.tfi30**	**vmd.s1.tfi40**	**vmd.s1.tfi30**	**Unit**
T_{fi}	40.00	35.00	30.00	40	30	°C
T_{fo}	37.5	33.39	29.39	37.5	29.39	°C
K_{ov}	4.10E-11	4.28E-11	3.93E-11	4.10E-11	3.93E-11	$m^3/m^2\,Pa\,s$
C_{fo}	1.39	1.22	1.17	1.39	1.31	mol/kg_{H2O}
			LCI			
Inputs						
Feed side Q_{fi}	83	83	83	55	55	kg
Membrane area	18	27	62	11	39	cm^2
Electricity	98	91	85	49	38	MJ
Outputs						
Feed side Q_{fo}	42	48	43	35	39	kg
Permeate side Q_{po}	41	39	37	20	16	kg

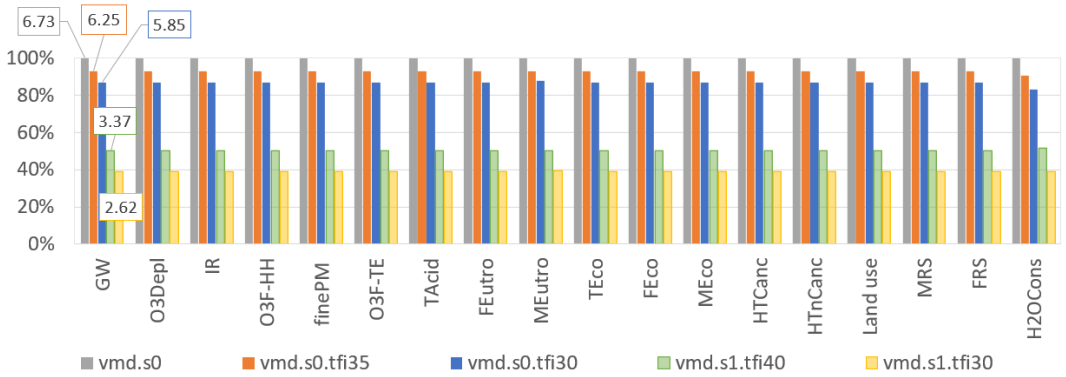

Figure 34 LCIA of VMD with different feed inlet temperature T_{fi} - characterisation. The data labels on the bar charts represent CO_2 emissions in [kgCO_2-eq]. VMD cases with s0 treat the generic absorption solution noted absoA.s0, operating with ARG at maximum K_{ov}. Vmd.s1.tfi40 and vmd.s1.tfi30 outline VMD operating at $T_{fi} = 40$ or $T_{fi} = 30$°C with former optimised absorption (absoS.kMax), with SAR and maximum $\kappa = 0.412$ [mol/kg]. Data labels on the bar charts represent global warming emissions in [kgCO_2-eq] Abbreviations on the x-axis refer to Table 24.

V.2.5 Post-treatment Post.s0

This section gives an indication on the emissions due to post-treatment of the $NaHCO_3$ concentrated solution and the benefits of crystals recovery. As a reminder, this step is not yet experimentally optimised and $NaHCO_3$ produced crystals are credited via *avoided product* in SimaPro.

In the last step of the process, $NaHCO_3$ crystals are further crystallised in a crystalliser tank, filtered and recovered for marketable uses. Water is also recovered and sent back to absorption. However, for simplicity, credits of water recovery are accounted in this step. Indeed the amount of recovered water depends on the MDC technology. Here generic DCMD (i.e. dcmd.s0) was considered. Nevertheless, it appears on Figure 35 that water recovery does not influence emissions as much as $NaHCO_3$ recovery does. As a matter of fact, revalorisation of CO_2 into $NaHCO_3$ has a significant positive influence regarding environmental concerns. Therefore, maximimisation of this recovery could be interesting. This is investigated in Section V.3.1.

In Figure 35, ionising radiation (IR) accounts for more emissions due to the high contribution of electricity. However, it should be recalled that the LCI model considers energy inputs as indicative and independent of the previous MDC step (Section IV.3). Indeed, the post-treatment is not yet optimised. Furthermore, these energy inputs are independent of the amount of flowrate to be treated. It can thus be expected that smaller equipment will be used to treat a lower solution flowrate. Therefore, the LCIA of post-treatment should result in effective lower IR emissions by incorporating energy consumption adapted to the incoming flowrate.

Future work may suggest that LCA should focus on CO_2 recovery (and on post-treatment) rather than CO_2 capture as is the case here. By doing so, the FU should be adapted. For example, it could be: 1 kg of $NaHCO_3$ produced per hour.

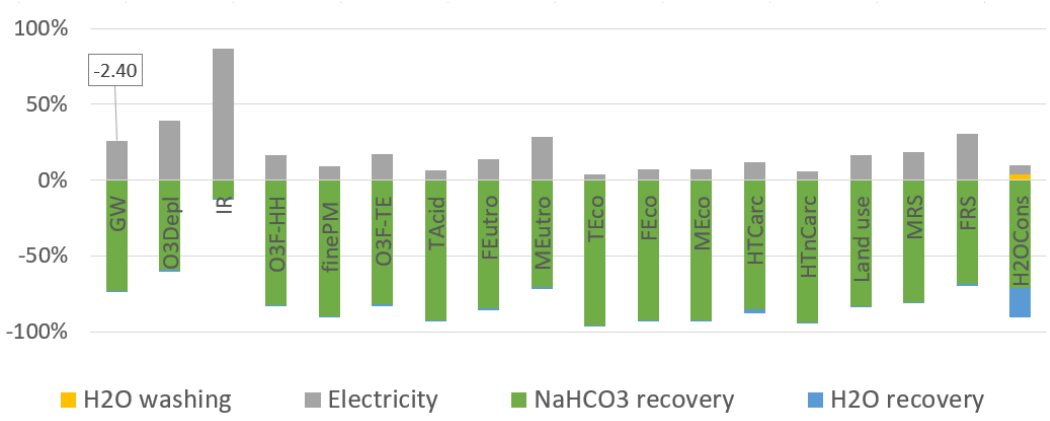

Figure 35 LCIA of Post.s0 standing for post-treatment with a water and crystals recovery of $\chi = 99\%$ - characterisation. The data label on the bar charts represents the total CO_2 emissions in [$kgCO_2$-eq]. Abbreviations on the x-axis refer to Table 24.

V.2.6 Saturation concentration C_{fo}

In this section, the 3 processes are studied and compared with regard to the environmental influence of the final desired concentration of $NaHCO_3$ (C_{fo} in $[mol/kg_{H2O}]$) when leaving MDC. Indeed, in the previous LCAs, it was assumed that MDC stops when the feed reaches the saturation level. The latter is defined in Figure 17 for different T_{fi}. Here, LCAs of the full processes via either OMD, DCMD or VMD were performed for a saturation level of 0, 30 and 50% above the saturation level (i.e. supersaturation). Results are available in Figure 36 to 38.

On one hand, OMD and DCMD presented in Figures 36 and 37 show that the increase of C_{fo} has only a significant impact on the water consumption (H2OCons). Indeed, for higher C_{fo}, more water evaporates from the feed to the permeate side and is recovered by seawater discharge for the OMD, and as pure water for the DCMD. For DCMD, the human carcinogenic toxicity (HTCarc) shows a decrease in emissions due to the higher water recovery (see Figure 30 for the water recovery contribution in DCMD). From the Ecoinvent *Unit* database, pure deionised water provokes HTCarc emissions due to the water supply network construction (see LCIA network of deionised water in Figure C.37). For OMD, it should be noted that for marine ecotoxicity (MEco) in OMD, a higher C_{fo} would increase emissions in this impact category, as shown in Figure 36. In fact, the outgoing permeate reaches a higher flowrate, which is accounted for in SimaPro as a higher brine discharge to the sea. But in practice, a higher C_{fo} will only dilute the brine permeate further and not increase MEco. Finally, C_{fo} would have an impact on the surface area of OMD and DCMD membranes. The latter increases with C_{fo}. Therefore, variations in C_{fo} could have a significant impact on the LCIA if the membrane lifetime becomes shorter (here the membrane lifetime is assumed to be about 5 years [62]). The membrane lifetimes are varied in Section V.3.2.

On the other hand, VMD gives significant results in Figure 38. The parameter C_{fo} has an impact on both the membrane area and electricity. High distillation and

crystallisation of $NaHCO_3$ crystals in the feed should be avoided for environmental reasons. Indeed, the higher the C_{fo}, the greater the quantity of permeate to be condensed (equation (19)) and the higher the electricity demand. It should be noted that water, as in the DCMD, is recovered after condensation of the permeate. However, the overall water footprint emissions (H2OCons) are positive as the water demand for electricity generation exceeds the negative contribution of the permeate recovery.

Finally, it should be noted that the level of supersaturation must be carefully determined. Allowing a too high C_{fo} can induce higher crystal growth and leads to the risk of **membrane clogging** [39]. A final remark could highlight the correlation between the MDC and the post-treatment (more precisely the crystalliser tank). With a highly crystallised solution coming out of the MDC, energy should be saved in the post-processing. However, this correlation has not been modelled in this thesis.

In conclusion, C_{fo} does not play a significant role in OMD and DCMD emissions when the membrane lifetime remains relatively long. However, the lowest C_{fo} should be selected for VMD in order to minimise the electricity required by the permeate condenser.

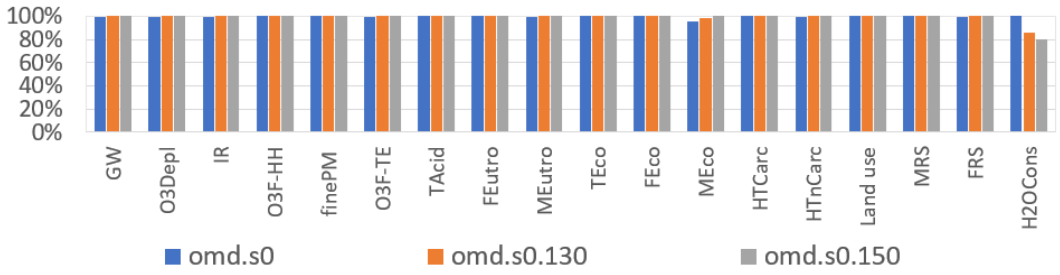

Figure 36 LCIA of OMD with different feed outlet $NaHCO_3$ concentrations C_{fo} - characterisation. The previous absorption step of all OMD cases is absoA.s0 with ARG and maximum K_{ov}. omd.s0 represents the reference case where C_{fo} is 100% the saturation level omd.s0.130 and omd.s0.150 represents OMD with C_{fo} respectively 130 and 150% times the saturation level. Abbreviations on the x-axis refer to Table 24.

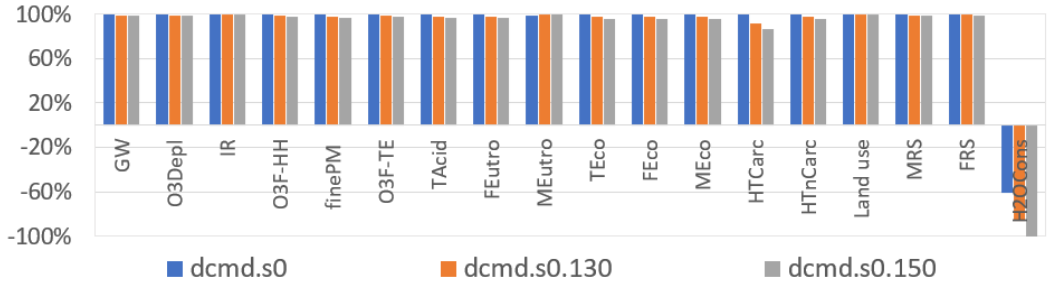

Figure 37 LCIA of DCMD with different feed outlet $NaHCO_3$ concentrations C_{fo} - characterisation. The previous absorption step of all DCMD cases is absoA.s0 with ARG and maximum K_{ov}. dcmd.s0 represents the reference case where C_{fo} is 100% the saturation level dcmd.s0.130 and dcmd.s0.150 represents DCMD with C_{fo} respectively 130 and 150% times the saturation level. Abbreviations on the x-axis refer to Table 24.

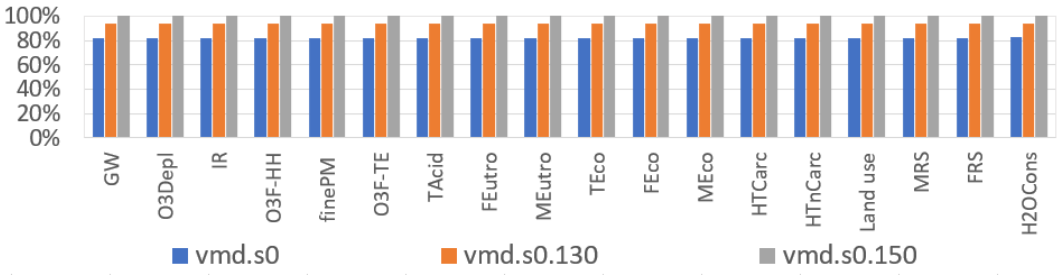

Figure 38 LCIA of VMD with different feed outlet $NaHCO_3$ concentrations C_{fo} - characterisation. The previous absorption step of all VMD cases is absoA.s0 with ARG and maximum K_{ov}. vmd.s0 represents the reference case where C_{fo} is 100% the saturation level vmd.s0.130 and vmd.s0.150 represents DCMD with C_{fo} respectively 130 and 150% times the saturation level. Abbreviations on the x-axis refer to Table 24.

V.2.7 Comparison of optimised OMD, DCMD and VMD

In the present document, different membrane technologies are investigated in order to concentrate and crystallise $NaHCO_3$ from the solution leaving membrane gas absorption. OMD, DCMD and VMD were optimised in previous sections. Therefore, in this section, there are compared with regards to their environmental impacts. LCIA results are available in Figure 39.

First, regarding global warming (GW), Figure 39 shows that OMD and DCMD have equivalent emissions and that VMD obtains a higher carbon footprint. However, other environmental impacts should be considered. Therefore, it appears that VMD scores in 12 categories, but OMD also emits more compared to DCMD and VMD in many impact categories (7).

As a result, this shows the importance of a LCA treating several impact categories in order to qualify conclusions and resulting environmental decisions. Moreover, it is interesting to remind that conversely to optimised scenarii, in the generic scenario, VMD scored in 7 impact categories, and OMD in 11 (see Figure C.23). As a matter of fact, OMD was greatly improved when coupled with desalination plants, decreasing subsequently emissions in many categories.

However, when OMD emits more in some impact categories, the difference of emissions between OMD and VMD is relatively small. Exception should be noticed regarding stratospheric ozone depletion (O3Depl). Indeed, the difference of O3Depl emissions for OMD and VMD is relatively important. OMD emits significantly more [kgCFC11-eq] due to tap water considerations when using brine from desalination plants.

Afterwards, DCMD recovers more water (H2OCons) than other MDC process. Compared to OMD, the permeate composed of pure water is continuously recycled inside DCMD. In comparison to VMD, a higher C_{fo} enables more water evaporation and recovery.

Next, if VMD has high scores in certain categories compared to OMD and DCMD,

this is largely explained by its higher electricity demands to condense the permeate.

To conclude, with regard to carbon footprint, OMD and DCMD have equivalent the lowest emissions (0.21 $kgCO_2$-eq) and VMD the higest (0.34 $kgCO_2$-eq). However, taking into account other types of emissions, DCMD proves to have less impact in the most categories compared.

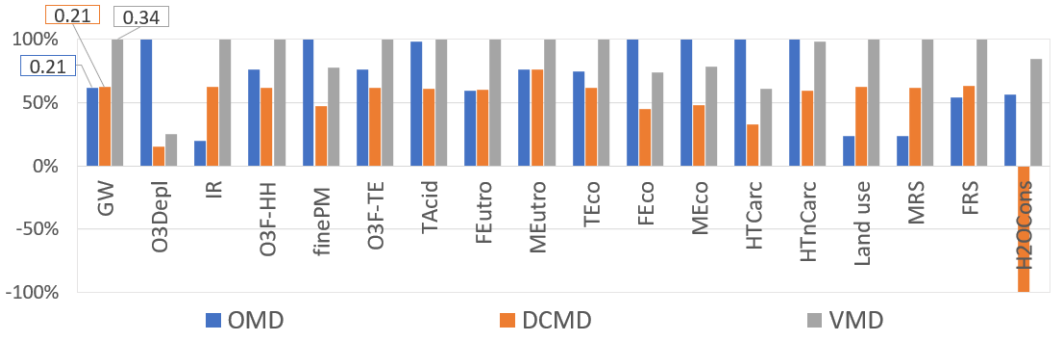

Figure 39 LCIA of the optimised MDCs (OMD, DCMD and VMD) with operating conditions - characterisation. Previous optimised absorption step is absoA.kmax and operates with ARG and maximum $\kappa = 0.561$ [mol/kg]. OMD is working until 50% above the saturation level and is coupled with desalination plant. DCMD is working until 50% above the saturation level and with $T_{fi} = 25°C$. VMD works at $T_{fi} = 30°C$ and up the the saturation level. Data labels on the bar charts represent global warming emissions of each MDC step in [$kgCO_2$-eq]. Abbreviations on the x-axis refer to Table 24.

V.2.8 Resume of best scenarii per LCA step

Here the different optimisation routes per LCA step that were described earlier are resumed. These optimisation routes aims to minimise as much as possible environmental emissions. Several operating conditions for absorption and the different MDC processes are chosen in order to obtain the lowest emissions. Results are presented in Figure 40 and 41.

The different optimised scenarii should be remined. First, regarding absorption, absorption with the maximum CO_2 load κ in the solvent is chosen as the best option. Therefore, absorption with ARG is selected, which results in a solvent flowrate about 42 kg/h.
Afterwards, the different optimised MDC processes were developped. All of them treat the former feed solution from optimised absorption. Optimised OMD is coupled with desalination plants to recycle brine by-product and optimised DCMD works at inlet feed temperature $T_{fi} = 25°C$. In addition OMD and DCMD distillate and crystallise $NaHCO_3$ up to a supersaturation level being 50% above the saturation level. Lastly, VMD operates at $T_{fi} = 30°C$ and at saturation level. Finally, post-treatment is considered with a recovery percentage around 99%. The amount of recovered water in post-treatment is also based on the optimised DCMD.

With these optimised scenarii, it clearly results in Figure 40 that the whole CO_2

capture and utilisation process would be environmentally interesting regarding global warming (GW) and many other environmental impacts. Indeed, by summing emissions from absorption with one MDC process and post-treatment, all 3 processes' carbon footprint would be below 1 kgCO2-eq. For instance, for 1 kg CO_2 captured, the process via VMD would additionally save 0.24 kgCO_2-eq. In other words, a total of 1.24 kgCO_2-eq are avoided.

However, in Figure 40, several impact categories do not show a global emissions reduction. These different results between impact categories have several explanations.
First, looking simultaneously at Figure 40 and 41, it can be seen that marine eutrophication (MEutro) has overall positive emissions. This is again explained by absorption and the use of ARG in the solvent mixture, which requires grains and manure for a fermentative production of ARG.
Regarding positive emissions of ionising radiation (IR) in Figure 41, the post-treatment step emits the most although it has the lowest emissions in every other impact categories. In fact, electricity demand as the most contributor factor to IR emissions in post-treatment, is considered constant regardless of the previous absorption and MDC steps.
In addition, fossil resource scarcity (FRS) presents overall positive emissions in Figure 40 and particularly for the process by VMD. This is explained again by the Na_2CO_3 production for the absorption' solvent and by a high electricity use in VMD.
Moreover, ozone depletion (O3Depl) is scoring in absorption and OMD due to Na_2CO_3 and tap water production respectively and their associated CFC emissions.

Afterwards, and comparing the 5 steps, Figure 41 shows that absorption is the most negative impactful step in all categories (except ionising radiation (IR)). This is due to the use of Na_2CO_3.

In Figure 42, the optimised LCIA results are normalised by the mean of the Recipe (H) midpoint method. This figure can be compared to the normalised results of the reference LCI (Figure 21). The focus is on the carbon footprint because the purpose of the process studied is carbon capture. But in the generic LCA, it was concluded that special attention should be paid to ecotoxic and carcinogenic emissions (see Section V.1). Indeed, they have higher normalised emissions. Nevertheless, optimised LCA allows for a reduction of normalised emissions in these categories too. In addition, when normalised emissions from absorption, one MDC step and post-treatment are added together (as shown in Figure C.29), the overall LCA shows negative emissions (except for ionising radiation (IR)). Therefore, the optimised global LCA would reduce emissions in all impact categories except IR. But note that IR could also become negative if the source of electricity is changed (see Section V.3.3). Lastly, note that endpoints results (characterisation and normalisation) are also available in Appendix C.2.5.

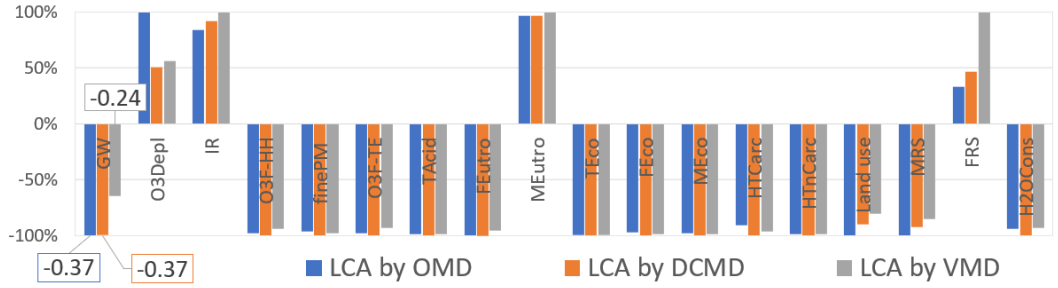

Figure 40 LCIA of the optimised LCA with operating conditions - characterisation. LCA by OMD/DCMD or VMD sums up emissions due to absorption + OMD/DCMD or VMD + post-treatment. Absorption step is operating with ARG and at maximum $\kappa = 0.561$ [mol/kg]. OMD is working until 50% above the saturation level and is coupled with desalination plant. DCMD is working until 50% above the saturation level and with $T_{fi} = 25°C$. VMD works at $T_{fi} = 30°C$ and up to the saturation level. Post-treatment works with a recovery χ=99%. Data labels on the bar charts represent global warming emissions in [kgCO_2-eq]. Abbreviations on the x-axis refer to Table 24.

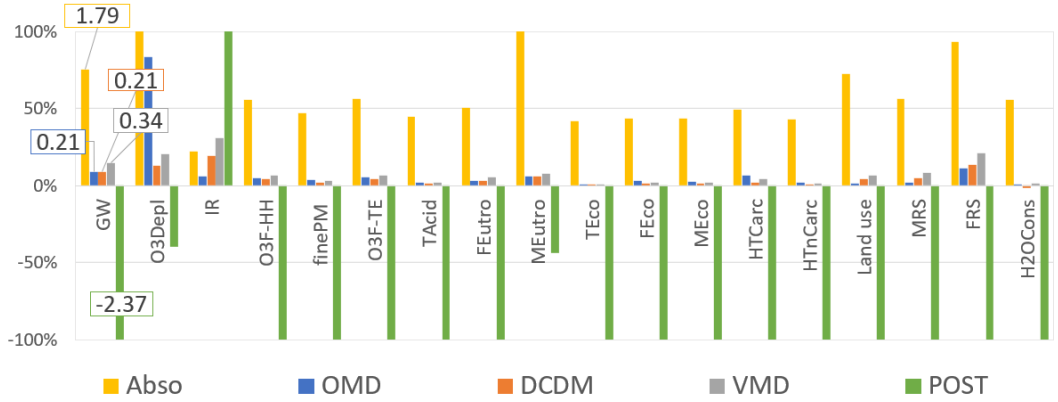

Figure 41 LCIA of the optimised LCA with operating conditions - characterisation. Abso is absorption with ARG and maximum $\kappa = 0.561$ [mol/kg]. OMD is working until 50% above the saturation level and is coupled with desalination plant. DCMD is working until 50% above the saturation level and with $T_{fi} = 25°C$. VMD works at $T_{fi} = 30°C$ and up the the saturation level. Post stands for post-treatment step with a recovery χ=99%. Data labels on the bar charts represent global warming emissions in [kgCO_2-eq]. Abbreviations on the x-axis refer to Table 24.

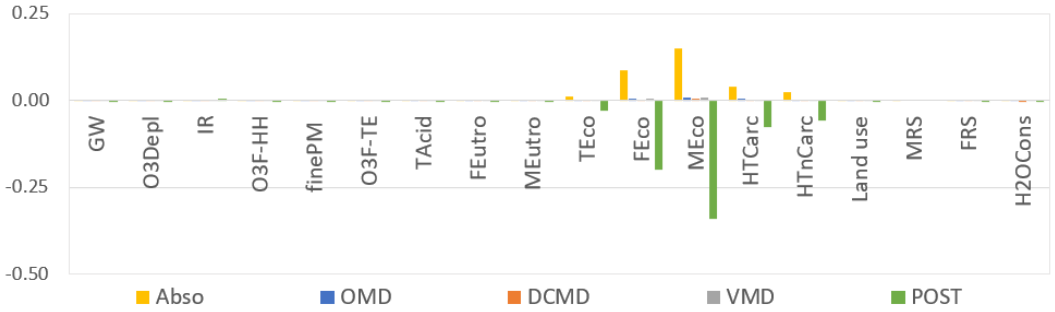

Figure 42 LCIA of the optimised LCA with operating conditions - normalisation. Abso is absorption with ARG and maximum $\kappa = 0.561$ [mol/kg]. OMD is working until 50% above the saturation level and is coupled with desalination plant. DCMD is working until 50% above the saturation level and with $T_{fi} = 25°C$. VMD works at $T_{fi} = 30°C$ and up the the saturation level. Post stands for post-treatment step with a recovery χ=99%. Abbreviations on the x-axis refer to Table 24.

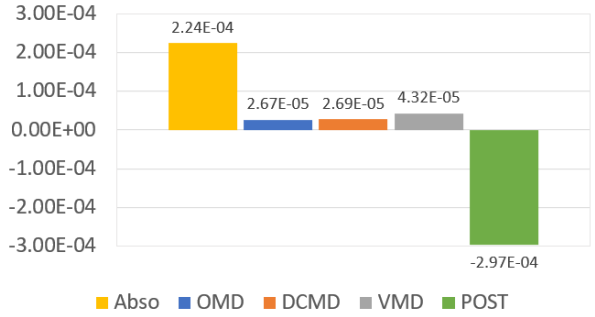

Figure 43 LCIA of optimised LCA with operating conditions - zoom on normalisation of global warming. Abso is absorption with ARG and maximum $\kappa = 0.561$ [mol/kg]. OMD is working until 50% above the saturation level and is coupled with desalination plant. DCMD is working until 50% above the saturation level and with $T_{fi} = 25°C$. VMD works at $T_{fi} = 30°C$ and up the the saturation level. Post stands for post-treatment step with a recovery χ=99%.

V.3 General LCA optimisation routes

Absorption, membrane distillation-crystallisation (MDC) with its 3 different potential processes (OMD, DCMD and VMD) and post-treatment have been extensively described in the previous sections with regard to environmental impacts. Points of attention have been highlighted, showing where emissions are relatively significant. Therefore, several operating conditions and specific to each step were studied. Each step was optimised by different means to reduce emissions.
Now, in this section, general assumptions made at the beginning of the model (i.e LCI in Chapter IV) are studied. Sensitivity analyses on the percentage of recovery, the lifetime of the membrane and the energy sources are performed. This allows the conclusions on the environmental impacts of the process to be qualified.

V.3.1 Recovery percentage χ

In the development of generic LCIs in Chapter IV, it was assumed that the overall recovery would be about $\chi = 99\%$. It implies that for 1 $kgCO_2$ absorbed per hour, 1% of recovered water, $NaHCO_3$ crystals and amino acid (AA) would be lost. However, this parameter represents a significant assumption, as there is not yet a continuous, large-scale installation. In addition, it has been shown in the results sections above that crystal recovery has a real quantitative positive impact on emissions. Therefore, a χ sensitivity analysis might be of interest to qualify the LCIA results and interpretations.

Moreover, it should be reminded that AAs recovery is accounted in the absorption step whilst water and crystals recovered are accounted in the post-treatment. By consequent, absorption and post-treatment are influenced by χ, and MDC remains unchanged. In this section, different recovery percentages χ were investigated: 100, 99 (reference case), 90 and 80 % where the optimised absorption absoA.kMax was considered. Results are available in Figure 44 showing only the absorption and post-treatment steps.

It appears on Figure 44, from a global warming (GW) perspective in the absorption step, that χ plays a important role. Indeed, between an ARG recovery about 100 or 80%, GW emissions change from 1.58 to 5.78 $kgCO_2$-eq which is relatively significant compared to the functional unit (FU) of 1 $kgCO_2$-eq absorbed per hour. Moreover, note that regarding GW emissions, ARG is more sensible to χ than H_2O and $NaHCO_3$ recovery. The same conclusion can be drawn regarding marine eutrophication (MEutro) since this category is relatively more sensible to ARG due to grain cultivation (see Figure C.34).

Additionally, ionising radiation (IR) emissions in post-treatment shows to be relatively independent from χ. As presented earlier in Figure 35, the impact category is mainly affected by electricity demand. The latter was assumed constant in post-treatment, such that χ variations do not impact IR.

To summarise, GW is globally impacted by a lower χ. Other categories as MEutro show the same trend. Therefore, it is worth maximising χ.

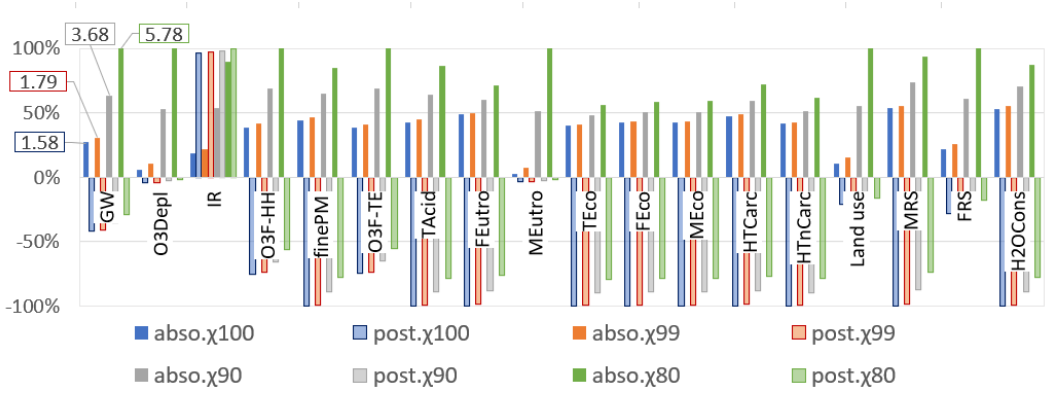

Figure 44 LCIA of absorption and post-treatment with different recoveries χ - characterisation. abso.χ99 refers to the reference case absoA.s0 with ARG and maximum $\kappa = 0.561$ [mol/kg] and where recovery is $\chi = 99\%$ (i.e. post.χ99). All other absorption scenarii with different recovery rates (χ =100, 90 and 80 %) are operated with ARG and under maximum $\kappa = 0.561$ [mol/kg]. Absorption accounts for AA recovery whilst crystals and water recovery is credited to post-treatment. Data labels on the bar charts represent global warming emissions in [kgCO_2-eq]. Abbreviations on the x-axis refer to Table 24.

V.3.2 Membrane lifetime

In this section, the effect on membrane lifetime is studied. In previous LCIAs, the lifetime was considered to be about 5 years [62; 87]. This average value can be subject to a sensitivity analysis since at the laboratory scale, the life span is shorter (1-2 years) and at the industrial and commercial scale, the membranes are used up to 10-15 years [88]. Furthermore, it can be recalled that the optimisation of OMD and DCMD via the saturation level and/or inlet temperature increases the membrane area. These parameters could have greater environmental consequences if the lifetime variations. This section analyses the effect of membrane lifetime on the overall LCAs for: 1, 2, 5 (reference case) and 10 years.

The results are presented in Figure 45, where the complete LCAs by DCMD, i.e. absorption followed by DCMD and post-treatment steps, are presented. DCMD was chosen since the high final concentration C_{fo} and the low inlet temperature T_{fi} considerably increase the membrane area and therefore the amount of membrane to be produced. Therefore, it can be seen from Figure 45 that membrane lifetime has only a small impact on the environmental emissions. Only global warming (GW), marine eutrophication (MEutro) and fossil fuel depletion (FRS) show relatively large variations for different lifetimes.

As a reminder, the different materials and energy inputs to produce a hollow fibre membrane in polypropylene (PP) are given in Table 8. By decreasing the membrane lifetime, some components of the membrane production become significant with respect to environmental emissions. For example, in Figure 45, global warming (GW) has increasing emissions when considering one year of lifetime, mainly due to the increased demand for electricity and solvent to produce more polymer membrane. The solvent considered is dimethylacetamide (DMAC). Figure C.39 shows the different contributors to membrane production in relation to GW. It

confirms the conclusions of the LCA study on polymer membrane production which identified solvent and electricity as the main determinants of environmental emissions [58]. Note that this paper also highlighted the significant contribution of the polymer to environmental emissions. Nevertheless, the polymer selected (PP) in this case does not contribute significantly to carbon emissions (see Figure C.39). Indeed, the quantity of polymer to produce a given membrane area was adapted to the case studied by taking into account a lower density for the PP than for the polymers studied in [58] (i.e. polysulfone, polyvinylidene fluoride or cellulose acetate).

In addition, fossil resources scarcity (FRS) differs due to the need for electricity and the solvent DMAC increasing with shorter lifetimes. (Figure C.40). Variations in marine eutrophication (MEutro) are mainly influenced by the solvent DMAC only (Figure C.41).

In conclusion, membrane lifetime can play a role in reducing emissions. Although, in the already optimised case, a 10-year membrane would reduce emissions by a few tenths of kg/CO_2-eq compared to a one-year lifetime. However, the most affected categories are FRS, MEutro and GW, whilst the other types of emissions are hardly influenced by this parameter. It should be remembered that in the laboratory, the lifetime of membranes is shorter (1-2 years) whereas on an industrial scale, membranes can be operated for a longer period of time (10-15 years [88]), but this depends on the maintenance conditions [88]. If longer lifetime is considered, maintenance should then be included within the system boundaries.

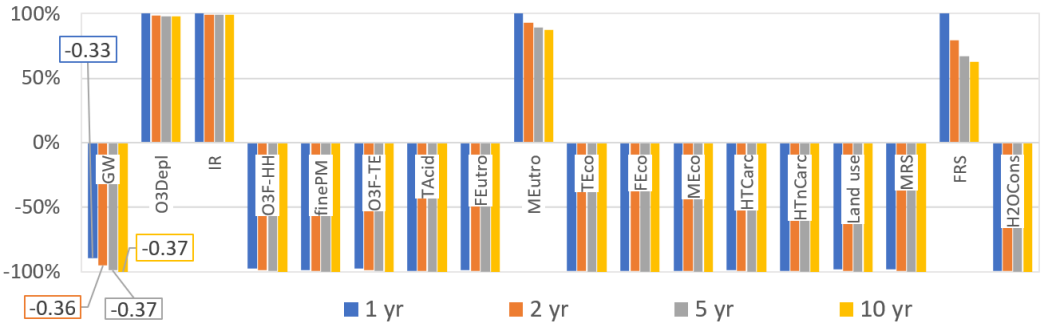

Figure 45 LCIA of full LCA by DCMD for different membrane lifetimes - characterisation. Absorption step is operating with ARG and at maximum $\kappa = 0.561$ [mol/kg]. DCMD is working until 50% above the saturation level and with $T_{fi} = 25°C$. Post-treatment works with a recovery χ=99%. Data labels on the bar charts represent global warming emissions in [kgCO_2-eq]. Abbreviations on the x-axis refer to Table 24.

V.3.3 Electricity source

In a screening report of CE Delft on LCA of CCU routes [51], the different pathways were investigated for fossil and renewable energies. It concludes that environmental conclusions greatly depend on the energy source used by the CCU.
In this paper, the LCI has so far considered energy supplied by and an electricity mix from Ecoinvent. The mix combines electricity from imports, natural gas, nuclear generation, CHP, etc. (see Figure C.42). However, it has been shown in

the previous results that ionising radiation can have a significant impact on the environment due to nuclear energy. In addition, VMD and DCMD have emissions highly determined by the electricity need. In this case, comparing LCAs with different energy sources could be an interesting sensitivity analysis.

In this section, different energy sources are compared: electricity mix (generic case), solar energy (photovoltaic panels), wind energy (onshore wind turbines) and nuclear energy. The results are presented in Figure 46, which shows the complete LCA by VMD, i.e. the sum of the emissions caused by absorption, VMD and post-processing. VMD was chosen as it was shown in Figure 41 that VMD was the worst case scenario and the most emitting MDC process for the majority of the impact categories. The absorption, VMD and post-treatment scenarios here work with optimised scenarios for the operating conditions.

Figure 46 shows that the use of renewable or nuclear energy has a large overall impact on emissions reductions. Solar and wind energy emit less than an electricity mix in many impact categories (12). Nuclear energy has the lowest impacts in many categories (11), including global warming (GW). However, its impact on ionising radiation (IR) and marine eutrophication (MEutro) is the highest compared to other energy types. The electricity mix was already composed of nuclear energy sources (see figure C.43). This explains the higher IR and MEutro emissions when opting for a full nuclear source. It should be noted that uranium is mainly responsible for MEutro emissions from nuclear energy (see Figures C.44 and C.45).

In addition, the electricity mix is found to be relatively high in stratospheric ozone depletion (O3Depl) and MEutro. As mentioned above, nuclear electricity, which is part of the electricity mix, is strongly responsible for MEutro emissions because of uranium. In addition, O3Depl is caused by nuclear, biogas and natural gas from the electricity mix (see Figures C.46 and C.47).

In conclusion, the choice of an energy source is a delicate task. Beyond material and economic considerations, each energy source is the most emitting in one or more impact categories. Nuclear power emits the least carbon, but its IR and MEutro emissions are the highest. Solar and wind power emit less than an electricity mix in the majority of categories, whilst renewable energy by wind depicts a less emitting source compared to solar energy in every categories.

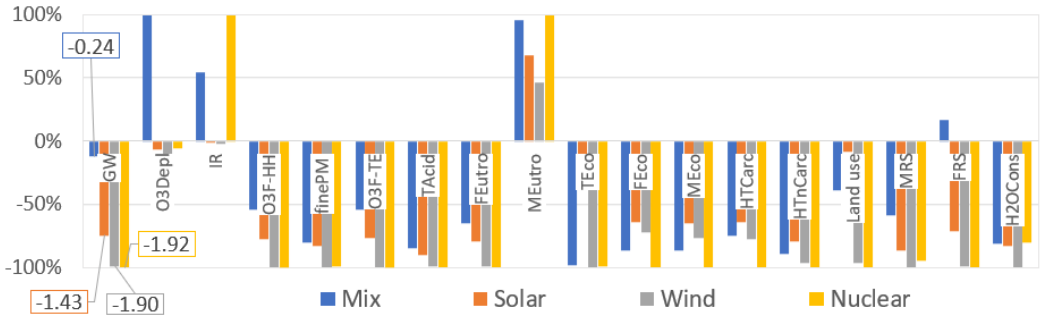

Figure 46 LCIA of full LCA by MD for different energy sources - characterisation. LCA by VMD sums up emissions due to absorption, VMD and post-treatment. Absorption step is operating with ARG and at maximum $\kappa = 0.561$ [mol/kg]. VMD is working up to the saturation level and with $T_{fi} = 30°C$. Post-treatment works with a recovery χ=99%. Membrane lifetime is worth 5 years. All energy source are data for Belgium. Mix represents an electricity mix, solar energy is produced via photo-voltaic panels, wind via onshore wind turbines, and nuclear via Belgian power plants. Data labels on the bar charts represent global warming emissions in [kgCO_2-eq]. Abbreviations on the x-axis refer to Table 24.

Chapter VI

Conclusion and future work

The purpose of this thesis is to quantify the environmental impacts of a specific process of carbon capture and utilisation (CCU) still under development in the laboratories of UCLouvain. To this end, a life cycle assessment (LCA) is carried out on the process following the 4-step LCA methodology.

The capture process studied aims at absorbing CO_2 emissions from flue gases by means of membrane gas absorption using an aqueous Na_2CO_3 solution and promoted by amino acids. Two types of amino acids are studied: arginine (ARG) and sarcosine (SAR). A chemical reaction absorbs CO_2 into $NaHCO_3$ in the aqueous solvent. Then, the distillation-crystallisation of this compound is operated thanks to a membrane contactor. This step can be performed via 3 different membrane distillation-crystallisation (MDC) processes: osmotic membrane distillation (OMD), direct contact membrane distillation (DCMD) and vacuum membrane distillation (VMD). Each membrane technology is experimented at UCLouvain on a laboratory scale and under batch mode. Part of the work of the thesis aims at scaling up the membrane set-ups and making them evolve towards continuous modes. Finally, a post-processing step allows the recovery of the $NaHCO_3$ crystals.

The thesis reveals that the studied CCU process could be a promising technology to reduce carbon emissions by storing CO_2 and revaluing it into $NaHCO_3$ crystals. Several scenarii and their LCAs are established to highlight the environmental issues of the CCU. The different optimisation pathways and the life cycle impact assessment (LCIA) are summarised in Figure 47 and Table 30. Furthermore, it is shown that the 3 MDC processes have different advantages and disadvantages depending on the impact category considered. For example, VMD causes the highest carbon emissions, while OMD and DCMD have a lower and equivalent carbon footprint. In an other impact category, OMD presents the highest stratospheric ozone depletion and DCMD the lowest.

First of all, the membrane gas absorption step reveals to be the most emitting step among the MDC and post-treatment processes, for almost all types of emissions. The reduction of Na_2CO_3 use is the key point to minimise emissions related to absorption. Therefore, the solvent flowrate must be reduced. To do this, κ, the loading of CO_2 into the solvent, must be maximised so that the solvent reaches

absorption saturation. Simultaneously, this leads to a decrease in absorption performance due to an overall decrease in K_{ov}. Moreover, a higher K_{ov} is achieved with a solvent promoted by ARG than by SAR. Therefore, and with respect to environmental concerns, absorption should be performed by saturating the ARG-promoted solvent.

Secondly, with regard to MDC, none of the 3 potential processes (OMD, DCMD or VMD) has the lowest impacts for all types of emissions. However, DCMD occupies an overall intermediate position with moderate emissions compared to OMD and VMD. In addition, MDCs are subjected to different sensitivity analyses in order to identify the preferred operating conditions in relation to environmental issues.
OMD should be operated when coupled with a desalination plant. In this case, the osmotic solution comes from the residual brine of the reverse osmosis desalination.
DCMD minimises emissions most when the temperature at the feed inlet T_{fi} is 25°C and at the permeate inlet 5°C. The permeate inlet temperature T_{pi} could also be changed to be closer to room temperature. However, the emissions savings were greater with $T_{fi} = 25°$ than with $T_{pi} = 20°$. In addition, OMD and DCMD should distil the solution as much as possible. A saturation level about 50% of the $NaHCO_3$ is considered acceptable to avoid membrane clogging.
VMD have emissions where the electricity consumption for permeate condensation is the main determining factor. Therefore, minimisation of emissions from VMD can be achieved by a low saturation level. Further emission reductions are achieved when $T_{fi} = 30$°C.
An overall conclusion shows that reducing the solvent flowrate in absorption is a win-win situation, leading to a reduction of the emissions in MDC too.

Thirdly, the post-treatment stage depicts a significant reduction in environmental emissions through the recovery of $NaHCO_3$ crystals. These are taken into account in the LCA through *avoided products*.

General assumptions are subsequently analysed: membrane lifetime, recovery rate and energy source were subjected to sensitivity analysis. To further reduce emissions, the recovery rate should be maximised. In addition, the lifetime of the membrane was found to have a relatively small influence on the environment compared to the other parameters. Nuclear power has the lowest carbon footprint, but the highest emissions of ionising radiation and marine eutrophication. And wind power has lower overall emissions than solar power.

In addition, the environmental LCIAs are normalised by the means of Recipe (H) midpoint. This allows different types of emissions to be compared. Indeed, the carbon footprint is the quantitative focus such that emissions at a characterisation level must be kept below 1 $kgCO_2$-eq in order to save more than it emits. However, normalised LCIA reveals that the process causes higher normalised emissions for ecotoxicity and carcinogenicity than for carbon footprint. Nevertheless, when optimised, the overall CCU process shows negative emissions in these categories as well.

The insights gained from this process with regards to environmental concerns could provide a reference point for further research. The development of the process in

the laboratory in continuous mode and research to optimise the post-treatment should be carried out. The LCI model could also be the subject of future work for further improvements, such as:

- The recycling of Na_2CO_3 particles from the post-treatment to the absorption could be accounted for.
- Heat recovery in the DCMD could be explored.
- The remaining particles of Na_2CO_3 in the solution could be taken into account in MDC (for K_{ov} and water activities).
- The extension of the system boundaries can be done since a LCA is an iterative study. Transport emissions, nano-filtration, control devices (flow regulation, temperature control, flow meters, etc. [89]), maintenance and end of life of the membrane [88] could be evaluated within the LCA.

As other LCAs on CCU technologies published in the scientific literature [51; 53; 47], the CCU studied here could be a process of potential interest to reduce environmental emissions and especially the carbon footprint. However, further experimental research and LCA modelling could be carried out to pursue a more accurate quantification of emissions. Further work suggests focusing on a LCA on the CO_2 revalorisation in order to determine whether the production of $NaHCO_3$ by capturing CO_2 is indeed more environment-friendly than conventional $NaHCO_3$ production. It could also be interesting to compare LCAs of membrane gas absorption promoted by amino acids against conventional monoethanolamine (MEA). Or to compare the LCA of the present CCU process with other LCAs on CCU technologies. The resulting LCA could also be integrated to a techno-economic assessment to examine its technological feasibility and economic profitability [52]. Lastly, the Intergovernmental Panel on Climate Change (IPCC) recently published its 6th report on climate change [90]. In this report, carbon capture and storage (CCS) is presented as a potential means of CO_2 removal. However, the report focuses more on CCS than on CCU. This is partly due to a lack of literature allowing for a better assessment. Nevertheless, one could expect that CCU will be widely developed in the future, with increasing interest and publications, as is the case for their LCAs [56].

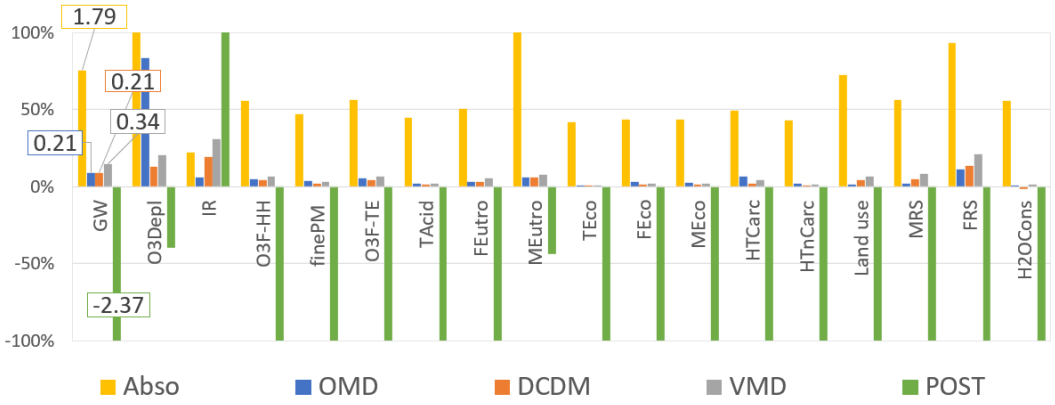

Figure 47 Resume of LCIA of the optimised LCA - characterisation, Recipe (H) midpoint method. Abso is absorption operating until saturation and with ARG and a maximum $\kappa = 0.561$ [mol/kg]. OMD is working until 50% above the saturation level and is coupled with desalination plant. DCMD is working until 50% above the saturation level and with $T_{fi} = 25°C$. VMD works at $T_{fi} = 30°C$ and up the the saturation level. Post stands for post-treatment step with a recovery χ=99%. Data labels on the bar charts represent global warming emissions in [kgCO_2-eq]. Abbreviations on the x-axis refer to Table 24.

Table 30 Summary of optimisation routes and consequences regarding environmental emissions. The optimisation routes resume the operating conditions and general assumptions that result in the lowering of environmental emissions. The range of experiences on parameters were T_{pi} between 5-20°C, and T_{fi} in DCMD between 25-40°C and in VMD between 40-30°C. C_{fo} ranges between 0-50% above the saturation level. The recovery rate χ was between 80-100%. The membrane lifetime changed from 1 to 10 years.

	Optimisation routes	**Consequences**	
		Advantages	**Drawbacks**
Absorption	Maximisation of CO_2 load Arginine as promoting agent	ABSO : lower solvent flowrate Global : higher C_{fi} OMD : less permeate DCMC: less electricity to heat/cool the feed/permeate VMD : less electricity for condensing	Abso : lower K_{ov}
OMD	Coupling with desalination plant	OMD: osmotic solution comes from recycled brine	ALL : geographical limitations
	High C_{fo}	OMD : higher brine dilution going to brine treatment	OMD : higher A_m
DCMD	High T_{pi}	DCMD : less electricity to cool the permeate	DCMD : higher A_m
	Low T_{fi}	DCMD : less electricity to heat feed	DCMD : higher A_m
	High C_{fo}	DCMD: higher H_2O recovery	DCMD : higher A_m
VMD	Low T_{fi}	VMD : less electricity to heat the feed	VMD : higher A_m POST : important post-treatment (crystalliser tank)
	Low C_{fo}	VMD : less electricity for the condenser	
Recovery χ	Highest, near 100% is the best	ABSO: higher AA recovery POST : higher H_2O and $NaHCO_3$ recovery	
Membrane lifetime	Longest possible	ALL: lower A_m per FU	Membrane maintenance, feasibility
Energy source	Nuclear power	Global : lowest global warming	Global : highest IR
	Wind power	Global : lower emissions than solar	

Appendices

Appendix A

Literature review

A.1 CO_2 absorption

A.1.1 Amino acids reaction mechanism

Amino acids, used as CO_2 capture agents and promoted by sodium carbonates, are organic compounds with a carboxyl (-COOH) and amine (-NH_2) functional group (Figure 7a). A side chain (R group) is present in the molecule and is specific to each amino acid. In total, there are 20 different types of amino acids. The general structure is illustrated in Figure 7a. In order to identify the isomeric and enantiomeric amino acids, the letters L and D are used respectively to define the amino acids. However, D isomers are rarely found in nature.[8] In the present document, arginine (arginine (ARG)) and sarcosine (sarcosine (SAR)) in aqueous solution favoured by sodium carbonate are studied as potential solvents for CO_2 absorption. The molecular structure of these two amino acids is shown in Figures 7b and 7c.

The generally accepted reaction mechanism for describing CO_2 absorption by amino acid promoters is the zwitterion mechanism. In the case of the use of ARG as an amino acid, the CO_2 reacts with the salt of the amino acid (here sodium salt of arginine, NaArg), and forms the zwitterion (Reaction (21)). This intermediate is further deprotonated with the bases B (CO_3^{2-}, H_2O, OH^-, ...) present in the solution, producing, among others, bicarbonates $NaHCO_3$ (Reaction (22)) [8; 20]

$$CO_2 + H_2N{-}CHR'{-}COO^-Na^+ \longrightarrow {}^-COO^+H_2N - CHR'{-}COO^-Na^+ \quad (21)$$

$${}^-COO^+H_2N{-}CHR'{-}COO^-Na^+ + B \longrightarrow {}^-COOHN{-}CHR'{-}COO^-Na^+ + BH^+ \quad (22)$$

A similar mechanism can be applied in the case of a sarcosine amino acid.

Another important reaction during the absorption process is the dissociation of water:

$$2H_2O \rightleftharpoons OH^- + H_3O^+$$

Depending on the pH, the mechanism is different, and some reactions may be neglected. With a pH<8, the dissolved CO_2 is hydrated to form carbonic acid, then the carbonic acid reacts again with OH^-. Here, the rate control step is Reaction (23).[91]

$$\begin{aligned} CO_2 + 2\,H_2O &\rightleftharpoons HCO_3^- + H_3O^+ \qquad (Fast) \\ HCO_3^- + H_2O &\rightleftharpoons CO_3^{2-} + H_3O^+ \qquad (Instantaneous) \end{aligned} \tag{23}$$

In the case of pH>8 that corresponds to interesting commercial application, the reaction of CO_2 and H_2O that produces bircarbonates HCO_3^- can be neglected. In this basic solution, the formation of bicarbonate take place with the reaction of CO_2 and OH^- and the reaction of HCO_3^- with OH^-. The rate-limiting reaction is given by the other Reaction (24) of CO_2 reacting with OH^-.[20; 91]

$$\begin{aligned} CO_2 + OH^- &\rightleftharpoons HCO_3^- \quad (Fast) \\ HCO_3^- + OH^- &\rightleftharpoons CO_3^{2-} + H_2O \quad (Instantaneous) \end{aligned} \tag{24}$$

Simultaneously to that, the carbonate Na_2CO_3 presents in the aqueous solution will also react with CO_2. The carbonate is transformed into bicarbonate via an exothermic reaction [91] :

$$CO_2 + H_2O + Na_2CO_3 \rightleftharpoons 2\,NaHCO_3$$

After the absorption of CO_2 by amino acids and the carbonates, the liquid outstream is mostly composed of a solution of sodium bicarbonates ($NaHCO_3$) in liquid phase and amino acids.

A simplified flowsheet of the studied process is presented next page on Figure 11.

A.1.2 Driving Force

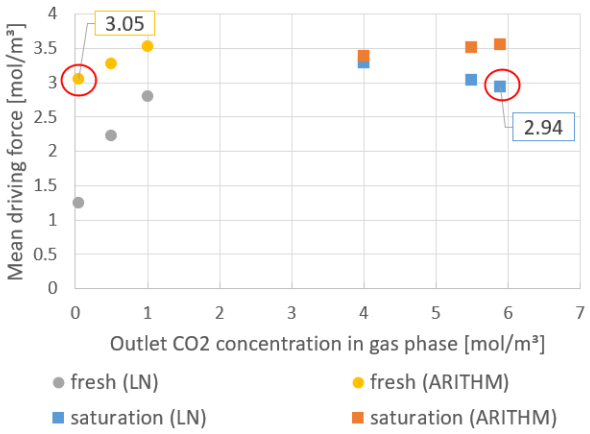

Figure A.1 Driving force of membrane gas absorption based on CO_2 concentration gradients. Two extreme cases are outlined: fresh solvent and saturation. Two average ways to calculated the driving force were studied: arithmetic and logarithmic means. On a physical point of view, the driving force of a fresh solvent should be higher than for a saturated solvent.

Appendix B

LCI

B.1 Impact categories

Midpoint impact category	Indicator	CF_m	Unit
Climate change	Infrared radiative forcing increase	Global warming potential (GWP)	kg CO_2-eq to air
Ozone depletion	Stratospheric ozone decrease	Ozone depletion potential (ODP)	kg CFC-11-eq to air
Ionising radiation	Absorbed dose increase	Ionising radiation potential (IRP)	kBq Co-60-eq to air
Fine particulate matter formation	PM2.5 population intake increase	Particulate matter formation potential (PMFP)	kg PM2.5-eq to air
Photochemical oxidant formation: terrestrial ecosystems	Tropospheric ozone increase	Photochemical oxidant formation potential: ecosystems (EOFP)	kg NOx-eq to air
Photochemical oxidant formation: human health	Tropospheric ozone population intake increase	Photochemical oxidant formation potential: humans (HOFP)	kg NOx-eq to air
Terrestrial acidification	Proton increase in natural soils	Terrestrial acidification potential (TAP)	kg SO_2-eq to air
Freshwater eutrophication	Phosphorus increase in freshwater	Freshwater eutrophication potential (FEP)	kg P-eq to freshwater
Human toxicity: cancer	Risk increase of cancer disease incidence	Human toxicity potential (HTPc)	kg 1,4-DCB-eq to urban air
Human toxicity: non-cancer	Risk increase of non-cancer disease incidence	Human toxicity potential (HTPnc)	kg 1,4-DCB-eq to urban air
Terrestrial ecotoxicity	Hazard-weighted increase in natural soils	Terrestrial ecotoxicity potential (TETP)	kg 1,4-DCB-eq to industrial soil
Freshwater ecotoxicity	Hazard-weighted increase in freshwaters	Freshwater ecotoxicity potential (FETP)	kg 1,4-DCB-eq to freshwater
Marine ecotoxicity	Hazard-weighted increase in marine water	Marine ecotoxicity potential (METP)	kg 1,4-DCB-eq to marine water
Land use	Occupation and time-integrated land transformation	Agricultural land occupation potential (LOP)	$m^2 \times$ yr annual cropland-eq
Water use	Increase of water consumed	Water consumption potential (WCP)	m^3 water-eq consumed
Mineral resource scarcity	Increase of ore extracted	Surplus ore potential (SOP)	kg Cu-eq
Fossil resource scarcity	Upper heating value	Fossil fuel potential (FFP)	kg oil-eq

Figure B.2 Overview of the midpoint impact categories of Recipe 2016.[92]

B.2 Library selection

Ecoinvent [83] releases 3 versions of the library database: cut-off allocation (cut-off), allocation at the point of substitution (APOS) and consequent (conseq). Each version has a different methodological approach to multifunctionality and data types. The main differences are summarised in Table B.3.

Multifunctionality involves a process that creates multiple products and there are different approaches to deciding how to assess the burdens associated with **multifunctionality**. The first approach is to avoid allocation. System expansion or subdivision can therefore be applied. With **system expansion** in conseq, by-product inventories could be subtracted from multi-product outputs, leading to the use of *avoided products* in SimaPro. A second alternative is to opt for **allocation**, which can be done on the basis of physical relationships (mass or energy) or economic factors (cut-off and APOS). [59] However, "*ISO 14044 states that allocation should be avoided where possible*". [93]

The end-of-life scenario is also a central point of allocation, where it has to be decided which life cycle benefits from the benefits and burdens of the recycling process and/or the virgin materials avoided. For example, when plastic bottles are burnt and energy is recovered, is this electricity allocated to the life cycle of the plastic bottles or to the life cycle using this generated electricity? On the one hand, the **cut-off** approach allocates recycling activities to the life cycle using recycled materials as inputs. Indeed from ISO 14044:2006 [93] : "*Specification of the amount of material or energy flow or level of environmental significance associated with the unit processes or product system to be excluded from a study*". On the other hand, **APOS** will allocate the loads at the point of substitution taking into account the allocation factors.[93]

As far as data is concerned, **conseq** is different as it uses marginal data. Indeed, conseq evaluates the change in the consequences of a change in an existing, marginal and outdated system or process. This library is used for perspective studies.

The choice of the most appropriate library is important to maintain consistency between the background and foreground databases. However, as the benefits of pure water recovery in DCMD and VMD and $NaHCO_3$ in post-treatment are taken into account the LCA, the use of the cut-off approach is to be excluded here. As far as conseq is concerned, the assessment of benefits via *avoided products* could be very interesting. However, $NaHCO_3$ is not available in the consequential database. Indeed, the current production of this crystal is not marginal, and the production of $NaHCO_3$ by the CCU could not substitute the current productions of $NaHCO_3$. Moreover, the definition of the function and its FU (see Table 3) deals with CO_2 absorption as the primary interest. Therefore $NaHCO_3$ is more a by-product than the main product which would aim to compete with conventional $NaHCO_3$ production units. For these different reasons, the conseq library in Ecoinvent should also be excluded, and APOS is therefore adopted.

By **choosing APOS**, allocation factor is the consistent methodology for allocating the benefits of water and $NaHCO_3$ recovery, rejecting the use of *avoided*

products.

However, regarding the benefits of $NaHCO_3$ production and despite APOS as background model, it was decided to use **avoided products** in order to clearly illustrate the positive environmental impacts of this production throughout the LCA. Inconsistencies between the background and foreground have already been noted in previous scientific papers [94]. Furthermore, water recovery from DCMD and VMD is also accounted via avoided product. Note that future work could perform a sensitivity analysis to compare several multifunctionality approaches (avoided product vs allocation factors by mass or value).

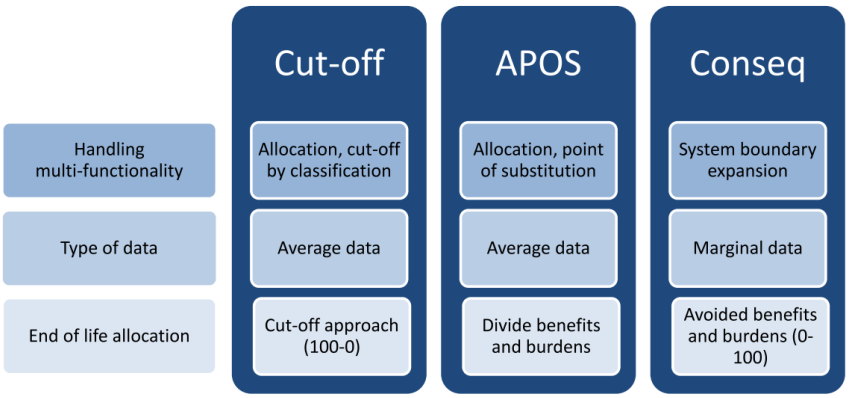

Figure B.3 Libraries in Ecoinvent.[93]

B.3 Membrane characteristics

Table B.1 Technical characteristics of membrane contactor, the 3M™ Liqui-Cel™ MM-1x5.5 Series hollow fiber membrane contactor, Germany [21; 33].

Membrane characteristics	**Data**	**Unit**
Module configuration	Hollow fibers	
Membrane material	polypropylene (PP)	
Effective membrane surface area	0.18	m^2
Number of fibers	2300	
Effective fiber length	0.1397	m
Wall thickness	40	μm
Outer radius r_o	150	μm
Inner radius r_i	120	μm
Density PP ρ_p	0.9	g/cm^3

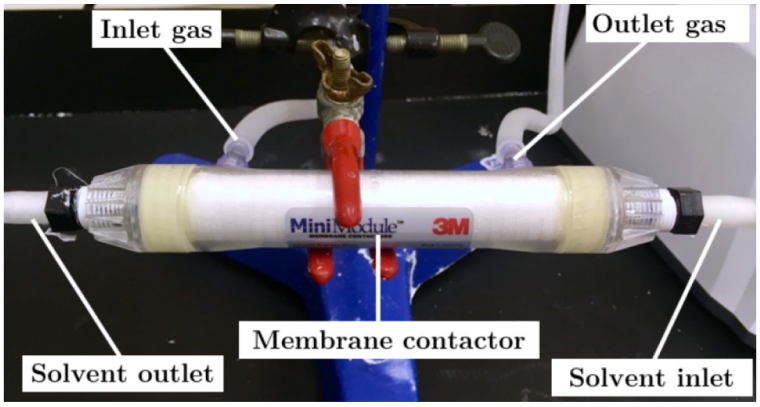

Figure B.4 Membrane contactors inlets and outlets.[21]

B.4 Amino acids production pathway selection

Because arginine (ARG) and sarcosine (SAR) are not available in the background database of Ecoinvent, the required materials and energy inputs for their production must be found in the literature. Different sources and possible production pathways are simulated in SimaPro and compared to keep the best and representative pathways production of ARG and SAR.
The production of amino acids can be performed either by **chemical synthesis or fermentation** (Figure B.5). ARG is most commonly industrially synthesised by a fermentation pathway production, while SAR is produced via chemical synthesis or fermentation. [95]

B.4.1 ARG

The most common biobased industrial production of amino acids is fermentation from glucose. However, the industrial production capacity of amino acids by microbial synthesis is usually low while its range of applications is growing (pharmaceutical, cosmetic, food, and agricultural industries) [96]. Therefore, to improve the production yields and meet the market demand, *Corynebacterium glutamicum* bacteria is used. Nowayadays, this *Corynebacterium* is selected as strain for the breeding of ARG and is used on a commercial scale. [97; 98; 95] The fermentation metabolic pathway of ARG in *Corynebacterium glutamicum* can be seen in Figure B.6.

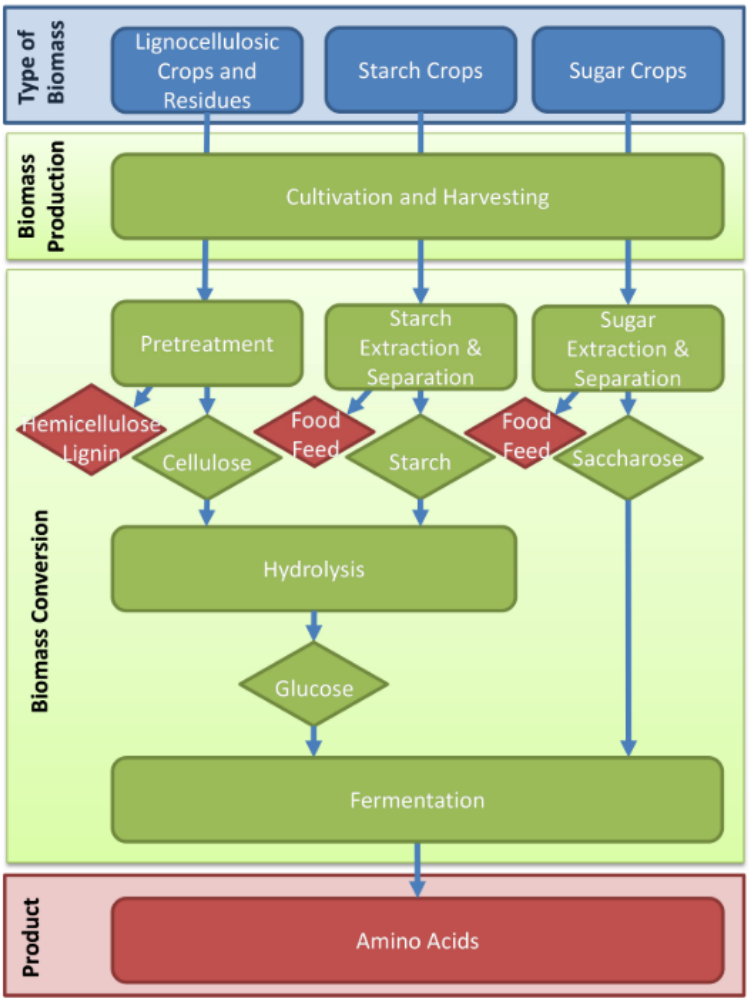

Figure B.5 Fermentation chains of amino acids.[95]

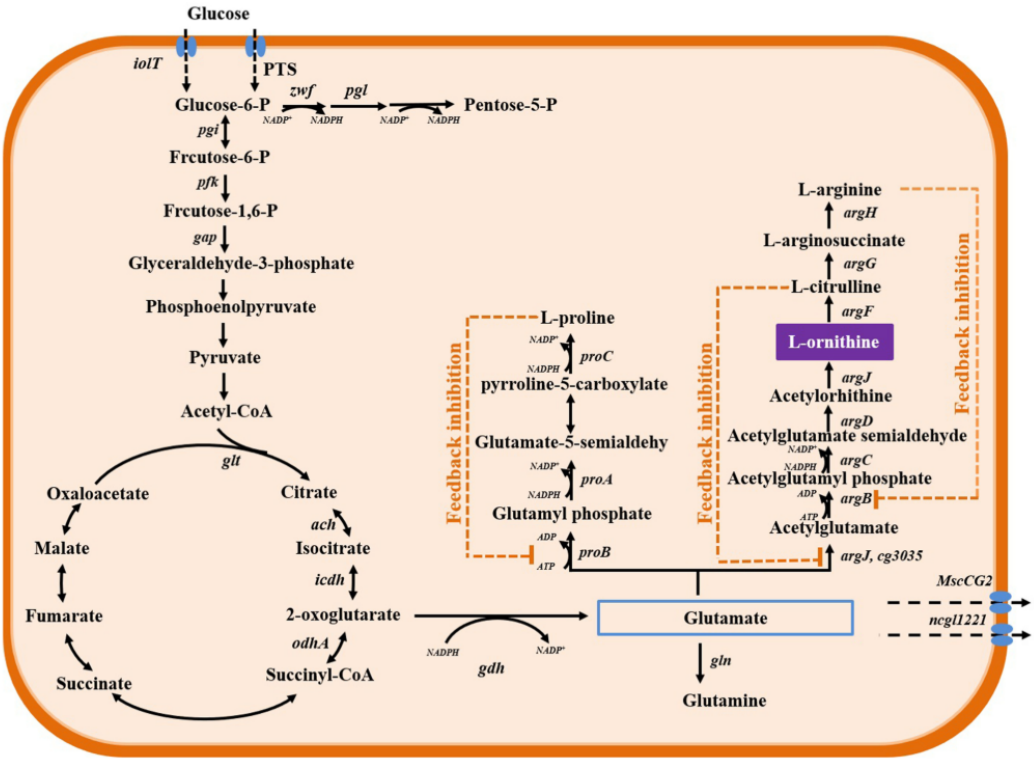

Figure B.6 Biosynthesis of ARG in *Corynebacterium*.[98]

ARG by raw materials

A first model to simulate the production of ARG is given by [97] where only materials inputs are considered. Glucose, ammonia and oxygen are the essential raw materials. Note that ammonia is the nitrogen source since arginine contains 4 nitrogen atoms (Figure B.7). [97]

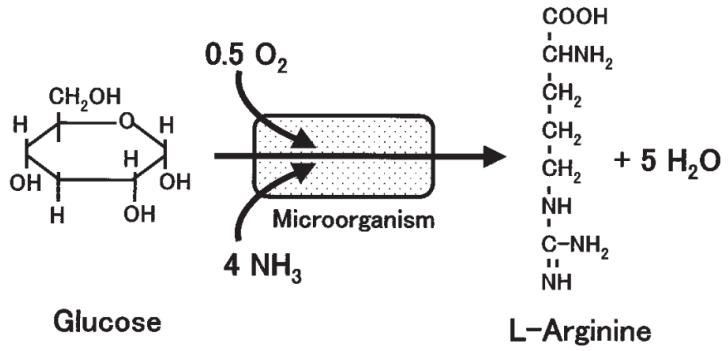

Figure B.7 Biological synthesis of ARG production from raw materials.[97]

ARG by E. Coli

To meet and improve the growing market demand on ARG, research is also performed using *Escherichia coli* strains. As a matter of fact, for environmental concerns, renewable raw materials widely available and not competing with food industry should be promoted. Lignocellulosic biomass as feedstock presents these advantages, but it includes other monosaccharides besides glucose (i.e, xylose, mannose, galactose). *Corynebacterium* strains can only handle pentoses, while *Escherichia coli* is able to use pentoses as well as hexoses. Therefore, *Escherichia coli* is a potential candidate for fermentation production of ARG. As a result, research showed that ARG can be produced with a yield of 0.17 $g_{arg}/g_{glucose}$ and a C/N molar ratio of 6, where NH_4Cl is the nitrogen source. [99]

ARG by lysine

Furthermore, another model to simulate the ARG production is based of lysine. Lysine is an amino acids which has a similar industrial fermentation pathway to ARG as it can be seen in Figure B.8. It is therefore assumed that the materials and energy required to produce lysine are similar to those for arginine. [100] Information on the lysine production was studied in a previous study [61], where data were supplied by a working group on feed-use amino acids of EU Association of Specialty Feed Ingredients and their Mixtures (FEFANA). These data are available in Table B.2. [61]

Table B.2 LCI inputs for the production of 1 kg lysine.[61]

Components	Amount	Unit
Sugar	1	kg
Maize starch	0.5	kg
Wheat starch	0.5	kg
Liquid ammonia	0.3	kg
Energy		
Electricity mix	18	MJ
Natural gas	18	MJ

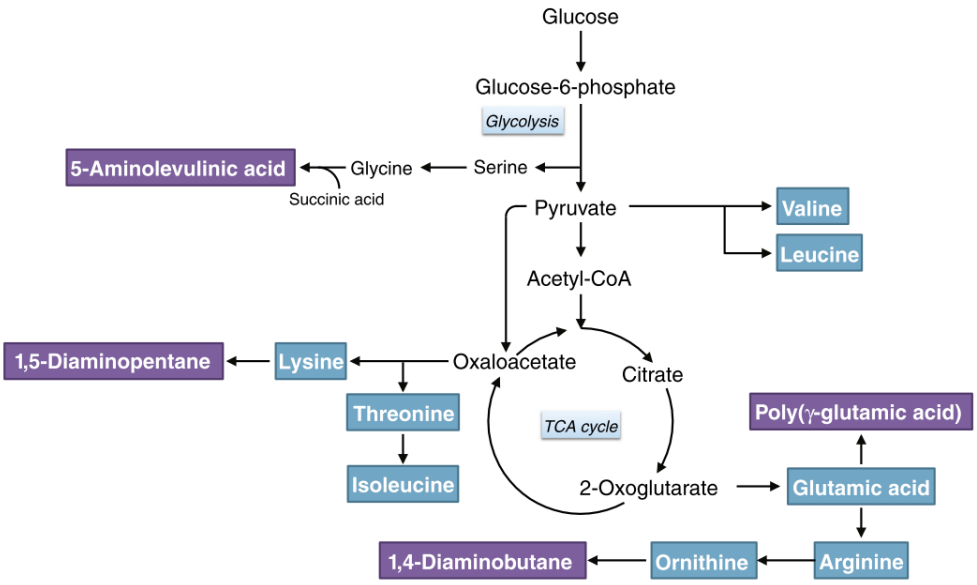

Figure B.8 Metabolic pathway for production of arginine and lysine.[100]

ARG by MSG

Finally, a last model of ARG production consists in using the glutamate production pathway. Indeed, ARG is produced, among other things, from the intermediate product glutamate (Figure B.8). An previous LCA study [101] was carried out on the production of MSG. The system boundaries added one step, refining, where the salts Na_2CO_3 and Na_2PO_4 are needed to convert glutamic acids into monosodium glutamate (MSG). These salts were therefore not taken into account to fit the LCA of MSG to ARG. [101] The inputs data are given in Table B.3.

ARG production pathway selection

Considering the 4 potential ARG production models, their respective LCAs were performed on SimaPro with the Recipe 2016 (H) midpoint method, for the production of 1kg of ARG.

The results are presented in Figure B.9. It is concluded that the production of ARG using *Escherichia coli* strains is not interesting and that the commercially used strain *Corynebacterium* is more optimised. Moreover, the production of ARG via *E.coli* and based exclusively on raw materials is to be excluded because the energy inputs are not taken into account. Finally, it can be noted that the simulation of

Table B.3 LCI inputs for the production of 1 ton MSG.[101]

Components	Amount	Unit
Maize grain	1.82	t
Liquid ammonia	0.24	t
H_2SO_4	0.33	t
Active carbon	0.01	t
SO_2	2.76	kg
water	8.28	t
Energy		
Electricity mix	916.58	kWh
Steam	7.14	t

ARG via MSG and lysine takes into account both material and energy inputs, and that these 2 simulations give results of the same order of magnitude.

However, the data on MSG inputs were collected in China, while the lysine input data are collected in Europe and are therefore more relevant. Furthermore, to remain consistent with SAR and to present a more reliable comparison between ARG and SAR, ARG with lysine is considered as a better production model.

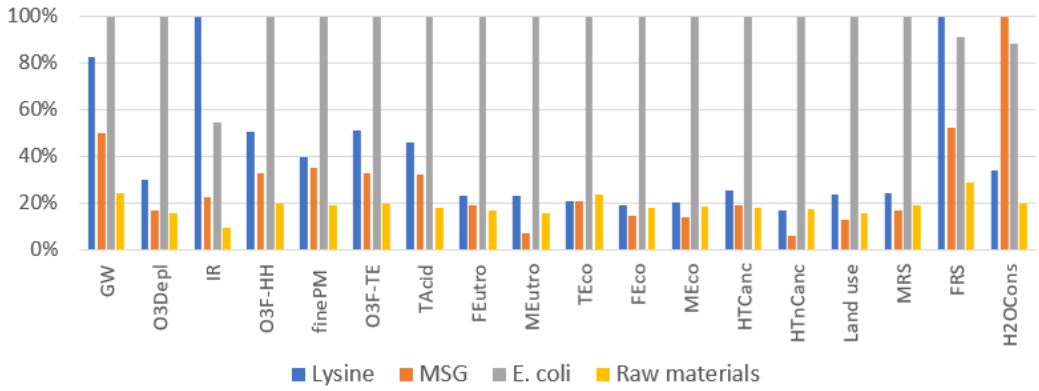

Figure B.9 LCIA comparison of different production pathways of ARG. Abbreviations on the x-axis refers to Table 24.

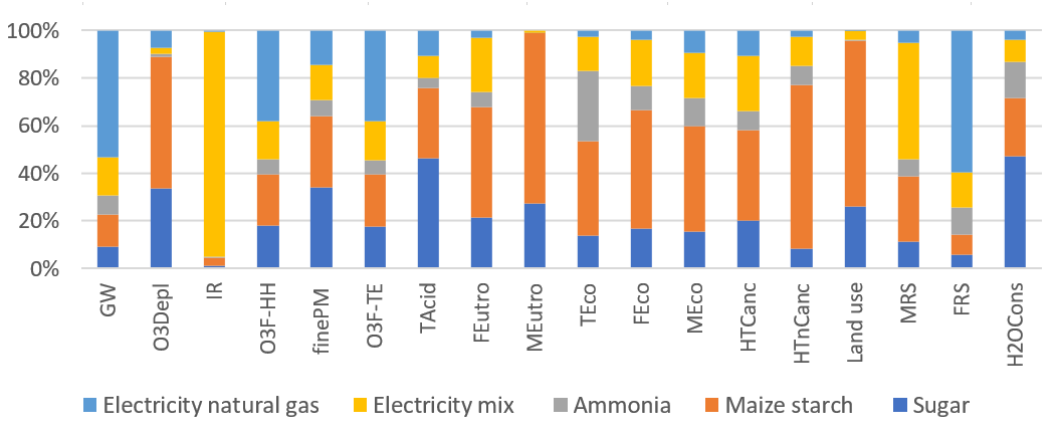

Figure B.10 LCIA for the production of 1kg ARG by lysine. Abbreviations on the x-axis refers to Table 24.

B.4.2 SAR

Currently, sarcosine is produced either chemically or based on fermentation in *Corynebacterium glutamicum* strains. [102]

SAR by glucose fermentation

Firstly, a production method of SAR by fermentation has been carried out in [102] based on a mixture of glucose, potassium acetate and monoethylamibe. Glucose in *C. glutamicum* is the source of carbon and energy in SAR production. Different case study were performed, and the simpliest scenario was here considered. The data are given in Table B.4. [102]

Table B.4 LCI inputs for the production of 2 g SAR from fermentation.[102]

Components	Amount	Unit
Glucose	12	g
Potassium acetate	20	g
Monoethylamine	3.1	g

SAR by glycine

Furthermore, sarcosine can be seen as an intermediate product in glycine production. SAR is degraded to glycine by the enzyme dehydrogenase in the metabolic pathway (Figure B.11).[103] Therefore it can be considered to model the production of SAR by the production of glycine available in the Ecoinvent database.

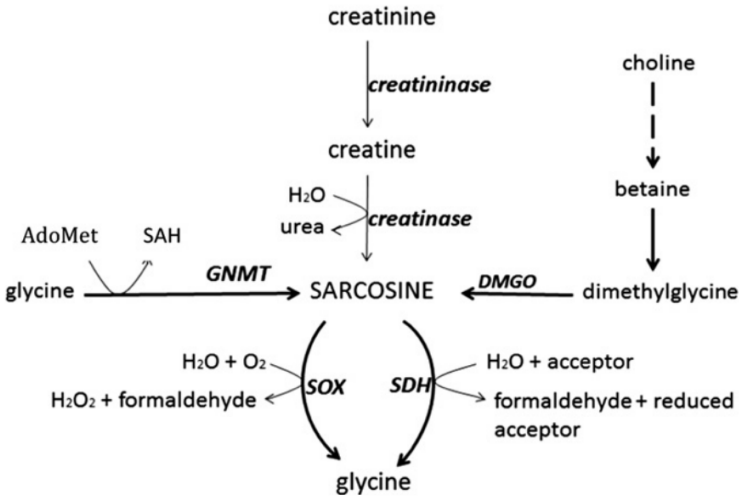

Figure B.11 SAR metabolism by glycine.[103]

SAR by methionine

SAR and methionine are similar in their production processes. Indeed, SAR can be an intermediate product of the fermentation production of methionine. In addition, both RAS and glycine can be produced by chemical synthesis. [95; 104] As a result, it can be assumed that the materials and energy required to produce methionine are similar to those for sarcosine. Information on the chemical and industrial production of methionine has been provided previously by FEFANA and is presented in Table B.5 [61].

Table B.5 LCI inputs for the production of 1kg methionine.[61]

Components	Amount	Unit
Propylene	0.43	kg
Hydrogene sulfide	0.27	kg
Methanol	0.39	kg
Hydrogen cyanide	0.21	kg
Energy		
Electricity mix	3.7	MJ
Natural gas	3.7	MJ

SAR by chemical reaction with chloroacetic acid

Next, model of SAR production exists and is based on chemical synthesis and the interaction of chloroacetic acid and methylamine [105]. The materials required for the chemical synthesis are given in Table B.6.

SAR by chemical reaction with formaldehyde

A last model was found in the literature. This chemical synthesis of SAR is based on the reaction of methylamine and formaldehyde solution. The materials data are given in Table B.7 [106].

SAR production pathway selection

As for the ARG, the production of 1 kg of SAR was simulated in SimaPro to

Table B.6 LCI inputs for the production of 18 g SAR chloroacetic acid.[105] No precise data was given for ethanol (needed for post-treatmentà, such that it was decided to take 0.2L of it.

Components	**Amount**	**Unit**
Chloroacetic acid	47.5	g
Methylamine	462	g
DI water	1.33	kg
Ethanol	0.2	L

Table B.7 LCI inputs for the production of 22 g SAR from formaldehyde solution. It is mentionned that a *"little amount"* is added to the solution, which was decided to be 5g.[106]

Components	**Amount**	**Unit**
Formaldehyde solution (37%)	120	cm^3
Methylamine hydrochloride	67.5	g
Chloroacetic acid	47.5	g
Potassium cyanide	65	g
Ethanol	5	g

compare the 5 production models. The Recipe 2016 (H) midpoint method was applied. The results of the different impact categories are presented in Figure B.12.

First of all, it can be concluded that SAR production from glucose fermentation and chemical synthesis of chloroacetic acid performs the poorest results and should be excluded.Furthermore, the model based on formaldehyde dates back to 1915 and does not show to be applicable on an industrial scale, so it can be assumed that this technology is not relevant. Furthermore, these 3 models (glucose fermentation, chloroacetic acid and formaldehyde) only take material inputs.

Concerning glycine, it was mentioned that SAR is an intermediate product of glycine fermentation. However, the glycine process developed in Ecoinvent is based on the chemical synthesis of glycine from chloroacetic acid [83]. SAR by glycine is also to be excluded.

Finally, the methionine-based model for SAR production seems more practical. Although in this model methionine is obtained chemically and the SAR is a by-product of fermentative methionine production, the methionine SAR has the advantage that the data are taken from the same scientific paper [61]. Therefore, both data for ARG and SAR were collected in Europe and are considered with the same weighting and reliability.

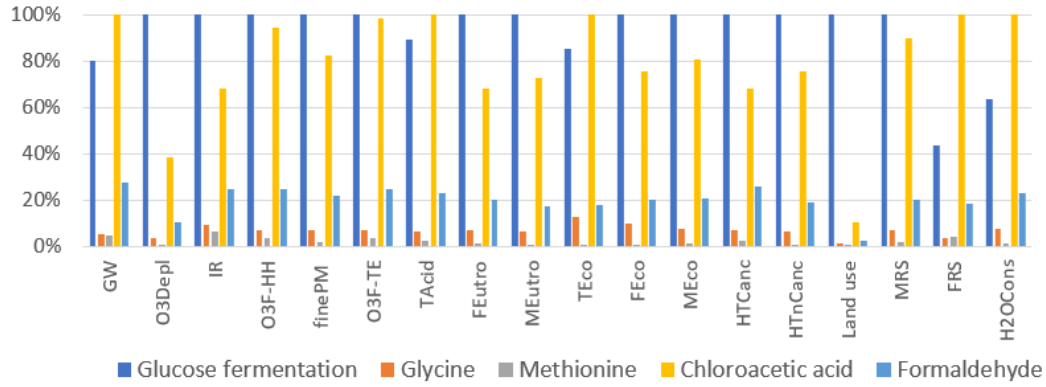

Figure B.12 LCIA comparison of different production pathways of SAR. The abbreviations of impact categories on the x-axis are defined in Table 24

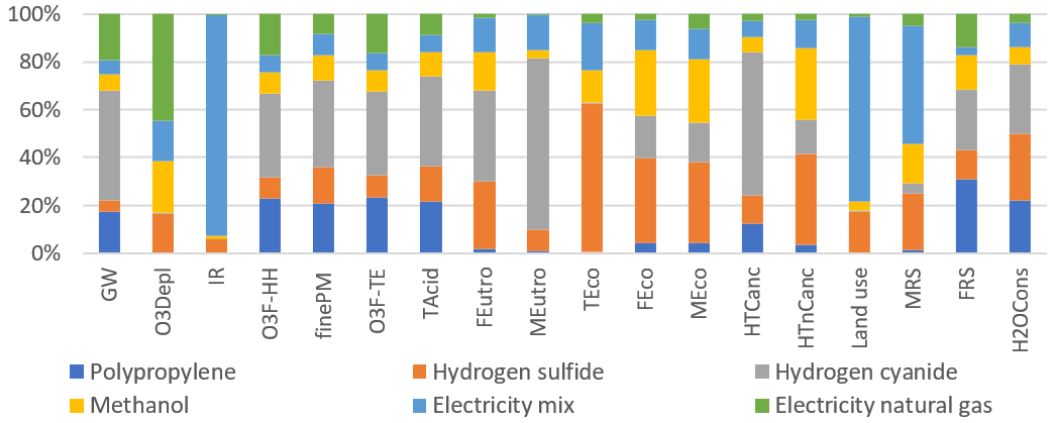

Figure B.13 LCIA for the production of 1kg ARG by methionine. Abbreviations on the x-axis refers to Table 24. Abbreviations on the x-axis refers to Table 24.

B.5 Membrane distillation-crystallisation

B.5.1 Driving force

Table B.8 Comparison of different calculations methods of the driving force $\Delta\overline{P}$ in $[Pa]$ of VMD. Several scenarii of VMD are presented. Vmd.s0 considers the generic VMD scenario treating the previous reference absorption case, i.e. absoA.s0 (with ARG and maximum K_{ov}). In this reference case vmd.s0, the feed inlet temperature is $T_{fi} = 40°$C. vmd.s0.tfi$x$ represents VMD treating the previous absoA.s0 for different $T_{fi} = x°$C. vmd.s1 is VMD treating the previous absorption step working with SAR and the maximum CO_2 load $\kappa = 0.412$ [mol/kg]. It appears from the Table, that $\Delta\overline{P}$ in VMD (and more generally in membrane distillation-crystallisation (MDC)) can be computed either via an arithmetic or natural logarithmic mean. The difference between both types of driving force is negligible.

	Driving force	
	Arithm	**LN**
vmd.s0	3586	3570
vms.s0.tfi35	2118	2113
vms.s0.tfi30	957	958
vmd.s1.tfi40	3094	3094
vmd.s1.tfi30	676	657

B.5.2 Water Activities

g/L	mol/L	aw
0.058	0.001	1.000
0.117	0.002	1.000
0.175	0.003	1.000
0.234	0.004	1.000
0.292	0.005	1.000
0.351	0.006	1.000
0.409	0.007	1.000
0.468	0.008	1.000
0.526	0.009	1.000
0.585	0.010	1.000
1.169	0.020	0.999
1.752	0.030	0.999
2.335	0.040	0.999
2.916	0.050	0.998
3.498	0.060	0.998
4.078	0.070	0.998
4.658	0.080	0.997
5.237	0.090	0.997
5.816	0.099	0.997

g/L	mol/L	aw
11.565	0.198	0.993
17.247	0.295	0.990
22.865	0.391	0.987
28.419	0.486	0.984
33.910	0.580	0.980
39.339	0.672	0.977
44.708	0.764	0.974
50.017	0.855	0.970
55.267	0.945	0.967
80.671	1.379	0.949
104.745	1.791	0.931
127.590	2.181	0.911
149.298	2.552	0.891
169.952	2.905	0.870
189.627	3.241	0.849
333.312	5.698	0.695
300.000	5.133	0.742
200.000	3.422	0.840
250.000	4.277	0.788

Figure B.14 NaCl water activity.[]

moL/L	aw
0.001	0.99996
0.002	0.99993
0.003	0.99989
0.004	0.99986
0.005	0.99982
0.006	0.99979
0.007	0.99976
0.008	0.99972
0.009	0.99969
0.01	0.99965
0.02	0.9993
0.03	0.99897
0.04	0.9983
0.05	0.998
0.06	0.998
0.07	0.997

moL/L	aw
0.08	0.997
0.09	0.997
0.1	0.993
0.2	0.990
0.3	0.987
0.4	0.987
0.5	0.984
0.6	0.981
0.7	0.978
0.8	0.975
0.9	0.973
1	0.970
1.223	0.964
1.25	0.963
1.3	0.962
1.1	0.957

Figure B.15 $NaHCO_3$ water activity.[107; 108]

mol/L	aw
0.14555488	0.998
0.21750586	0.997
0.29041332	0.996
0.34726757	0.995
0.44112457	0.994
0.51388312	0.992
0.59193456	0.992
0.66526642	0.99
0.73365586	0.989

Figure B.16 ARG water activity.[109; 110]

mol/L	aw
0.200	0.786
0.302	0.849
0.506	0.911
0.709	0.945
1.018	0.978
1.226	0.996
1.538	1.021
2.057	1.062
2.579	1.103
3.095	1.152
3.610	1.202
4.126	1.258
5.158	1.376
6.189	1.499
7.221	1.614

Figure B.17 SAR water activity.[111]

B.6 OMD post-treatment of brine

In the case of the OMD, the wastewater is the outlet stream of the permeate. This is a solution with a high salt content (NaCl), commonly called brine. Here, the brine has a salt content of about 200 g/kg, whereas the seawater contains 35 g/kg of NaCl. In fact, wastewater can be defined as high salinity when its salinity is about 10-35 g/kg. [112] Therefore, osmotic permeate with a higher salinity cannot be treated by a common wastewater treatment (WWT).

Different methods exist to manage these saline waters. The most common are: deep well injection, land application, evaporation ponds, sewer discharge or seawater discharge. The choice of the most appropriate disposal method depends on a number of factors: quantity, composition, geographical location of the disposal site, legal factors, capital and operating costs, etc. [84] However, brine discharge is the most common and widely adopted method worldwide, with 45% of total capacity in the US. It has the advantage of being suitable for treating large volumes with low costs and energy demands. However, brine discharge is disruptive to aquatic ecosystems. [84; 113] Thus, brine discharge is assumed to be a realistic waste treatment scenario for the waste output permeate of the OMD. Its management can be modelled by the background process in Ecoinvent: "*discharge of water from oil extraction (on/off-shore)*". [83].

The extraction and production of oil generates a by-product called *produced water*. The chemical composition of produced water depends considerably on the geographical location of the field where the oil was extracted. The main components of produced water are salt, oils and inorganic and organic toxic compounds. Most produced water is saltier than sea water and can exceed 300 g/kg. Therefore, the salinity is comparable to that of wastewater in the OMDs. In addition, oil emissions are available for different production areas and are assessed directly in the crude oil production inventory. This means that oil emissions are not used for "water discharge from oil extraction". Hence, this WWT can be appropriately applied to the resulting osmotic permeate. [114]

Next, onshore or offshore water discharge is available in Ecoinvent. On the one hand, offshore discharge releases the brine into the sea water. On the other hand, onshore discharge uses the same data but leads to more uncertainties because different data are expected for different geographical regions. [114]

Finally, OMD wastewater is managed by a seawater discharge which is simulated by the background database associated with the offshore discharge of produced water.

Appendix C

LCIA and interpretation

C.1 Classification and characterisation

C.1.1 Method selection

The selection of the LCA method is an important step where it should complies ISO standards, be on the scope of the LCA study and compatible with the selected impact categories. The purpose of a LCA method is to class inventory results into impact categories. Many reference methods are available and scientifically recognised by the ISO Standards.[48]

Characterisation can be assessed at two mainstreams ways : with **midpoint** and **endpoint** impact categories both presenting advantages and drawbacks. Firstly, the midpoint characterisation (i.e. problem-oriented) presents more robust but less environmentally relevant results, while the opposite is true for the endpoint indicators (i.e. damage-oriented). Secondly, in the endpoint indicators, more assumptions are made than in the midpoint indicators, which leads to a higher level of uncertainty for the endpoint indicators. Thirdly, the results of the endpoint indicators are easier to communicate, but they are accompanied by a significant loss of valuable information, which leads to limited interpretation. However, the two indicators are complementary rather than alternative to each other, such it is relevant to make the key mid- and end-point LCA results available in this study. [115; 116] As a results, "*a quick screening using an endpoint method will be used to "flag" relevant issues; even if the study will not use endpoint methods for the final results*" [59].

The **Recipe** method [78] has the advantage of presenting both midpoint and endpoint indicators. In fact, Recipe 2016 is an updated and extended version of Recipe 2008 and mixes an improved version of the CML-oriented problems [117], and the damage-oriented approach of the Eco-Indicator 99 [118; 115]. At the midpoint level and endpoint level, 18 impact and 3 impact categories are respectively available. To quantify them, the 18 impact categories are multiplied by a damage factor and aggregated into the 3 endpoint protection zones (see Figure C.18). [116]

In addition, three **perspectives** (i.e. scenarii) are proposed in the Recipe method: Individualistic (I), Hierarchistic (H), Equalitarian (E). For the sake of consistency with other LCAs on CCU available in the literature [119; 54; 120; 121], the Recipe **Hierarchistic** method is chosen, which is based "*on scientific consensus regarding the timing and plausibility of impact mechanisms*" [78].

Furthermore, it is mentioned that single-issue methods do not comply with ISO 14044, as they exclude impact categories whose results could be significant for the study. To avoid this, ISO standards have started to develop single-issue methods [59]. Hence, even if the carbon footprint is not the only relevant impact category, the robustness of this impact category is of paramount importance for a CCU process focused on CO_2 absorption performance.
In fact, several LCA methods (IPCC 2013, Recipe 2016, Impact 2002+ etc.) have an impact category on **climate change** (or sometimes called *global warming*), for which the use of IPCC GWPs as characterisation factors at the midpoint level leads to a wide consensus. However, there are some differences in the use of GWPs, so the International Reference Life Cycle Data (ILCD) Handbook [122] recommends that the IPCC 2013 method should be used for the assessment of the climate change impact category. Indeed, the latter uses the most recent GWPs. Nevertheless, the Recipe 2016 GWP is based on the same 2013 IPCC Report 5 consulted for the IPCC 2013 method [78], so that the Recipe 2016 carbon footprint assessment is considered appropriate for the present study.

Finally, the ILCD Handbook stresses that from a scientific and sustainability point of view, a scenario with a **time horizon** of 500 years should be preferred to assess climate change, even though many policy instruments (e.g. the Kyoto Protocol) are based on a time horizon of 100 years. Therefore, a **sensitivity analysis** is recommended for CO_2 equivalent emissions, and for comparing different time horizons (20 (I) -100 (H) -1000 (E) years) [78].

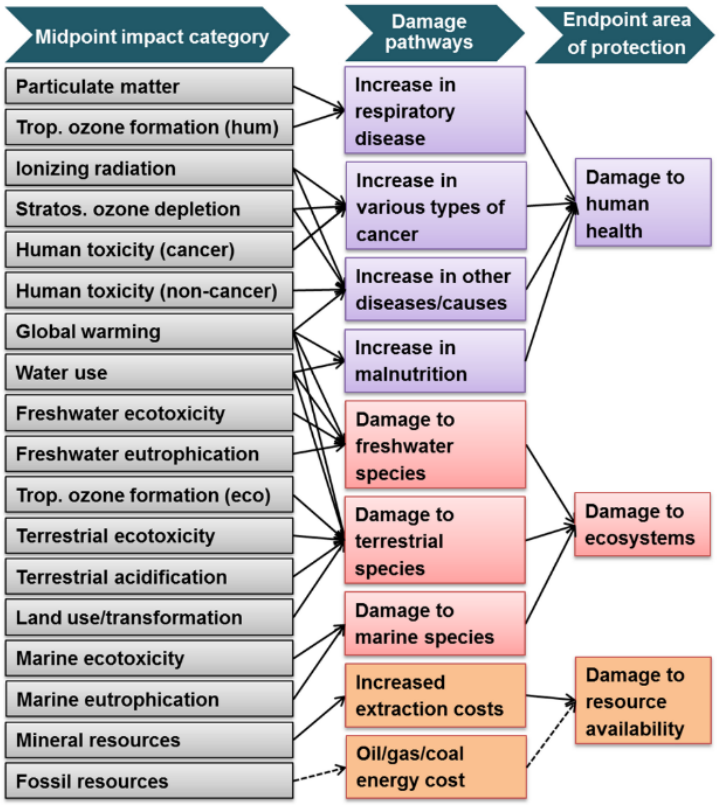

Figure C.18 Representation of the relations between the impact categories midpoint and the areas of production (endpoint).[78] Damage to human health is expressed in Disability adjusted life years (DALY), to the ecosystem in [species.yr] and to resources in US dollars reference year 2013 (USD2013).

C.2 Results and discussion

C.2.1 Sensitivity analysis on LCA methods

Different LCA methods were compared in order to highlight potential contradictions and nuances in these results based on the 5 steps of the generic LCI. The report "*Techno-Economic Assessment & Life-Cycle Assessment Guidelines for CO_2 Utilization*" [52] suggests using the CML [117] method for CCU studies as used in [123; 124; 125]. For this purpose, the results of the LCA by CML have been added to the paper and are presented. Other papers on LCA of CCU technologies [47; 126] have been carried out with the IPCC method. Therefore, the global warming impact category is closely analysed by comparing Recipe 2016, CML and IPCC. Finally, a sensitivity analysis regarding the time horizons of global warming is performed.

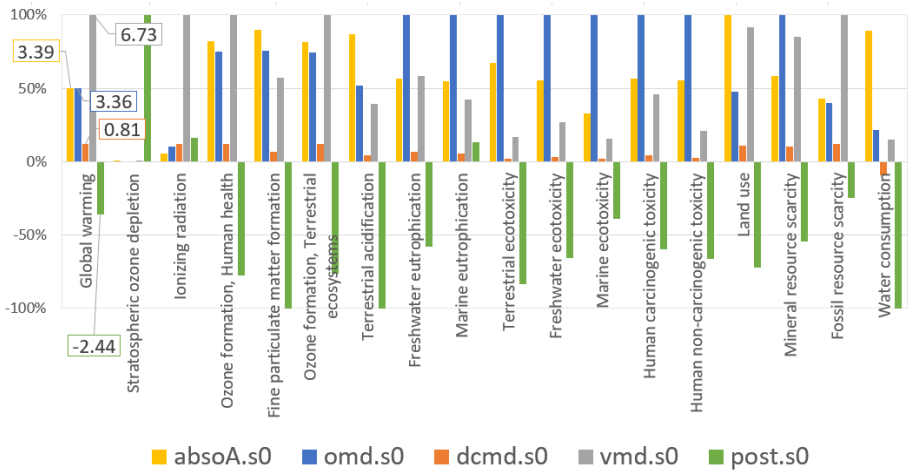

Figure C.19 LCIA results for Recipe 2016 (H) midpoint method - characterisation. The 5 steps refer to reference cases. AbsoA.s0 is absorption considering ARG and the maximum K_{ov}. Omd.s0, dcmd.s0 and vmd.s0 are for OMD, DCMD and VMD treating the former AbsoA.s0. Post.s0 is post-treatment with a recovery $\chi = 99\%$.

CML vs Recipe

A global comparison of all impact categories between Recipe 2016 (Figure C.19) and CML (Figure C.20) shows the same trend: VMD by vmd.s0 proves the biggest impact regarding global warming, followed by OMD and absorption. Note that in CML, the ozone depletion (in kg CFC11 eq) has a higher impact than its equivalent impact category, stratospheric ozone depletion, in Recipe method.

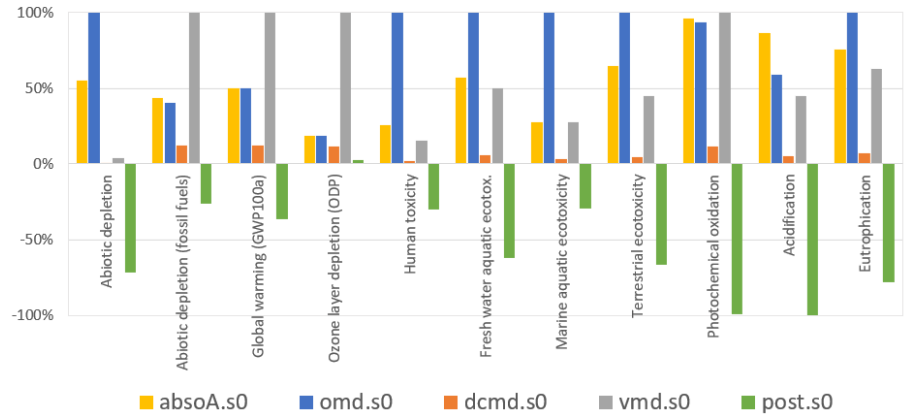

Figure C.20 LCIA results for CML method - characterisation. The 5 steps refer to reference cases. AbsoA.s0 is absorption considering ARG and the maximum K_{ov}. Omd.s0, dcmd.s0 and vmd.s0 are for OMD, DCMD and VMD treating the former AbsoA.s0. Post.s0 is post-treatment with a recovery $\chi = 99\%$.

Global warming

As the LCA concerns a CCU where the FU is expressed in terms of CO_2 kg, a particular interest is given to global warming in [$kgCO_2$-eq]. It is thus relevant to perform a sensitivity analysis on this particular impact category comparing different

LCA methods. For this purpose, Recipe 2016 (H), CML and the IPCC single issue method are performed in the case of the generic LCI. Figure C.21 shows the results where it is observed that Recipe 2016 has a higher global warming impact in each steps, compared to the other 2 methods. CML and IPCC show the same quantitative results. Indeed, the characterisation factors (GWP) selected for both the CML and IPCC methods are based on the IPCC report with a time horizon of 100 years. When examining the characterisation factor of each method in SimaPro, it appears that all methods have 212 items but the GWPs have different values : for GWPs < 1, Recipe method rounds them either 0 or 1. [78].

Nevertheless, Recipe gives the highest CO_2 equivalent emissions and is therefore a good worst-case approximation, although the difference with other methods is not really significant.

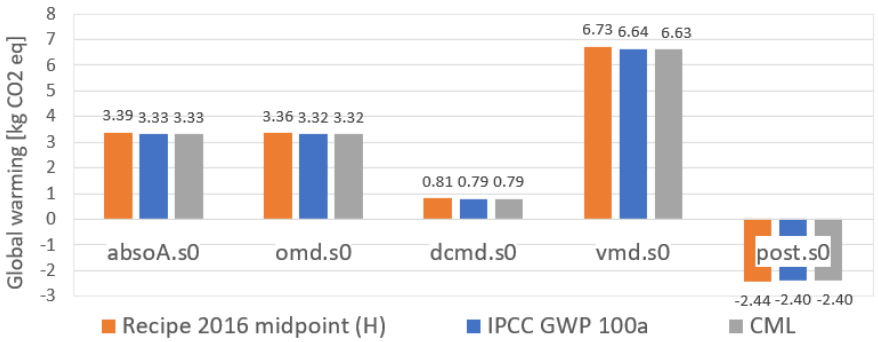

Figure C.21 LCIA comparison of methods on global warming - characterisation. The 5 steps refer to reference cases. AbsoA.s0 is absorption considering ARG and the maximum K_{ov}. Omd.s0, dcmd.s0 and vmd.s0 are for OMD, DCMD and VMD treating the former AbsoA.s0. Post.s0 is post-treatment with a recovery $\chi = 99\%$.

Time horizons

As suggested in Appendix C.1.1 by [122] and [127] concerning the method selection, a sensitivity analysis over the time horizon should be carried out, comparing the different perspectives (I-H-E) of the Recipe 2016 midpoint methods regarding climate change. A number of uncertainties are clustered in the 3 perspectives that represent similar types of assumptions or choices. Indeed, the climate metric differs in multiple ways (physical endpoints, cumulative, etc.) and the choice of time horizon in the GWPs can have a significant effect on the GWPs. For example, the GWP-100 (corresponding to a time horizon of 100 years) of methane is 30 while the GWP-20 is about 85. [127]

The choice of values for the 3 scenarii is presented in Table C.9 and the LCIA comparison in Figure C.22. It appears that with short-term time horizons, the process generates higher emissions of CO_2 eq. One reason could be that "*long-term changes include sea level recovery driven by relatively slow processes that can influence global ocean warming*" [128].

Nevertheless, the hierarchical perspective (H) is used for the other life cycle impact assessment (LCIA) results in this project, bearing in mind that, over a time

horizon of 20 years, the climate change impact category has higher CO_2 equivalent emissions.

Table C.9 Value choices in the derivation of characterisation factors for different perspectives in Recipe 2016 [78].

Climate Change	Individualist	Hierarchist	Egalitarian
Time Horizon	20 years	100 years	1000 years
Climate-carbon feed-back	No	Yes	No
Future socio-economic developments	Optimistic	Baseline	Pessimistic
Adaptation potential	Adaptive	Controlling	Comprehensive

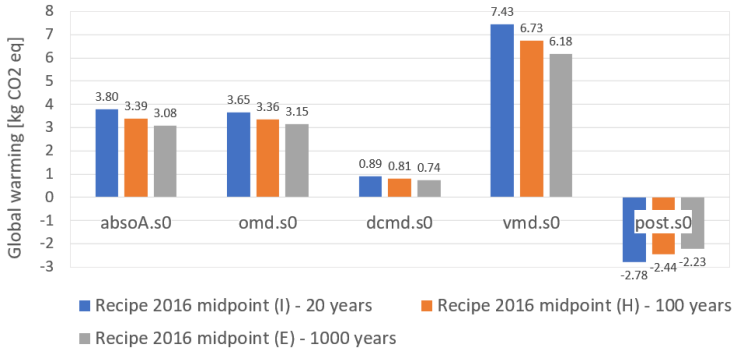

Figure C.22 LCIA comparison of time horizons - characterisation. The 5 steps refer to reference cases. AbsoA.s0 is absorption considering ARG and the maximum K_{ov}. Omd.s0, dcmd.s0 and vmd.s0 are for OMD, DCMD and VMD treating the former AbsoA.s0. Post.s0 is post-treatment with a recovery $\chi = 99\%$.

C.2.2 Overview of the generic LCI

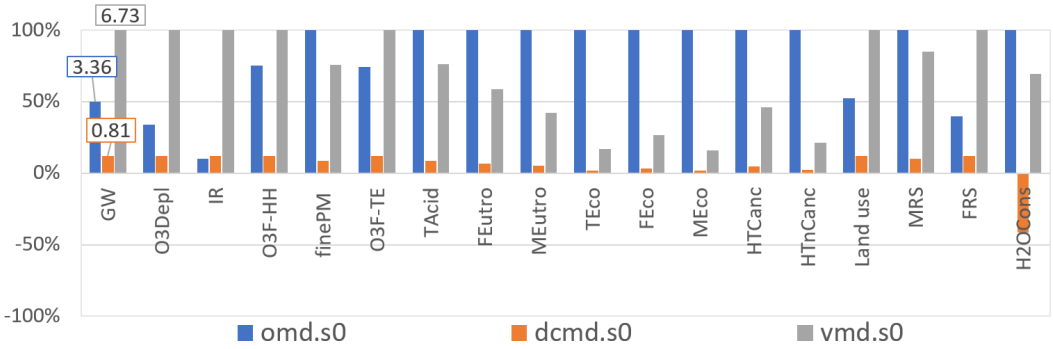

Figure C.23 LCIA results of generic membrane distillation-crystallisation (MDC) (omd.s0, dcmd.s0, vmd.s0) - characterisation. Generic MDC processes treat former absoA.s0 (absorption with ARG and maximum K_{ov}). Data labels on the bar charts represent global warming emissions in [kgCO_2-eq] Abbreviations on the x-axis refer to Table 24.

C.2.2.1 Endpoints

As explained at length in Appendix C.1.1, it is interesting to represent the environmental impacts of the LCA in terms of endpoint areas of protection by the means of Recipe 2016 endpoint (H) method presented earlier in Figure C.18. Damage-oriented results (i.e endpoint) are presented in Figures C.24 (characterisation) and C.25 (normalisation) for the cases of generic LCIs.

By characterisation in Figure C.24, in a quantified way, post.s0 has the best score in human health, but the OMD has the worst impact. In addition, vmd.s0 case of VMD has the highest impacts in the protection areas of ecosystems and resources. It also appears that dcmd.s0 has the lowest impact on these endpoint indicators.

In terms of normalised environmental impacts, Figure C.25 reveals that human health is the most impacted damage category compared to the other two.

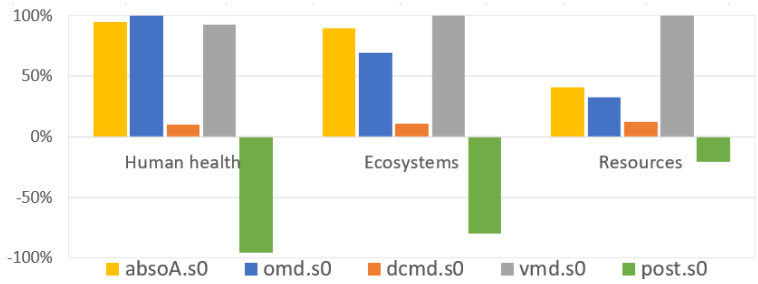

Figure C.24 LCIA results of generic LCA with Recipe endpoint (H) - characterisation. The 5 steps refer to reference cases. AbsoA.s0 is absorption considering ARG and the maximum K_{ov}. Omd.s0, dcmd.s0 and vmd.s0 are for OMD, DCMD and VMD treating the former AbsoA.s0. Post.s0 is post-treatment with a recovery $\chi = 99\%$.

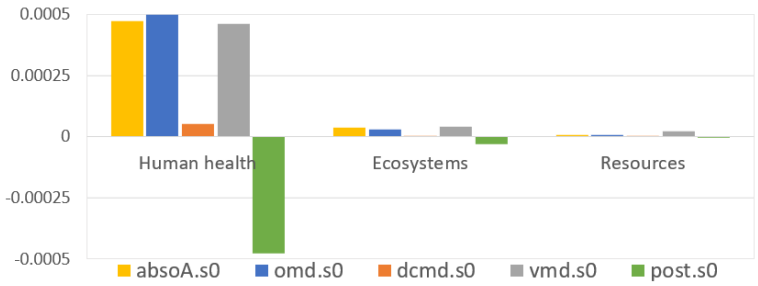

Figure C.25 LCIA results of generic LCA with Recipe endpoint (H) - normalisation. The 5 steps refer to reference cases. AbsoA.s0 is absorption considering ARG and the maximum K_{ov}. Omd.s0, dcmd.s0 and vmd.s0 are for OMD, DCMD and VMD treating the former AbsoA.s0. Post.s0 is post-treatment with a recovery $\chi = 99\%$.

C.2.3 Osmotic membrane distillation

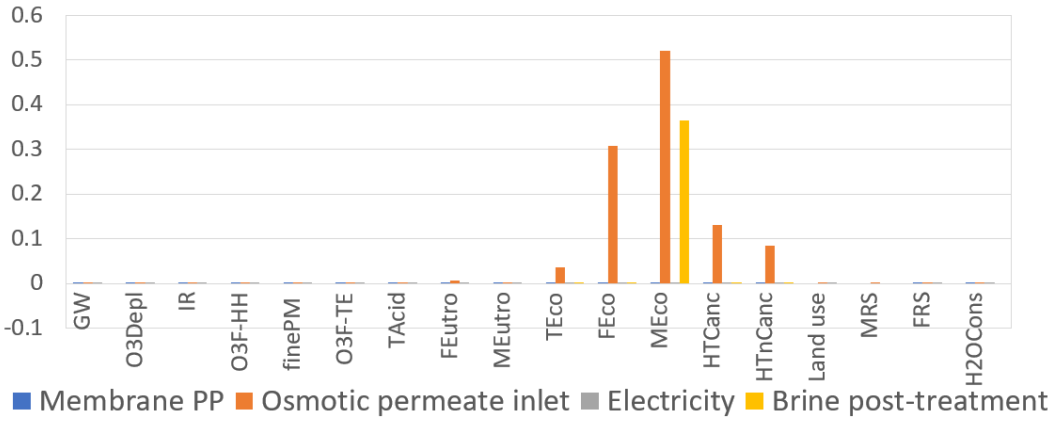

Figure C.26 LCIA of osmotic solution for omd.s0 with previous absoA.s0 - **normalisation**. absoA.s0 stand for generic absorption with ARG and maximum K_{ov}. omd.s0 is OMD treating previous absoA.s0. WWT stands for wastewater treatment. Abbreviations on thex-axis refers to Table 24.

C.2.4 Direct contact membrane distillation

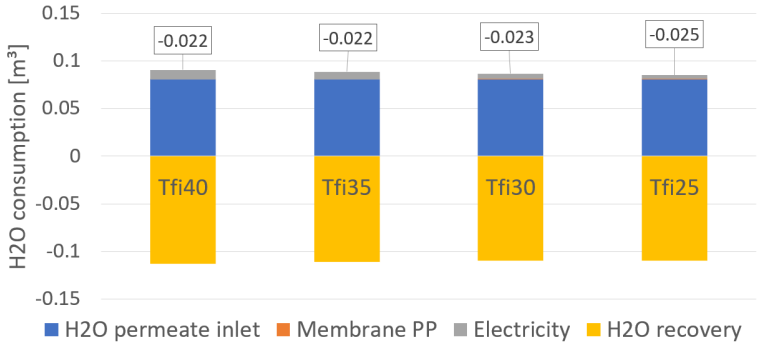

Figure C.27 LCIA results of DCMD with different feed inlet temperature T_{fi}, **water consumption** category (H2OCons) in $[m^3]$ - characterisation. The previous absorption step is AbsoA.s0 operating with ARG and at maximum K_{ov}. The data labels on the bar charts represents the total water consumption of DCMD. The case Tfi40 represents the reference case of DCMD, also previously noted dcmd.s0.

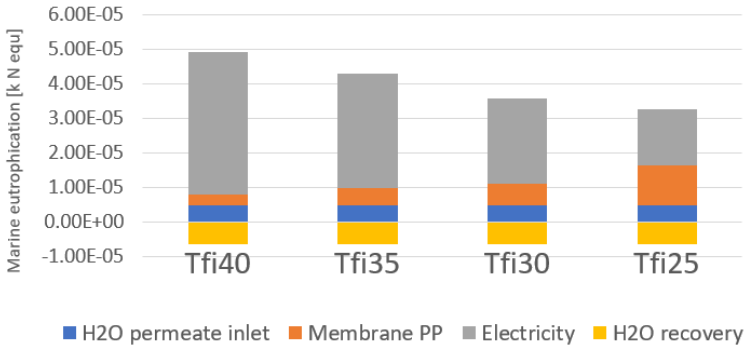

Figure C.28 LCIA results of DCMD with different feed inlet temperature T_{fi}, **marine eutrophication** category (MEutro) in [kN-eq] - characterisation. The previous absorption step is AbsoA.s0 operating with ARG and at maximum K_{ov}. The data labels on the bar charts represents the total water consumption of DCMD. The case Tfi40 represents the reference case of DCMD, also previously noted dcmd.s0.

C.2.5 Optimised LCA steps

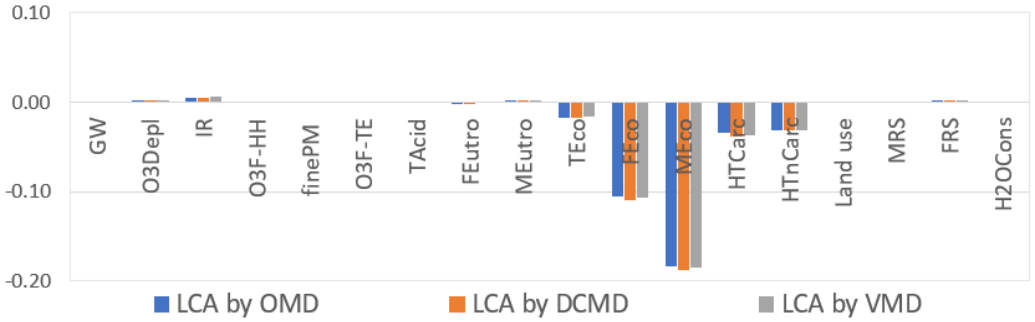

Figure C.29 LCIA of the optimised LCA with operating conditions - normalisation. LCA by OMD/DCMD or VMD sums up emissions due to absorption = OMD/DCMD or VMD + post-treatment. The absorption step is operating with ARG and at maximum $\kappa = 0.561$ [mol/kg]. OMD is working until 50% above the saturation level and is coupled with desalination plant. DCMD is working until 50% above the saturation level and with $T_{fi} = 25°C$. VMD works at $T_{fi} = 30°C$ and up the the saturation level. Abbreviations on the x-axis refer to Table 24.

Optimised Endpoints results

Endpoints of the optimised LCA are presented in the 2 following figures. Note that if LCIA results at midpoints indicators showed that the whole process via OMD, DCMD or VMD gives emissions reductions in almost every impact categories, this is also true for endpoint results. Figures C.30 and C.31 shows that in the 3 damage categories, post-treatments has a great reducing impact, leading to overall negative impacts.

These figures could also be compared to Figure C.24 and C.25 that outline endpoint results of the generic LCA.

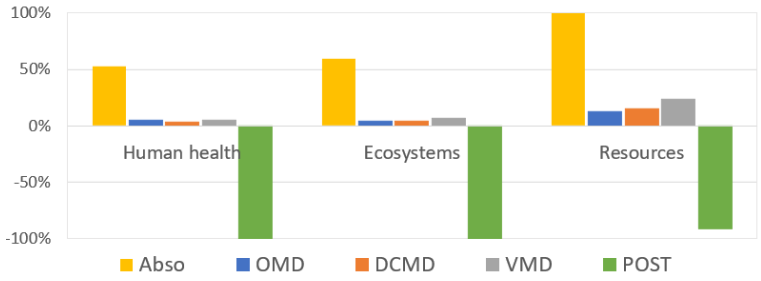

Figure C.30 LCIA of the optimised LCA with operating conditions, Recipe (H) endpoints - characterisation. Abso is absorption with ARG and maximum $\kappa = 0.561$ [mol/kg]. OMD is working until 50% above the saturation level and is coupled with desalination plant. DCMD is working until 50% above the saturation level and with $T_{fi} = 25°C$. VMD works at $T_{fi} = 30°C$ and up the the saturation level. Post stands for post-treatment step with a recovery χ=99%.

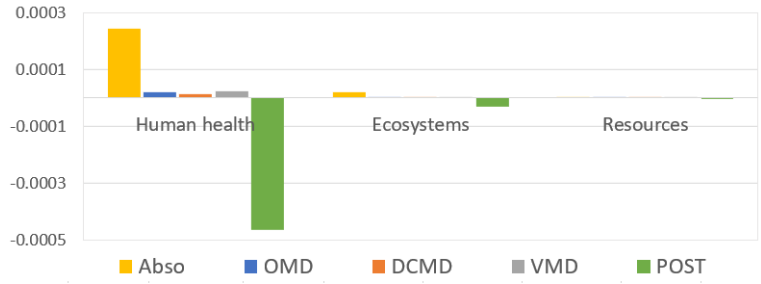

Figure C.31 LCIA of the optimised LCA with operating conditions, Recipe (H) endpoints - normalisation. Abso is absorption with ARG and maximum $\kappa = 0.561$ [mol/kg]. OMD is working until 50% above the saturation level and is coupled with desalination plant. DCMD is working until 50% above the saturation level and with $T_{fi} = 25°C$. VMD works at $T_{fi} = 30°C$ and up the the saturation level. Post stands for post-treatment step with a recovery χ=99%.

C.2.6 LCIA networks

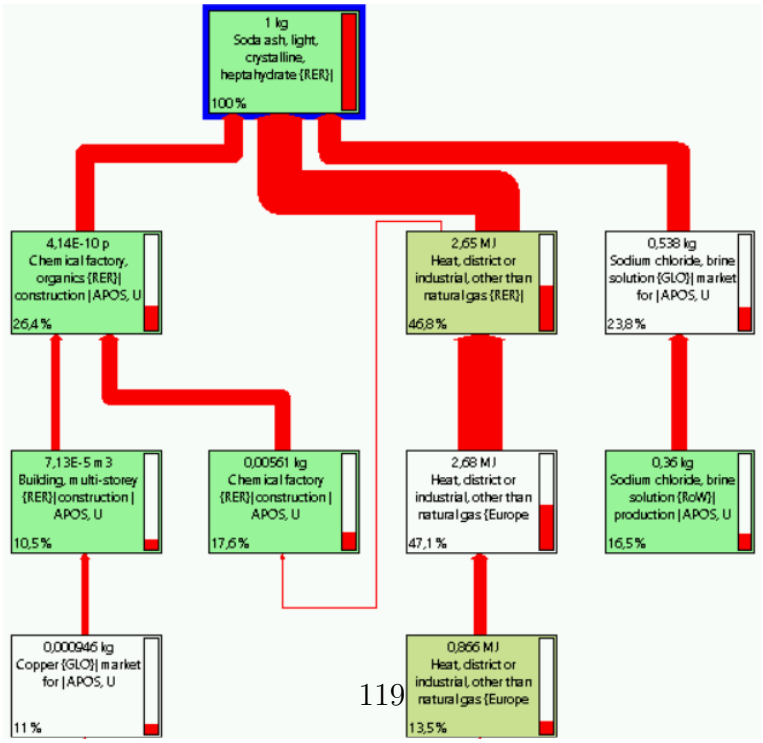

Figure C.32 LCIA network of Na_2CO_3, **global warming** (GW), soda ashes, in Ecoinvent Unit database. This represents the main factors in the production of soda ashes regarding global warming. Soda ashes are used in the solvent mixture of absorption, as Na_2CO_3 compounds.

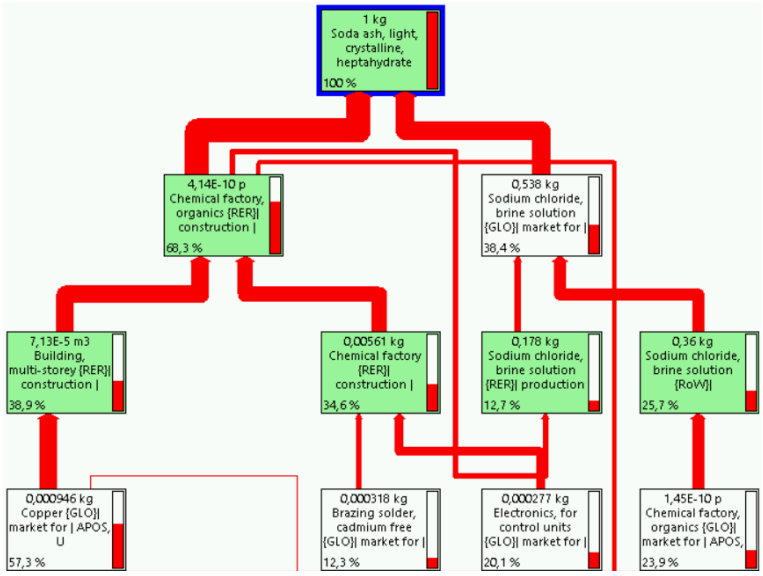

Figure C.33 LCIA network of Na_2CO_3, **marine ecotoxicity** (MEco), soda ashes, in Ecoinvent Unit database. This represents the main factors in the production of soda ashes regarding global warming. Soda ashes are used in the solvent mixture of absorption, as Na_2CO_3 compounds.

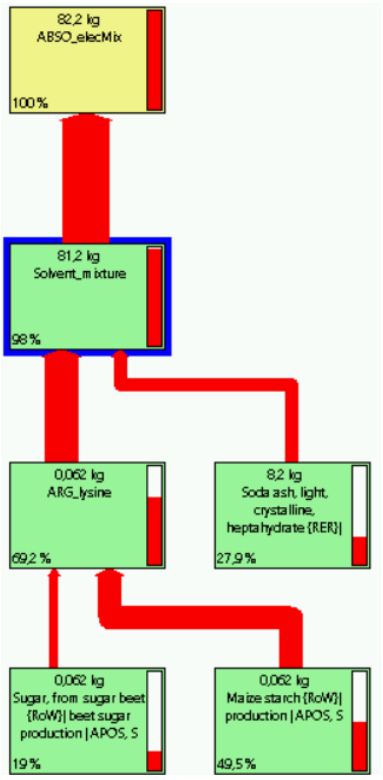

Figure C.34 LCIA network of absorption for absoA.s0, **marine eutrophication** (MEutro) category in [kg N-eq] - characterisation. AbsoA.s0 stands for reference absorption case operating with ARG and at maximum K_{ov}. The marine eutrophication category is primarily impacted by the production of ARG from maize starch, which in turn is primarily impacted by the production of maize grain and green manure.

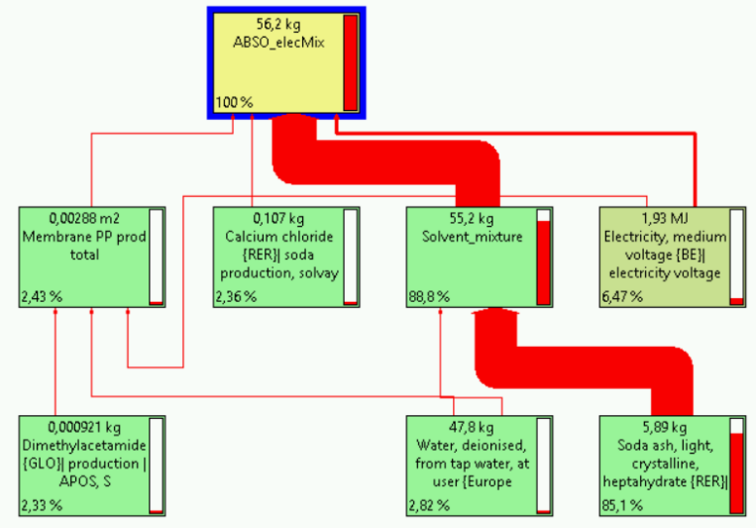

Figure C.35 LCIA network of absorption for absoS.s0, **marine eutrophication** (MEutro) category in [kg N-eq] - characterisation. AbsoS.s0 stands for reference absorption case operating with SAR and at maximum K_{ov}. The marine eutrophication category is primarily impacted by the production of soda ashes unlike absorption with ARG, where marine eutrophication is primarily impacted by the production of ARG due to maize starch production (see Figure C.34).

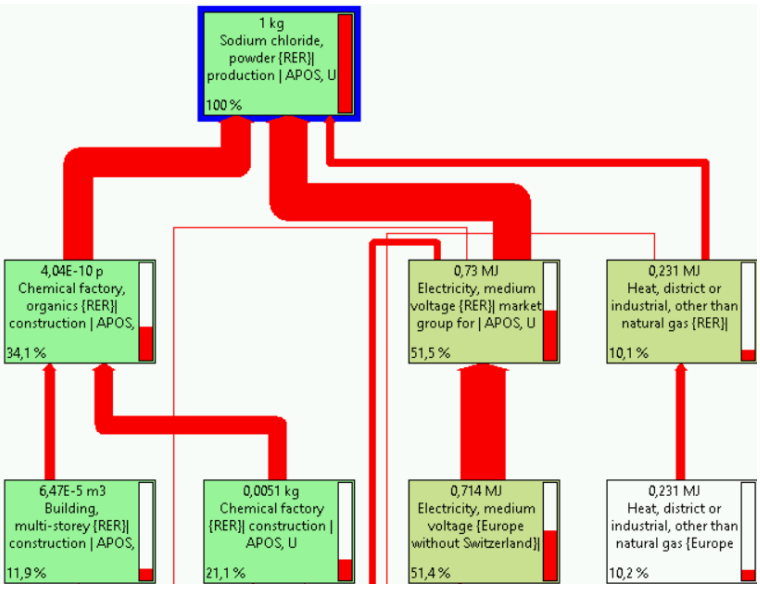

Figure C.36 LCIA network of NaCl production, **global warming** category in [kgCO_2-eq] - characterisation, from Ecoinvent Unit database. The global warming of NaCl category is primarily impacted by the use of electricity and heat (near 60%) and the construction of the chemical factory (34%).

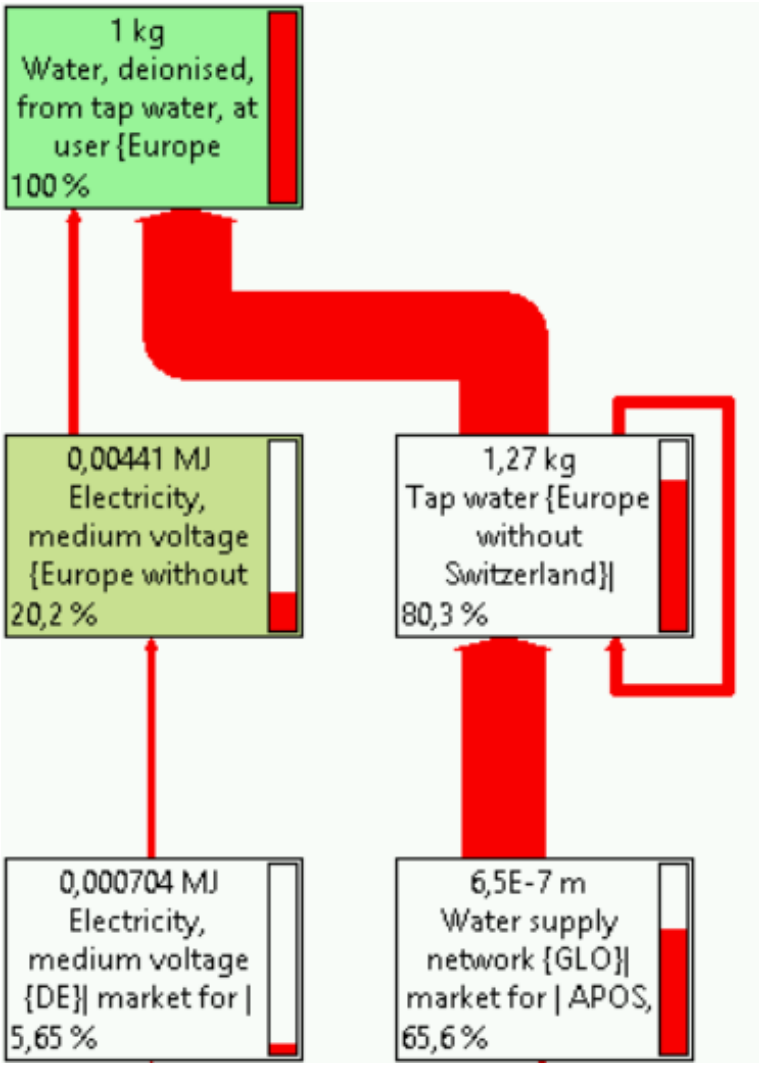

Figure C.37 LCIA network of deinonised water production, **human carcinogenic toxocity** category in [kgCO_2-eq] - characterisation, from Ecoinvent Unit database.

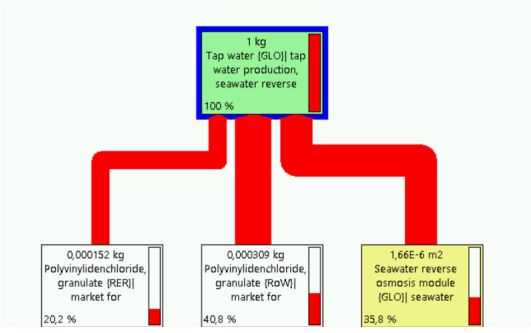

Figure C.38 LCIA network of tap water production by reverse osmosis (RO), **stratospheric ozone depletion** (O3Depl) in [kgCFC11-eq] - characterisation, from Ecoinvent Unit database.

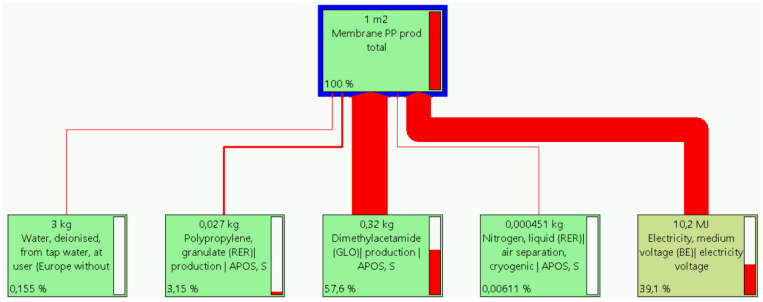

Figure C.39 LCIA network of membrane production [58], **global warming** (GW) in [kgCO_2-eq] - characterisation. Solvent dimethylacetamide (DMAC), followed by electricity are the 2 major determinants for environmental impacts due to polymeric membrane production.

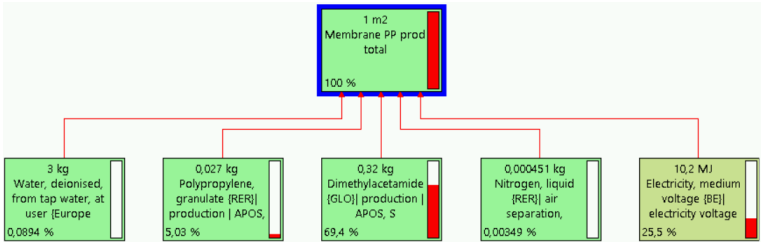

Figure C.40 LCIA network of membrane production [58], **fossil resource scarcity** (FRS) in [kgCO_2-eq] - characterisation. Solvent DMAC, followed by electricity are the 2 major determinants for environmental impacts due to polymeric membrane production.

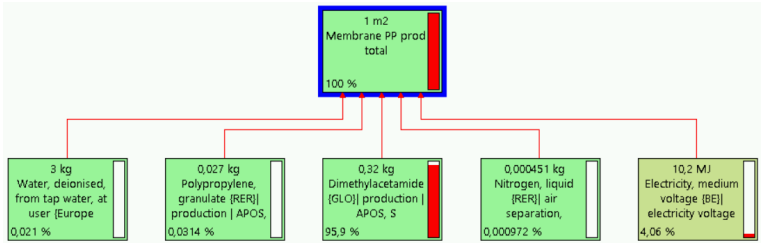

Figure C.41 LCIA network of membrane production [58], **marine eutrophication** (MEutro) in [kgCO_2-eq] - characterisation. Solvent DMAC is the major determinant for environmental impacts due to polymeric membrane production.

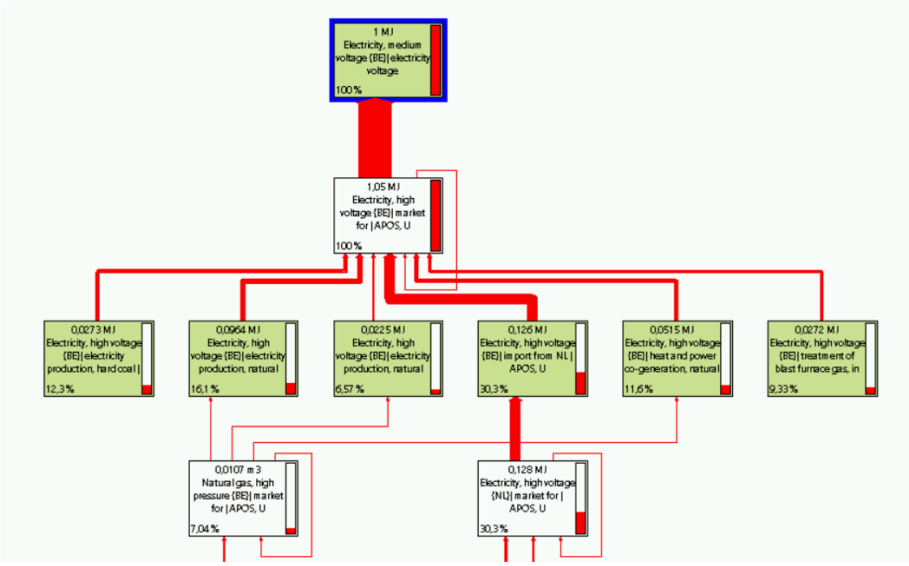

Figure C.42 LCIA network of Belgian electricity mix, **global warming** (GW) category in [kCO2-eq] - characterisation.

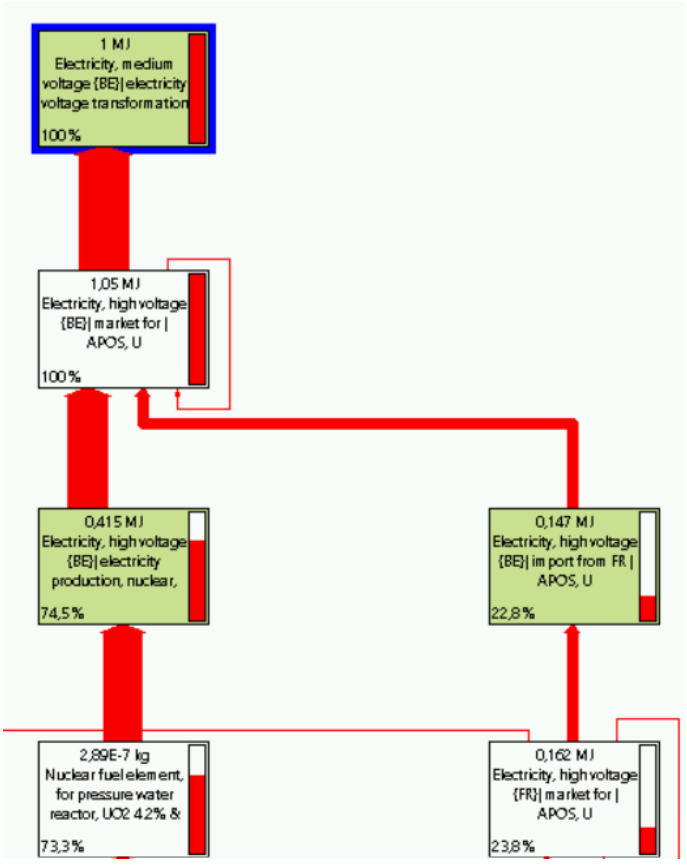

Figure C.43 LCIA network of Belgian electricity mix, **ionising radiation** (IR) category in [kBq Cobalt-60 eq] - characterisation. IR is primarily impacted by nuclear energy in the electricity mix. While global warming impact category is impacted by other energy inputs in the electricity mix (see Figure C.42).

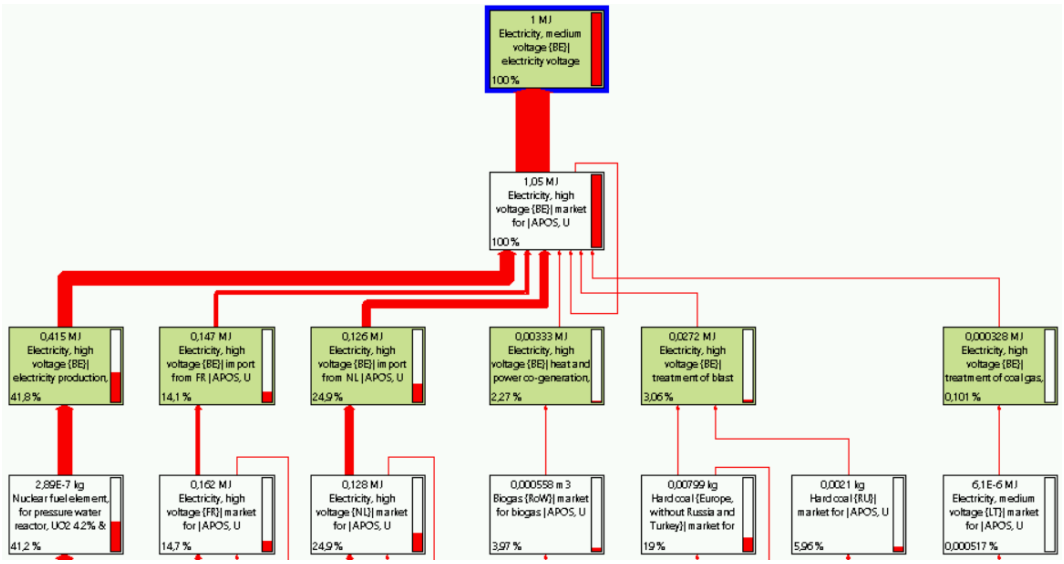

Figure C.44 LCIA network of Belgian electricity mix, Part 1,**marine eutrophication** (MEutro) in [kgN-eq] - characterisation.

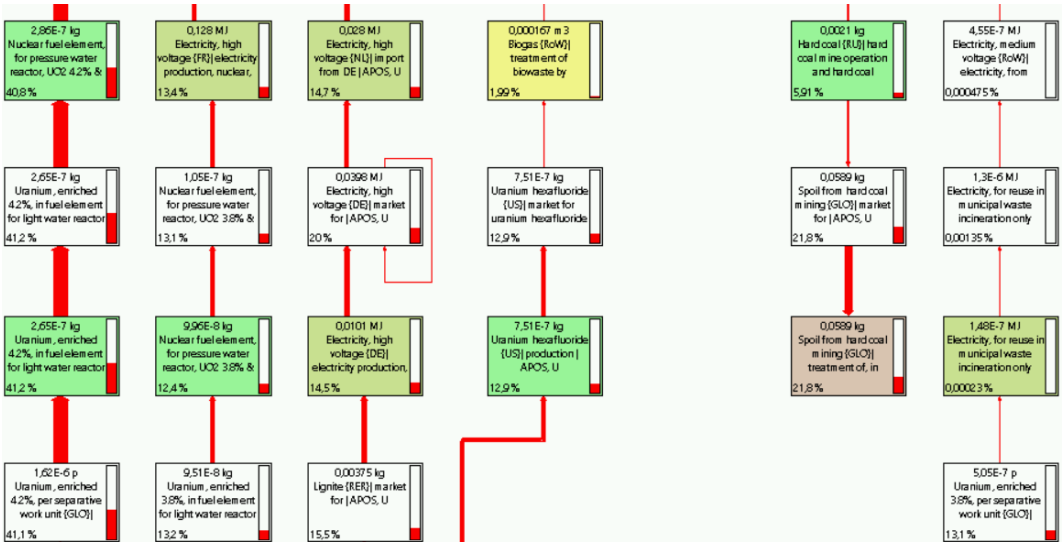

Figure C.45 LCIA network of Belgian electricity mix, Part 2, **marine eutrophication** (MEutro) in [kgN-eq] - characterisation.

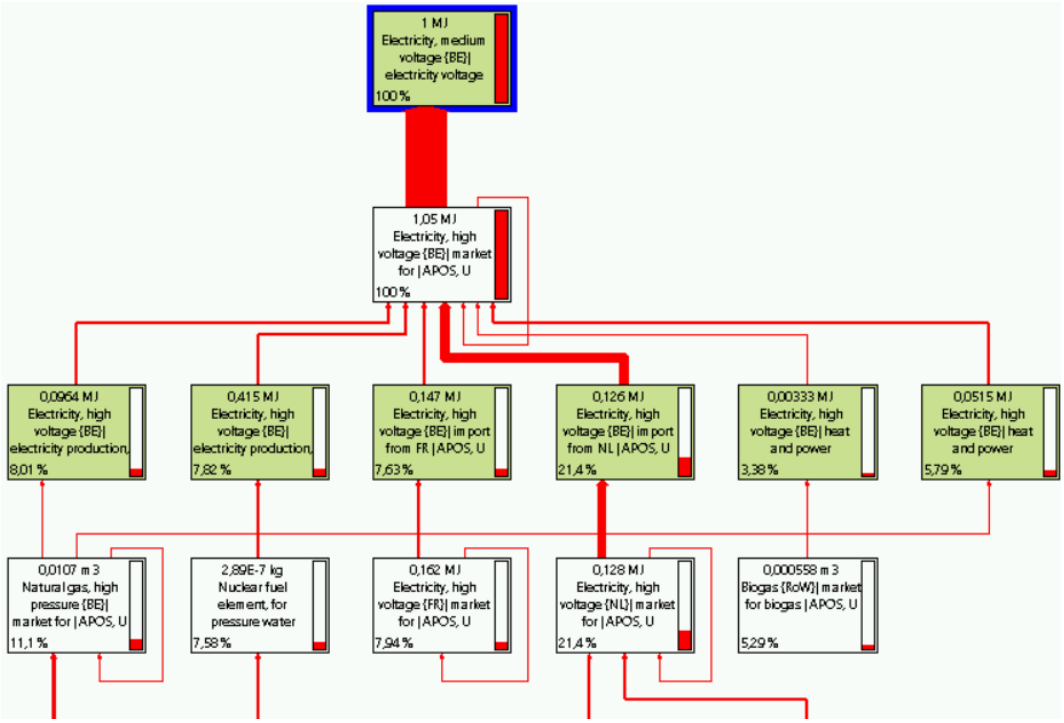

Figure C.46 LCIA network of Belgian electricity mix, Part 1, **stratospheric ozone depletion** (O3Depl) in [kgN-eq] - characterisation.

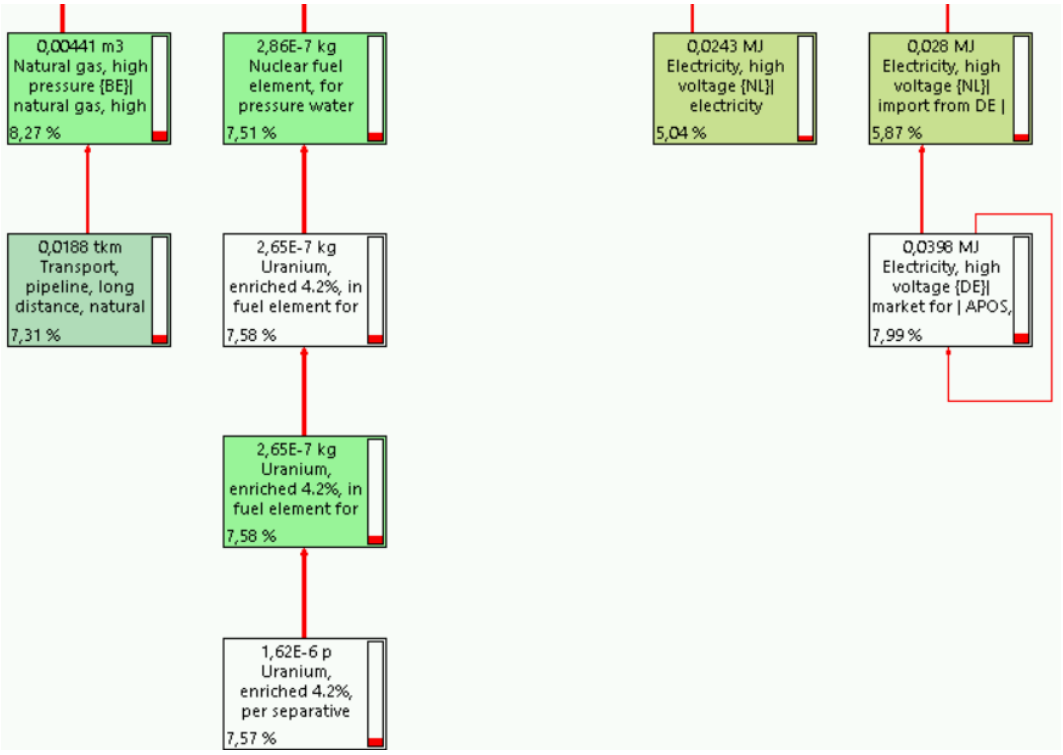

Figure C.47 LCIA network of Belgian electricity mix, Part 2, **stratospheric ozone depletion** (O3Depl) in [kgN-eq] - characterisation.

Appendix D

Tutorial on SimaPro model

SimaPro has been the world's leading life cycle assessment (LCA) software for 30 years. It is widely used in industry and academia. The licence provided by UCLouvain allows SimaPro to be used as a tool to quantify the environmental performance of a product or process. [129]

SimaPro is well documented. And different manuals are available in open source:

- **Introduction to LCA with SimaPro** : a deep explanation on LCA methodology, modelling choices (libraries, multi-functionality, methods etc.) [59]
- **SimaPro Tutorial** : a manual divided in different lessons to get used to the LCA software. [130]

The following figures show screenshots of the SimaPro model used for the present project. This guide is intended for potential users of the simulation.

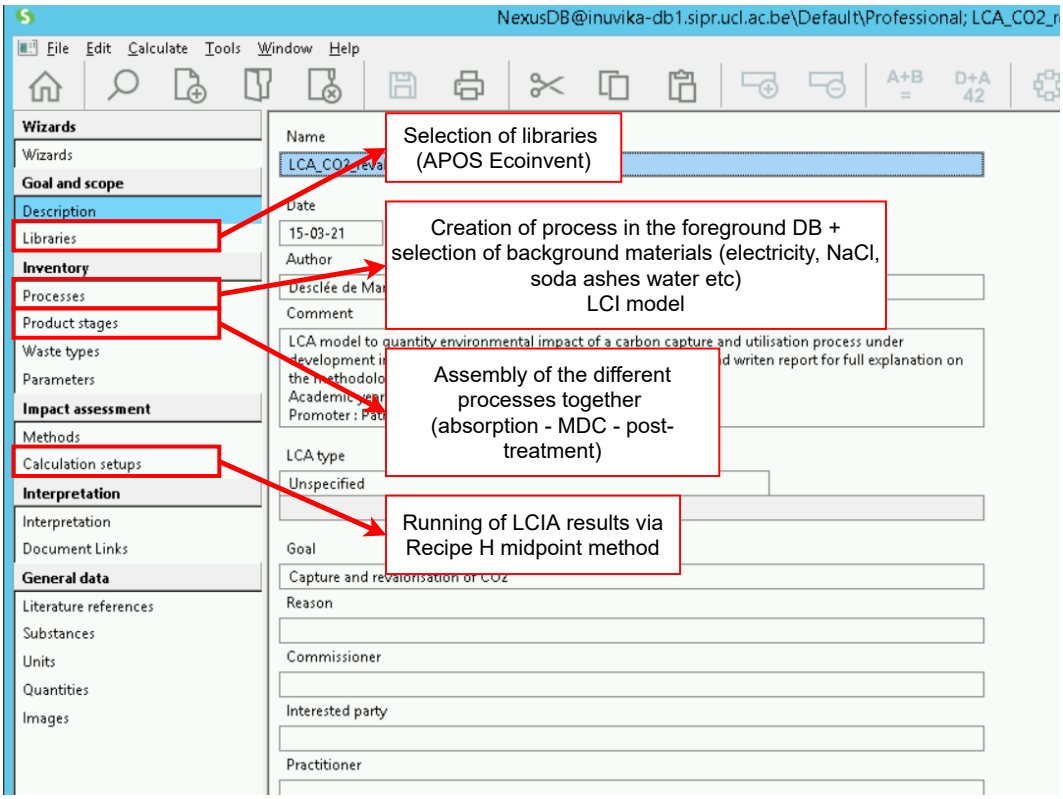

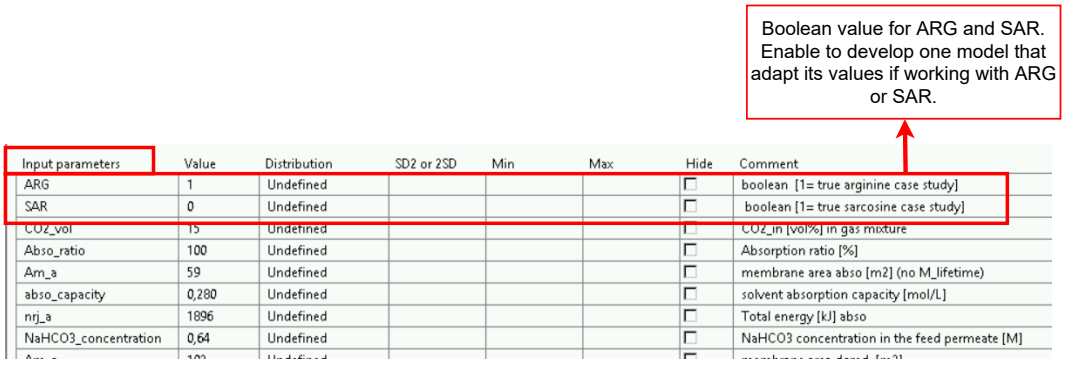

Input parameters	Value	Distribution	SD2 or 2SD	Min	Max	Hide	Comment
ARG	1	Undefined				☐	boolean [1= true arginine case study]
SAR	0	Undefined				☐	boolean [1= true sarcosine case study]
CO2_vol	15	Undefined				☐	CO2_in [vol%] in gas mixture
Abso_ratio	100	Undefined				☐	Absorption ratio [%]
Am_a	59	Undefined				☐	membrane area abso [m2] (no M_lifetime)
abso_capacity	0,280	Undefined				☐	solvent absorption capacity [mol/L]
nrj_a	1896	Undefined				☐	Total energy [kJ] abso
NaHCO3_concentration	0,64	Undefined				☐	NaHCO3 concentration in the feed permeate [M]

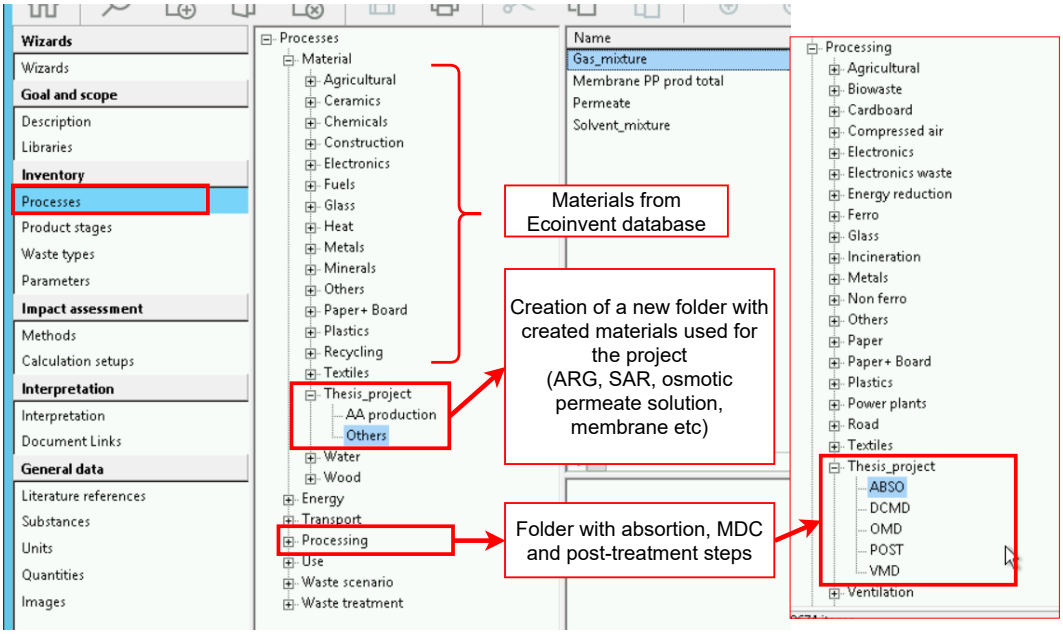
Wizards
Wizards
Goal and scope
Description
Libraries
Inventory
Processes
Product stages
Waste types
Parameters
Impact assessment
Methods
Calculation setups
Interpretation
Interpretation
Document Links
General data
Literature references
Substances
Units
Quantities
Images
Processes
Material
Agricultural
Ceramics
Chemicals
Construction
Electronics
Fuels
Glass
Heat
Metals
Minerals
Others
Paper+ Board
Plastics
Recycling
Textiles
Thesis_project
AA production
Others
Water
Wood
Energy
Transport
Processing
Use
Waste scenario
Waste treatment
Name
Gas_mixture
Membrane PP prod total
Permeate
Solvent_mixture
Materials from Ecoinvent database
Creation of a new folder with created materials used for the project (ARG, SAR, osmotic permeate solution, membrane etc)
Folder with absortion, MDC and post-treatment steps
Processing
Agricultural
Biowaste
Cardboard
Compressed air
Electronics
Electronics waste
Energy reduction
Ferro
Glass
Incineration
Metals
Non ferro
Others
Paper
Paper+ Board
Plastics
Power plants
Road
Textiles
Thesis_project
ABSO
DCMD
OMD
POST
VMD
Ventilation

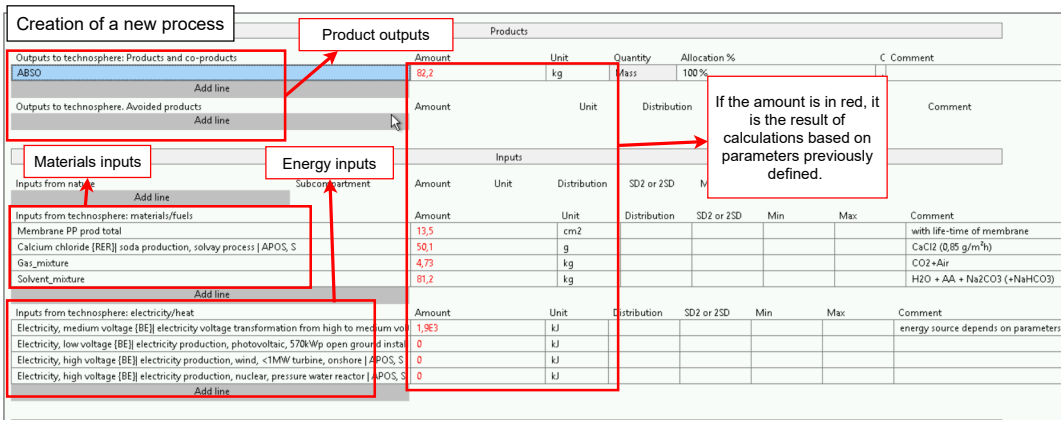
Creation of a new process
Product outputs
Products
Outputs to technosphere: Products and co-products
ABSO
Add line
Outputs to technosphere. Avoided products
Add line
Amount
Unit
Quantity
Allocation %
Comment
82,2
kg
Mass
100 %
Distribution
If the amount is in red, it is the result of calculations based on parameters previously defined.
Materials inputs
Energy inputs
Inputs
Inputs from nature
Subcompartment
SD2 or 2SD
Min
Max
Inputs from technosphere: materials/fuels
Membrane PP prod total
Calcium chloride {RER}| soda production, solvay process | APOS, S
Gas_mixture
Solvent_mixture
13,5
50,1
4,73
81,2
cm2
g
kg
kg
with life-time of membrane
CaCl2 (0,85 g/m²h)
CO2+Air
H2O + AA + Na2CO3 (+NaHCO3)
Inputs from technosphere: electricity/heat
Electricity, medium voltage {BE}| electricity voltage transformation from high to medium vol
Electricity, low voltage {BE}| electricity production, photovoltaic, 570kWp open ground instal
Electricity, high voltage {BE}| electricity production, wind, <1MW turbine, onshore | APOS, S
Electricity, high voltage {BE}| electricity production, nuclear, pressure water reactor | APOS, S
1,9E3
0
0
0
kJ
energy source depends on parameters

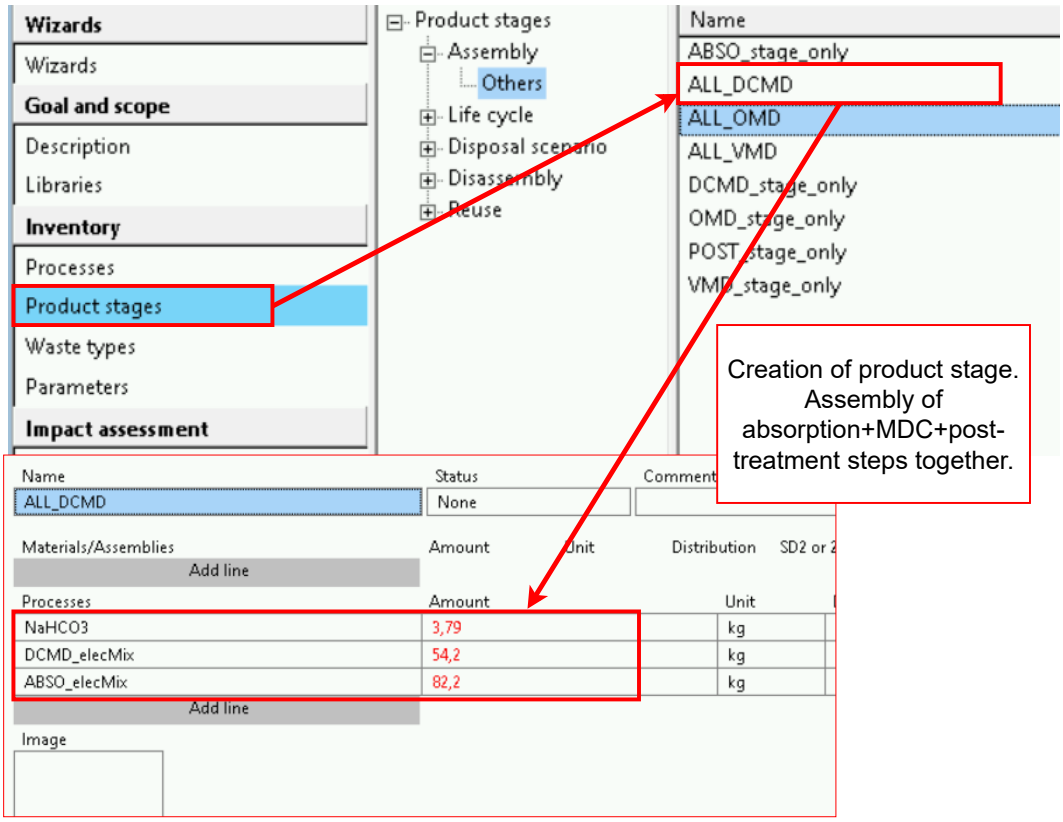
Wizards
Wizards
Goal and scope
Description
Libraries
Inventory
Processes
Product stages
Waste types
Parameters
Impact assessment
Product stages
Assembly
Others
Life cycle
Disposal scenario
Disassembly
Reuse
Name
ABSO_stage_only
ALL_DCMD
ALL_OMD
ALL_VMD
DCMD_stage_only
OMD_stage_only
POST_stage_only
VMD_stage_only
Creation of product stage. Assembly of absorption+MDC+post-treatment steps together.
Name
ALL_DCMD
Status
None
Comment
Materials/Assemblies
Amount
Unit
Distribution
Add line
Processes
Amount
Unit
NaHCO3
3,79
kg
DCMD_elecMix
54,2
kg
ABSO_elecMix
82,2
kg
Add line
Image

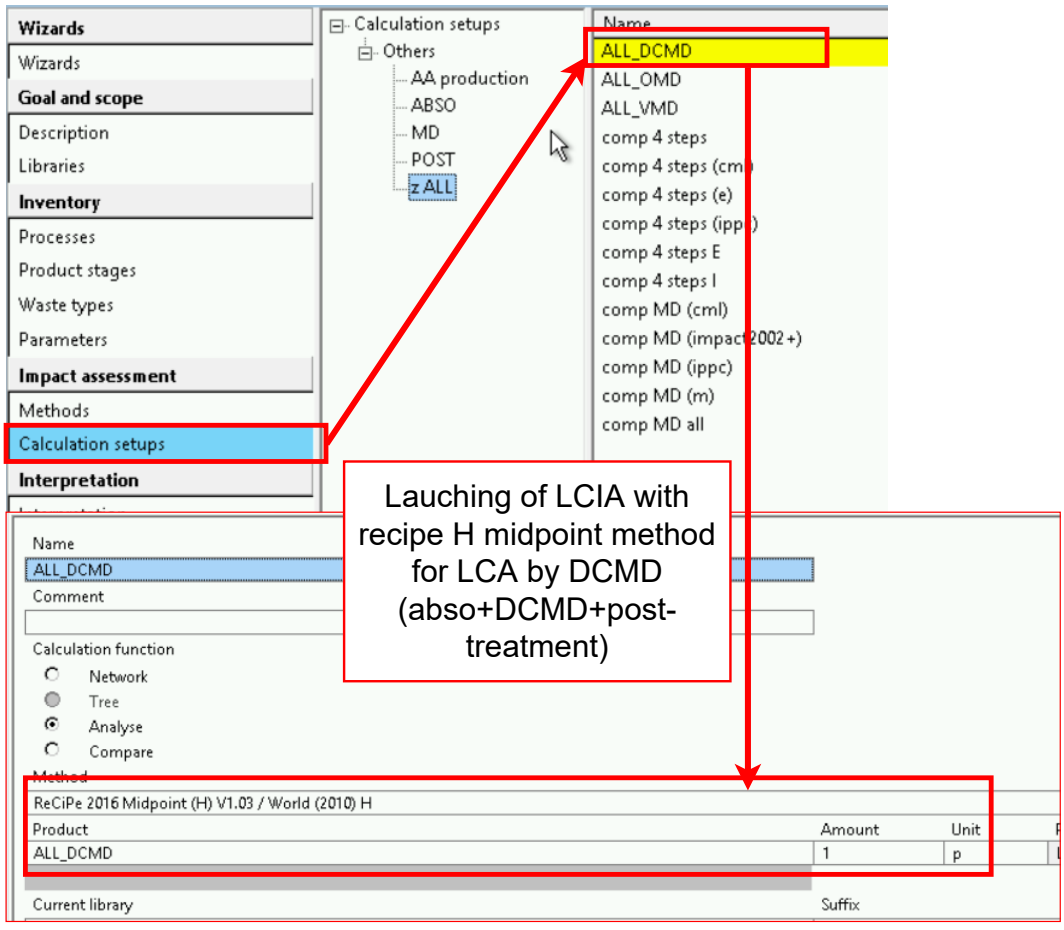
Wizards
Wizards
Goal and scope
Description
Libraries
Inventory
Processes
Product stages
Waste types
Parameters
Impact assessment
Methods
Calculation setups
Interpretation
Calculation setups
Others
AA production
ABSO
MD
POST
z ALL
Name
ALL_DCMD
ALL_OMD
ALL_VMD
comp 4 steps
comp 4 steps (cml)
comp 4 steps (e)
comp 4 steps (ippc)
comp 4 steps E
comp 4 steps I
comp MD (cml)
comp MD (impact2002+)
comp MD (ippc)
comp MD (m)
comp MD all
Lauching of LCIA with recipe H midpoint method for LCA by DCMD (abso+DCMD+post-treatment)
Name
ALL_DCMD
Comment
Calculation function
Network
Tree
Analyse
Compare
Method
ReCiPe 2016 Midpoint (H) V1.03 / World (2010) H
Product
Amount
Unit
ALL_DCMD
1
p
Current library
Suffix


Change to characterisation or normalised results
Copy results (for table format) to past it in Excel
Inventory
Setup
Checks (567,0)
Product overview
Characterisation
Normalisation
Skip categories
Never
Go from table to graph charts
Standard
Group
Default units
Exclude long-term emissions
Per impact category
%
Global warming
Stratospheric ozone dep
Ionizing radiation
Ozone formation, Huma
Fine particulate matter
Ozone formation, Terres
Terrestrial acidification
Freshwater eutrophicati
Marine eutrophication
Terrestrial ecotoxicity
Freshwater ecotoxicity
Marine ecotoxicity
Human carcinogenic toxi
Human non-carcinogeni
Land use
Mineral resource scarcity
Fossil resource scarcity
Water consumption
NaHCO3
DCMD_elecMix
ABSO

Bibliography

[1] EPA, "Overview of greenhouse gases | greenhouse gas (ghg) emissions | us epa," https://www.epa.gov/ghgemissions/overview-greenhouse-gases, 2018, (Accessed on 02/03/2021).

[2] "Global energy-related co2 emissions by sector – charts – data & statistics - iea," https://www.iea.org/data-and-statistics/charts/global-energy-related-co2-emissions-by-sector, (Accessed on 06/09/2021).

[3] "Energy mix - our world in data," https://ourworldindata.org/energy-mix, (Accessed on 06/09/2021).

[4] R. Sathre, M. Chester, J. Cain, and E. Masanet, "A framework for environmental assessment of CO2 capture and storage systems," *Energy*, vol. 37, no. 1, pp. 540–548, 2012. [Online]. Available: http://dx.doi.org/10.1016/j.energy.2011.10.050

[5] E. Favre, "Membrane processes and postcombustion carbon dioxide capture: Challenges and prospects," *Chemical Engineering Journal*, vol. 171, no. 3, pp. 782–793, 2011. [Online]. Available: http://dx.doi.org/10.1016/j.cej.2011.01.010

[6] R. Bounaceur, C. Castel, S. Rode, D. Roizard, and E. Favre, "Membrane contactors for intensified post combustion carbon dioxide capture by gas-liquid absorption in MEA: A parametric study," *Chemical Engineering Research and Design*, vol. 90, no. 12, pp. 2325–2337, 2012. [Online]. Available: http://dx.doi.org/10.1016/j.cherd.2012.05.004

[7] I. R. Salmón, N. Cambier, and P. Luis, "CO2 capture by alkaline solution for carbonate production: A comparison between a packed column and a membrane contactor," *Applied Sciences (Switzerland)*, vol. 8, no. 6, 2018.

[8] V. Sang Sefidi and P. Luis, "Advanced Amino Acid-Based Technologies for CO2 Capture: A Review," *Industrial and Engineering Chemistry Research*, vol. 58, no. 44, pp. 20 181–20 194, 2019.

[9] A. Mansourizadeh and A. Ismail, "Hollow fiber gas–liquid membrane contactors for acid gas capture: a review," *Journal of hazardous materials*, vol. 171, no. 1-3, pp. 38–53, 2009.

[10] A. Gabelman and S.-T. Hwang, "Hollow fiber membrane contactors," *Journal of Membrane Science*, vol. 159, no. 1, pp. 61 – 106, 1999. [Online]. Available: http://www.sciencedirect.com/science/article/pii/S037673889900040X

[11] Raphael, C. Janssens, Molina, V. Fernández, Sang, and Sefidi, "Lmapr 2118: absorption column," 2020, uCLouvain.

[12] P. Luis, "Use of monoethanolamine (MEA) for CO2 capture in a global scenario: Consequences and alternatives," *Desalination*, vol. 380, pp. 93–99, 2016. [Online]. Available: http://dx.doi.org/10.1016/j.desal.2015.08.004

[13] "Éthanolamine — wikipédia," https://fr.wikipedia.org/wiki/%C3%89thanolamine#/media/Fichier:Ethanolamin_-_Ethanolamine.svg, (Accessed on 01/19/2021).

[14] W. Ye, J. Lin, J. Shen, P. Luis, and B. Van Der Bruggen, "Membrane crystallization of sodium carbonate for carbon dioxide recovery: Effect of impurities on the crystal morphology," *Crystal Growth and Design*, vol. 13, no. 6, pp. 2362–2372, 2013.

[15] P. C. Tseng, W. S. Ho, and D. W. Savage, "Carbon dioxide absorption into promoted carbonate solutions," *AIChE Journal*, vol. 34, no. 6, pp. 922–931, 1988.

[16] Y. Cai, W. Wang, L. Li, Z. Wang, S. Wang, H. Ding, Z. Zhang, L. Sun, and W. Wang, "Effective capture of carbon dioxide using hydrated sodium carbonate powders," *Materials*, vol. 11, no. 2, 2018.

[17] G. Hu, N. J. Nicholas, K. H. Smith, K. A. Mumford, S. E. Kentish, and G. W. Stevens, "Carbon dioxide absorption into promoted potassium carbonate solutions: A review," *International Journal of Greenhouse Gas Control*, vol. 53, pp. 28–40, 2016.

[18] D. Guo, H. Thee, C. Y. Tan, J. Chen, W. Fei, S. Kentish, G. W. Stevens, G. Da Silva, S. Shen, X. Feng, R. Zhao, U. K. Ghosh, and A. Chen, "Amino acids as carbon capture solvents: Chemical kinetics and mechanism of the glycine + CO2 reaction," *Energy and Fuels*, vol. 27, no. 7, pp. 478–487, 2013. [Online]. Available: http://dx.doi.org/10.1016/j.cej.2013.02.093

[19] K. Simons, W. Brilman, H. Mengers, K. Nijmeijer, and M. Wessling, "Kinetics of CO2 absorption in aqueous sarcosine salt solutions: Influence of concentration, temperature, and CO2 loading," *Industrial and Engineering Chemistry Research*, vol. 49, no. 20, pp. 9693–9702, 2010.

[20] S. Shen, X. Feng, R. Zhao, U. K. Ghosh, and A. Chen, "Kinetic study of carbon dioxide absorption with aqueous potassium carbonate promoted by arginine," *Chemical Engineering Journal*, vol. 222, no. April 2018, pp. 478–487, 2013. [Online]. Available: http://dx.doi.org/10.1016/j.cej.2013.02.093

[21] Alissa Pirson, "Promoted sodium carbonate solvent for CO 2 capture by amino acids using membrane contactor technology," Master's thesis, UCLouvain, 2020.

[22] "The astrophysics & astrochemistry laboratory: Amino acids and their production during the photolysis of astrophysically relevant ices," http://www.astrochem.org/sci/Amino_Acids.php, (Accessed on 01/20/2021).

[23] "Arginine - wikipedia," https://en.wikipedia.org/wiki/Arginine, (Accessed on 01/20/2021).

[24] "Sarcosine - wikipedia," https://en.wikipedia.org/wiki/Sarcosine#/media/File:Sarcosine.png, (Accessed on 01/20/2021).

[25] R. Sander, "Compilation of Henry's law constants (version 4.0) for water as solvent," *Atmospheric Chemistry and Physics*, vol. 15, no. 8, pp. 4399–4981, 2015.

[26] T. N. G. Borhani, A. Azarpour, V. Akbari, S. R. Wan Alwi, and Z. A. Manan, "CO2 capture with potassium carbonate solutions: A state-of-the-art review," *International Journal of Greenhouse Gas Control*, vol. 41, pp. 142–162, 2015. [Online]. Available: http://dx.doi.org/10.1016/j.ijggc.2015.06.026

[27] D. Hasse, J. Ma, S. Kulkarni, P. Terrien, J.-P. Tranier, E. Sanders, T. Chaubey, and J. Brumback, "Co2 capture by cold membrane operation," *Energy Procedia*, vol. 63, pp. 186–193, 2014.

[28] M.-c. Sparenberg, B. Hanot, and P. Luis, "Experimental mass transfer comparison between vacuum and direct contact membrane distillation for concentration of carbonate solutions," *To be published*, 2021.

[29] Martin Chinarro Carla, "Development of advanced membranes for CO2 capture",," Master's thesis, UCLouvain, 2020.

[30] J. Albo, P. Luis, and A. Irabien, "Absorption of coal combustion flue gases in ionic liquids using different membrane contactors," *Desalination and Water Treatment*, vol. 27, no. 1-3, pp. 54–59, 2011. [Online]. Available: https://www.tandfonline.com/doi/abs/10.5004/dwt.2011.2050

[31] E. Curcio, A. Criscuoli, and E. Drioli, "Membrane crystallizers," *Industrial and Engineering Chemistry Research*, vol. 40, no. 12, pp. 2679–2684, 2001.

[32] G. Jarvenin, "Precipitation and Crystallization Processes," *Los Alamos National Laboratory*, 2009.

[33] I. Ruiz Salmón, "CO 2 capture and crystallization as sodium carbonate using membrane contactors," Ph.D. dissertation, UCLouvain Université Catholique de Louvain, 2018.

[34] I. Ruiz Salmón and P. Luis, "Membrane crystallization via membrane distillation," *Chemical Engineering and Processing: Process Intensification*, vol. 123, no. June 2017, pp. 258–271, 2018. [Online]. Available: https://doi.org/10.1016/j.cep.2017.11.017

[35] C. Wylock, A. Larcy, T. Cartage, and B. Haut, "Compartmental modeling of an industrial column," *Chemical Product and Process Modeling*, vol. 4, p. 30, 09 2009.

[36] Solvay, "Solvay ® sodium bicarbonate," *Solvay product brochure*, pp. 1–32, 2013.

[37] G. Steinhauser, "Cleaner production in the solvay process: general strategies and recent developments," *Journal of Cleaner Production*, vol. 16, no. 7, pp. 833–841, May 2008. [Online]. Available: https://doi.org/10.1016/j.jclepro.2007.04.005

[38] "Environmental issues associated with the solvay process - easychem australia," https://easychem.com.au/industrial-chemistry/the-solvay-process-has-been-in-use-since-the-1860s/environmental-issues-associated-with-the-solvay-process/, (Accessed on 06/11/2021).

[39] Patricia Luis Alconero, "Lmapr 2380: Solid – fluid separation, membrane distillation-crystallization," 2020, uCLouvain.

[40] A. Alkhudhiri, N. Darwish, and N. Hilal, "Membrane distillation: A comprehensive review," *Desalination*, vol. 287, pp. 2–18, 2012.

[41] J. I. Mengual, M. Khayet, and M. P. Godino, "Heat and mass transfer in vacuum membrane distillation," *International Journal of Heat and Mass Transfer*, vol. 47, no. 4, pp. 865–875, 2004.

[42] I. Ruiz Salmón, R. Janssens, and P. Luis, "Mass and heat transfer study in osmotic membrane distillation-crystallization for CO2valorization as sodium carbonate," *Separation and Purification Technology*, vol. 176, pp. 173–183, 2017.

[43] W. Li, B. Van der Bruggen, and P. Luis, "Recovery of Na2CO3 and Na2SO4 from mixed solutions by membrane crystallization," *Chemical Engineering Research and Design*, vol. 106, pp. 315–326, 2016. [Online]. Available: http://dx.doi.org/10.1016/j.cherd.2015.12.022

[44] M. Gryta, "The long-term studies of osmotic membrane distillation," *Chemical Papers*, vol. 72, no. 1, pp. 99–107, Aug. 2017. [Online]. Available: https://doi.org/10.1007/s11696-017-0261-1

[45] N. Nagaraj, G. Patil, B. R. Babu, U. H. Hebbar, K. S. Raghavarao, and S. Nene, "Mass transfer in osmotic membrane distillation," *Journal of Membrane Science*, vol. 268, no. 1, pp. 48–56, 2006.

[46] I. Handbook, "International reference life cycle data system (ilcd) handbook-general guide for life cycle assessment," *European Commission-Joint Research Centre-Institute for Environment and Sustainability*, 2010.

[47] H. Ostovari, A. Sternberg, and A. Bardow, "Rock 'n' use of CO2: Carbon footprint of carbon capture and utilization by mineralization," *Sustainable Energy and Fuels*, vol. 4, no. 9, pp. 4482–4496, 2020.

[48] D. I. S. Belboom, "Life cycle assessment – introduction," 2020, université de Liège.

[49] H.-P. Xie, L.-Z. Xie, Y.-F. Wang, J.-H. Zhu, B. Liang, and Y. Ju, "Ccu: A more feasible and economic strategy than ccs for reducing co (2) emissions," *Journal of Sichuan University: Engineering Science Edition*, vol. 44, no. 4, pp. 1–5, 2012.

[50] P. Mathieu, *The IPCC special report on carbon dioxide capture and storage*. Cambridge University Press, 2006.

[51] D. J. Harry Croezen, Sanne Nusselder, Erik Roos Lindgreen, "Screening LCA for CCU routes connected to CO 2 Smart Grid Screening LCA for CCU routes connected to CO 2 Smart Grid This," CE Delft, Delft, Tech. Rep., 2018.

[52] A. Zimmerman, , J. Wunderlich, G. Buchner, L. Müller, K. Armstrong, S. Michailos, A. Marxen, H. Naims, F. Mason, G. Stokes, and E. Williams, "Techno-economic assessment & life-cycle assessment guidelines for CO2 utilization," Technische Universität Berlin,RWTH Aachen University,The University of Sheffield, Institute for Advanced Sustainability Studies e.V. Potsdam, Tech. Rep., 2018. [Online]. Available: https://doi.org/10.3998/2027.42/145436

[53] R. M. Cuéllar-Franca and A. Azapagic, "Carbon capture, storage and utilisation technologies: A critical analysis and comparison of their life cycle environmental impacts," *Journal of CO2 Utilization*, vol. 9, pp. 82–102, Mar. 2015. [Online]. Available: https://doi.org/10.1016/j.jcou.2014.12.001

[54] R. Salmon and L. Alconero, "" Life cycle assessment of CO2 capture for further reuse as sodium carbonate " Abstract :," in *6th European Conference on Renewable Energy Systems - ECRES 2018*, Istanbul, 2018, pp. 1–2.

[55] H. H. Khoo and R. B. H. Tan, "Life cycle investigation of CO2recovery and sequestration," *Environmental Science & Technology*, vol. 40, no. 12, pp. 4016–4024, Jun. 2006. [Online]. Available: https://doi.org/10.1021/es051882a

[56] G. Garcia-Garcia, M. C. Fernandez, K. Armstrong, S. Woolass, and P. Styring, "Analytical review of life-cycle environmental impacts of carbon capture and utilization technologies," *ChemSusChem*, Jan. 2021. [Online]. Available: https://doi.org/10.1002/cssc.202002126

[57] L. J. Müller, A. Kätelhön, M. Bachmann, A. Zimmermann, A. Sternberg, and A. Bardow, "A guideline for life cycle assessment of carbon capture and utilization," *Frontiers in Energy Research*, vol. 8, Feb. 2020. [Online]. Available: https://doi.org/10.3389/fenrg.2020.00015

[58] Pooja, N. Yadav, M. Ismail, M. Essalhi, D. Tysklind, N. Athanassiadis, and Tavajohi, "Assessment of the environmental impact of polymeric membrane production," *Journal of Membrane Science*, vol. 622, no. September 2020, p. 118987, 2021. [Online]. Available: https://doi.org/10.1016/j.memsci.2020.118987

[59] M. Goedkoop, M. Oele, J. Leijting, T. Ponsioen, and E. Meijer, "Introduction to LCA with SimaPro Colophon," *Introduction to LCA with SimaPro*, vol. 5.2, no. November, 2016.

[60] J. Davis and G. Rochelle, "Thermal degradation of monoethanolamine at stripper conditions," *Energy Procedia*, vol. 1, no. 1, pp. 327–333, 2009. [Online]. Available: http://dx.doi.org/10.1016/j.egypro.2009.01.045

[61] E. Mosnier, H. M. Van Der Werf, J. Boissy, and J. Y. Dourmad, "Evaluation of the environmental implications of the incorporation of feed-use amino acids in the manufacturing of pig and broiler feeds using Life Cycle Assessment," *Animal*, vol. 5, no. 12, pp. 1972–1983, 2011.

[62] E. Kimball, A. Al-Azki, A. Gomez, E. Goetheer, N. Booth, D. Adams, and D. Ferre, "Contacteurs à membrane à fibres creuses pour la capture de co2: Modé lisation et mise à l'échelle de la capture du co2d'une centrale électrique au charbon de 800 MWe," *Oil and Gas Science and Technology*, vol. 69, no. 6, pp. 1047–1058, 2014.

[63] Jun, T. Kamo, H. Hirai, K. Takahashi, and Kondou, "High-speed digital-to-RF converter."

[64] M. Cheryan, *Ultrafiltration and microfiltration handbook*. CRC press, 1998.

[65] Chromalytic, "Peristaltic Pumps P, Chromalytic Technology, ZT6001J Basic Peristaltic Pump," https://www.chromalytic.com.au/pdf2/MC09_Laboratory09_37-39.pdf.

[66] B. instrument, "GF40 / GF80 Brooks instrument, Elastomer and Metal Seal Digital Mass Flow Controllers and Meters."

[67] Emerson, "Rosemount X-STREAM Enhanced XEGK Continuous Gas Analyzer | Emerson US." [Online]. Available: https://www.emerson.com/en-us/catalog/rosemount-x-stream-enhanced-xegk-continuous-gas-analyzer

[68] B. Instrument, "0250 Series Brooks instrument, Power Supply, Readout and Setpoint Controller." [Online]. Available: https://www.brooksinstrument.com/en/{~}/media/brooks/documentation/products/accessoriesandsoftware/secondaryelectronics/0250/0250-series-secondary-electronics-data-sheet.pdf

[69] "Sanitary Stirring Tank For Liquid Mixing And Stirring." [Online]. Available: https://www.machinery-ly.com/sanitary-stirring-tank-for-liquid-mixing-and-stirring-no-electric-heating

[70] "Drum Agitators - 200L Drum mixers - Dosing tanks - Mixing tanks." [Online]. Available: http://www.frankberg.nl/drum-agitators-mixers.html

[71] R. H. P. D. W. Green, R. H. Perry, and D. W. Green, *Perry's chemical engineers' handbook*. McGraw-Hill Professional Pub, 2008, vol. 8.

[72] "ME 1 Pompe à membrane - VACUUBRAND." [Online]. Available: https://www.vacuubrand.com/fr/page994.html{#}comparison

[73] "Fluids - latent heat of evaporation," https://www.engineeringtoolbox.com/fluids-evaporation-latent-heat-d_147.html, (Accessed on 05/20/2021).

[74] S. Tarleton and R. Wakeman, *Solid/liquid separation: equipment selection and process design*. Elsevier, 2006.

[75] "Laboratory decanter - Lemitec Decanter centrifuge MD 60." [Online]. Available: http://www.lemitec.com/en/products/md60.php

[76] "BHS Rotary Pressure Filter – BHS Filtration." [Online]. Available: https://bhs-filtration.com/products/rotary-pressure-filter/

[77] "Agitateurs à hélices électriques, agitateurs de laboratoire." [Online]. Available: https://glasatelier-saillart.be/fr/glazen-reactoren-en-reactievaten-met-flensdeksels/elektrische-bovenroerders/

[78] National Institute for Public Health and the Environment, "ReCiPe 2016 v1.1," *RIVM Report 2016-0104*, p. 201, 2017. [Online]. Available: www.rivm.nl/en

[79] A. W. Sleeswijk, L. F. van Oers, J. B. Guinée, J. Struijs, and M. A. Huijbregts, "Normalisation in product life cycle assessment: An LCA of the global and european economic systems in the year 2000," *Science of The Total Environment*, vol. 390, no. 1, pp. 227–240, Feb. 2008. [Online]. Available: https://doi.org/10.1016/j.scitotenv.2007.09.040

[80] "The sources and solutions: Agriculture | us epa," https://www.epa.gov/nutrientpollution/sources-and-solutions-agriculture, (Accessed on 08/02/2021).

[81] "Fertilizer use responsible for increase in nitrous oxide in atmosphere | berkeley news," https://news.berkeley.edu/2012/04/02/fertilizer-use-responsible-for-increase-in-nitrous-oxide-in-atmosphere/, (Accessed on 08/20/2021).

[82] U. N. S. C. on the Effects of Atomic Radiation *et al.*, *Sources, Effects and Risks of Ionizing Radiation, United Nations Scientific Committee on the Effects of Atomic Radiation (UNSCEAR) 2016 Report: Report to the General Assembly, with Scientific Annexes*. United Nations, 2017.

[83] S. C. for Life Cycle Inventories, "The life cycle inventory data version 2.2." https://www.ecoinvent.ch/, 2010.

[84] A. Panagopoulos, K. J. Haralambous, and M. Loizidou, "Desalination brine disposal methods and treatment technologies - A review," *Science of the Total Environment*, vol. 693, p. 133545, 2019. [Online]. Available: https://doi.org/10.1016/j.scitotenv.2019.07.351

[85] "Calculating true costs of salt brine," https://www.sima.org/news2/2015/08/01/calculating-true-costs-of-salt-brine, (Accessed on 08/05/2021).

[86] "Une eau au juste prix - eau de paris," http://www.eaudeparis.fr/leau-au-quotidien/une-eau-au-juste-prix/, (Accessed on 08/05/2021).

[87] R. Klaassen, P. H. Feron, and A. E. Jansen, "Membrane contactors in industrial applications," *Chemical Engineering Research and Design*, vol. 83, no. 3 A, pp. 234–246, 2005.

[88] P. Cote, Z. Alam, and J. Penny, "Hollow fiber membrane life in membrane bioreactors (MBR)," *Desalination*, vol. 288, pp. 145–151, 2012. [Online]. Available: http://dx.doi.org/10.1016/j.desal.2011.12.026

[89] A. Criscuoli, M. C. Carnevale, and E. Drioli, "Evaluation of energy requirements in membrane distillation," *Chemical Engineering and Processing: Process Intensification*, vol. 47, no. 7, pp. 1098–1105, 2008.

[90] The Intergovernmental Panel on Climate Change , "Climate Change 2021 The Physical Science Basis," https://www.ipcc.ch/report/ar6/wg1/downloads/report/IPCC_AR6_WGI_Full_Report.pdf, August 2021, (Accessed on 08/16/2021).

[91] T. N. G. Borhani, A. Azarpour, V. Akbari, S. R. W. Alwi, and Z. A. Manan, "Co2 capture with potassium carbonate solutions: a state-of-the-art review," *International Journal of Greenhouse Gas Control*, vol. 41, pp. 142–162, 2015.

[92] M. A. Huijbregts, Z. J. Steinmann, P. M. Elshout, G. Stam, F. Verones, M. Vieira, M. Zijp, A. Hollander, and R. van Zelm, "ReCiPe2016: a harmonised life cycle impact assessment method at midpoint and endpoint level," *International Journal of Life Cycle Assessment*, vol. 22, no. 2, pp. 138–147, 2017. [Online]. Available: http://dx.doi.org/10.1007/s11367-016-1246-y

[93] Pré Sustainability, "LCA and SimaPro essentials, Conference slides Day 1."

[94] D. L. Sills, L. G. Van Doren, C. Beal, and E. Raynor, "The effect of functional unit and co-product handling methods on life cycle assessment of an algal biorefinery," *Algal Research*, vol. 46, no. September 2019, p. 101770, 2020. [Online]. Available: https://doi.org/10.1016/j.algal.2019.101770

[95] European Commission, "Environmental factsheet: amino acids," no. 1, pp. 1–4.

[96] D. R.-N. Mireille Ginésy and U. Rova, "Tuning of the Carbon-to-Nitrogen Ratio for the Production of L-Arginine by Escherichia coli."

[97] T. Utagawa, "and Clinical Significance Production of Arginine by Fermentation 1," *Journal of Nutritions*, vol. 134, pp. 2854–2857, 2004.

[98] X. Y. Wu, X. Y. Guo, B. Zhang, Y. Jiang, and B. C. Ye, "Recent Advances of L-ornithine Biosynthesis in Metabolically Engineered Corynebacterium glutamicum," *Frontiers in Bioengineering and Biotechnology*, vol. 7, no. January, pp. 1–12, 2020.

[99] M. Ginésy, D. Rusanova-Naydenova, and U. Rova, "Tuning of the carbon-to-nitrogen ratio for the production of L-Arginine by Escherichia coli," *Fermentation*, vol. 3, no. 4, 2017.

[100] T. Hirasawa and H. Shimizu, "Recent advances in amino acid production by microbial cells," *Current Opinion in Biotechnology*, vol. 42, pp. 133–146, 2016. [Online]. Available: http://dx.doi.org/10.1016/j.copbio.2016.04.017

[101] D. Yang, X. Jia, M. Dang, F. Han, F. Shi, H. Tanikawa, and J. J. Klemeš, "Life cycle assessment of cleaner production measures in monosodium glutamate production: A case study in China," *Journal of Cleaner Production*, vol. 270, 2020.

[102] M. Mindt, M. Heuser, and V. F. Wendisch, "Xylose as preferred substrate for sarcosine production by recombinant Corynebacterium glutamicum," *Bioresource Technology*, vol. 281, no. January, pp. 135–142, 2019. [Online]. Available: https://doi.org/10.1016/j.biortech.2019.02.084

[103] S. Umair, C. Ria, J. S. Knight, R. J. Bland, and H. V. Simpson, "Sarcosine metabolism in Haemonchus contortus and Teladorsagia circumcincta," *Experimental Parasitology*, vol. 134, no. 1, pp. 1–6, 2013. [Online]. Available: http://dx.doi.org/10.1016/j.exppara.2013.01.017

[104] L. Barra, C. Fontenelle, G. Ermel, A. Trautwetter, G. C. Walker, and C. Blanco, "Interrelations between glycine betaine catabolism and methionine biosynthesis in sinorhizobium meliloti strain 102f34," *Journal of Bacteriology*, vol. 188, no. 20, pp. 7195–7204, Oct. 2006. [Online]. Available: https://doi.org/10.1128/jb.00208-06

[105] F. F. Blicke and P. E. Norris, "The preparation of sarcosine and methyl α-methylamino-β-(3-indolyl)-propionate," *Journal of the American Chemical Society*, vol. 76, no. 12, pp. 3213–3214, 1954.

[106] L. Baumann, "the Preparation of Sarcosine," *Journal of Biological Chemistry*, vol. 21, no. 3, pp. 563–566, 1915. [Online]. Available: http://dx.doi.org/10.1016/S0021-9258(18)87691-8

[107] M. Sarbar, A. Covington, R. Nuttall, and R. Goldberg, "The activity and osmotic coefficients of aqueous sodium bicarbonate solutions," *The Journal of Chemical Thermodynamics*, vol. 14, no. 10, pp. 967–976, 1982.

[108] K. S. Pitzer and J. C. Peiper, "Activity coefficient of aqueous sodium bicarbonate," *The Journal of Physical Chemistry*, vol. 84, no. 19, pp. 2396–2398, 1980.

[109] A. Shadloo and K. Peyvandi, "Thermodynamic modeling of amino acid solutions: A new perspective on cpa eos," *The Journal of Chemical Thermodynamics*, vol. 124, pp. 21–31, 2018.

[110] L. Ninni and A. J. Meirelles, "Water activity, ph and density of aqueous amino acids solutions," *Biotechnology progress*, vol. 17, no. 4, pp. 703–711, 2001.

[111] E. R. Smith and P. K. Smith, "Thermodynamic properties of solutions of amino acids and related substances: Viii. the ionization of glycylglycien, ε-aminocaproic acid, and aspartic acid in aqueous solution from one to fifty degrees," *Journal of Biological Chemistry*, vol. 146, no. 1, pp. 187–195, 1942.

[112] Y. Zhao, X. Zhuang, S. Ahmad, S. Sung, and S. Q. Ni, "Biotreatment of high-salinity wastewater: current methods and future directions," *World Journal of Microbiology and Biotechnology*, vol. 36, no. 3, pp. 1–11, 2020. [Online]. Available: https://doi.org/10.1007/s11274-020-02815-4

[113] L. W. en luchtbehandeling, "Brine treatment," https://www.lenntech.nl/processes/brine-treatment.htm, (Accessed on 05/22/2021).

[114] C. Meili and N. Jungbluth, "Life cycle inventories of crude oil extraction Final repor," ESU-services Ltd, Customer : BAFU, BFE & Erdöl-Vereinigung, Tech. Rep. October, 2018.

[115] R. K. Rosenbaum, *Selection of Impact Categories, Category Indicators and Characterization Models in Goal and Scope Definition. Chapter 2 "Goal and Scope Definition in Life Cycle Assessment" (Curran M. ed)*, 2017. [Online]. Available: http://link.springer.com/chapter/10.1007/978-94-024-0855-3{_}2

[116] Pré Sustainability, "Simapro Database Manual - Methods library v.4.15," pp. 3–48, 2020. [Online]. Available: http://www.pre-sustainability.com/download/DatabaseManualMethods.pdf

[117] "Cml-ia characterisation factors - leiden university," https://www.universiteitleiden.nl/en/research/research-output/science/cml-ia-characterisation-factors, (Accessed on 05/24/2021).

[118] "Eco-indicator 99 | manuals - pré sustainability," https://pre-sustainability.com/articles/eco-indicator-99-manuals/, (Accessed on 05/24/2021).

[119] S. Troy, A. Schreiber, and P. Zapp, "Life cycle assessment of membrane-based carbon capture and storage," *Clean Technologies and Environmental Policy*, vol. 18, no. 6, pp. 1641–1654, 2016.

[120] D. J. Harry Croezen, Sanne Nusselder, Erik Roos Lindgreen, "Screening LCA for CCU routes connected to CO 2 Smart Grid Screening LCA for CCU routes connected to CO 2 Smart Grid This," CE Delft, Delft, Tech. Rep., 2018.

[121] S. Belboom, J. M. Digneffe, R. Renzoni, A. Germain, and A. Léonard, "Comparing technologies for municipal solid waste management using life cycle assessment methodology: A Belgian case study," *International Journal of Life Cycle Assessment*, vol. 18, no. 8, pp. 1513–1523, 2013.

[122] H. M. G. M. G. J. H. R. H. M. J. O. M. M. D. S. An, "Recommendations for Life Cycle Impact Assessment in the European context - based on existing environmental impact assessment models and factors (International Reference Life Cycle Data System - ILCD handbook)," JRC European Comission, Tech. Rep. 9, 2013. [Online]. Available: https://publications.jrc.ec.europa.eu/repository/handle/JRC61049

[123] L. Giordano, D. Roizard, and E. Favre, "Life cycle assessment of post-combustion CO2 capture: A comparison between membrane separation and chemical absorption processes," *International Journal of Greenhouse Gas Control*, vol. 68, no. May 2017, pp. 146–163, 2018. [Online]. Available: https://doi.org/10.1016/j.ijggc.2017.11.008

[124] R. Aldaco, I. Butnar, M. Margallo, J. Laso, M. Rumayor, A. Dominguez-Ramos, A. Irabien, and P. E. Dodds, "Bringing value to the chemical industry from capture, storage and use of CO 2 : A dynamic LCA of formic acid production," *Science of the Total Environment*, vol. 663, pp. 738–753, 2019. [Online]. Available: https://doi.org/10.1016/j.scitotenv.2019.01.395

[125] A. Korre, Z. Nie, and S. Durucan, "Life cycle modelling of fossil fuel power generation with post-combustion CO2 capture," *International Journal of Greenhouse Gas Control*, vol. 4, no. 2, pp. 289–300, 2010. [Online]. Available: http://dx.doi.org/10.1016/j.ijggc.2009.08.005

[126] M. Rosental, T. Fröhlich, and A. Liebich, "Life Cycle Assessment of Carbon Capture and Utilization for the Production of Large Volume Organic Chemicals," *Frontiers in Climate*, vol. 2, p. 586199, oct 2020. [Online]. Available: https://www.frontiersin.org/article/10.3389/fclim.2020.586199/full

[127] D. S. Mallapragada and B. K. Mignone, "A theoretical basis for the equivalence between physical and economic climate metrics and implications for the choice of Global Warming Potential time horizon," *Climatic Change*, vol. 158, no. 2, pp. 107–124, jan 2020.

[128] "GTI: Gas Technology Institute", "Implications of Using Different GWP Time Horizons," GTI, Illinois, Tech. Rep., 2019.

[129] "Simapro | the world's leading lca software," https://simapro.com/, (Accessed on 08/16/2021).

[130] E. M. Mark Goedkoop, Michiel Oele, Marisa Vieira, Jorrit Leijting, Tommie Ponsioen, “SimaPro Tutorial Colophon,” no. May, 2014.

UNIVERSITÉ CATHOLIQUE DE LOUVAIN
École polytechnique de Louvain
Rue Archimède, 1 bte L6.11.01, 1348 Louvain-la-Neuve, Belgique | **www.uclouvain.be/epl**